On the Conductivity of Strongly Correlated Low-Dimensional Systems

Proefschrift

ter verkrijging van de graad van Doctor
aan de Rijksuniversiteit te Leiden,
op gezag van de Rector Magnificus Dr. L. Leertouwer,
hoogleraar in de faculteit der Godgeleerdheid,
volgens besluit van het college van dekanen
te verdedigen op woensdag 23 maart 1994
te klokke 16.15 uur

door

Behzad Rejaei-Salmassi

geboren te Teheran, Iran in 1965

Promotiecommissie:

Promotor:	Prof. dr. C.W.J. Beenakker
Referent:	Prof. dr. ir. W. van Saarloos
Overige leden:	Prof. dr. J. Amesz
	Prof. dr. ir. G.E.W. Bauer (Technische Universiteit Delft)
	Prof. dr. J.M.J. van Leeuwen
	Dr. J.-L. Pichard (Centre d'Etudes de Saclay)

To my parents

Contents

Chapter 1

Introduction

1.1 Fractional statistics and anyon superconductivity

Quantum statistics

Almost any textbook on quantum mechanics introduces the notion of quantum statistics by looking at the way the wave function changes sign under permutation of identical particles. The usual argument is as follows. Let $\psi(\mathbf{r}_1, \mathbf{r}_2, \ldots, \mathbf{r}_N)$ denote the wave function of a system of N particles with coordinates $\mathbf{r}_1, \mathbf{r}_2, \ldots, \mathbf{r}_N$. Quantum mechanics requires that the observable properties of a system do not change under permutation of identical particles. Because the probability density $|\psi|^2$ is an observable, it should not be altered by a simple permutation of two particles. If for instance $\psi'(\mathbf{r}_1, \mathbf{r}_2, \ldots, \mathbf{r}_N) = \psi(\mathbf{r}_2, \mathbf{r}_1, \ldots, \mathbf{r}_N)$ is the wave function after permutation of particles 1 and 2, we must have

$$|\psi'|^2 = |\psi|^2, \tag{1.1.1}$$

which means that ψ' differs from ψ only by a simple phase:

$$\psi' = \eta\psi,\ \eta = \exp(\mathrm{i}\theta). \tag{1.1.2}$$

Because ψ is single-valued, after a second permutation of the first two particles we get $\eta^2 = 1$. Hence there are just two possibilities: $\eta = 1$ ($\theta = 0$) corresponding to bosons and $\eta = -1$ ($\theta = \pi$) corresponding to fermions. The choice of η determines the statistics, *i.e.*, the rules for occupying quantum states. Fermions obey Pauli principle: a single state can only be occupied by a single fermion. Therefore, even at very low temperatures, fermions occupy states up to a relatively large energy (Fermi energy). There is no limitation on the number of bosons in a single quantum state. When the temperature is very low, bosons macroscopically occupy a single state, leading to Bose condensation.

It seems that this simple argument leaves no room for particles other than bosons and fermions. Indeed, these are the only particles which have been discovered in nature. Yet, as we shall see, this limitation is inherently related to the three spatial

dimensions we live in. In one spatial dimension, for instance, the whole notion of statistics looses its meaning for particles with a hard-core interaction. The hard-core particles cannot pass through each other in one dimension so that their ordering does not change. Therefore, it is not important how the wave function behaves when two particles are exchanged. By far the most interesting is the situation in two spatial dimensions. We will see that a continuum of statistical possibilities arises there: particles interpolating between bosons and fermions as the two extremes.

Path-dependent exchange phase and fractional statistics

We usually think about quantum statistics in terms of the permutation of the arguments in a wave function. However, what is essential for the physics is not the mathematical interchange of two arguments, but the *adiabatic* exchange, *i.e.*, the physical process in which two particles are transported adiabatically until they change places. The phase which then arises might depend on the Hamiltonian of the system and the traversed path [1]. The only condition which is imposed is that paths which can be continuously deformed into each other should yield the same phase [2].

As an example, let us consider the case of two particles in three spatial dimensions and restrict our attention to their relative coordinate $\mathbf{r} = \mathbf{r}_1 - \mathbf{r}_2$. As the two particles are exchanged adiabatically, their relative coordinate moves along a path connecting the points $\mathbf{r}$ and $-\mathbf{r}$. The phase η that arises is independent from the chosen path. This is because, in three dimensions, all of the paths with the same endpoints can be continuously deformed into each other. To determine η we exchange the particles a second time, after which the relative coordinate returns to its initial position $\mathbf{r}$. The relative coordinate has now traversed a closed path. But, in three dimensions, this path can be continuously deformed into the point $\mathbf{r}$. Therefore, the phase arising from the two exchanges should equal the phase when there is no exchange, *i.e.*, $\eta^2 = 1$ regardless of the chosen path.

But what about two dimensions? Consider the path of the relative coordinate $\mathbf{r}$ as the two particles are adiabatically exchanged (cf. Fig. 1.1). We assume that the particles have a hard-core interaction so that they cannot pass through each other. After a little bit of thinking it becomes clear that not all the possible exchange paths can be deformed continuously into each other. An exchange path can be continuously deformed into another one if and only if they both have the same (half) winding number, which is the number of times the relative coordinate encircles the origin in the positive (counter-clockwise) direction. (Paths in the negative (clockwise) direction have a negative winding number.) Therefore, in two dimensions the exchange phase may depend on the path, or more precisely, on its winding number.

In order to determine the exchange phase, we consider the set of the closed paths of the relative coordinate in two dimensions. To each closed path with an integer winding number n we assign a phase χ_n. We require that χ_n satisfies the group property $\chi_n \chi_m = \chi_{n+m}$, since any two closed paths with winding numbers n and m can be combined into a single closed path with the winding number $n + m$. A

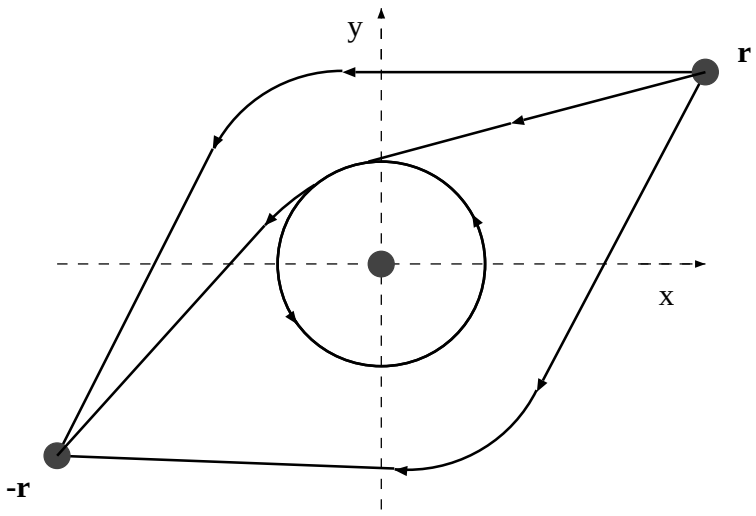

Fig. 1.1. Possible paths of the relative coordinate during the adiabatic exchange of two particles in two dimensions. The winding number of each path is the number of times it encircles the origin in the counter-clockwise direction. Paths with different winding numbers cannot be deformed into each other.

scalar representation of the group $\{\chi_n\}$ is given by $\chi_n = (\eta^2)^n$, where $\eta = \exp(\mathrm{i}\theta)$ is the phase arising from a simple exchange of the two particles (with zero winding number) in the positive direction. In contrast to three dimensions, closed paths with $n \neq 0$ cannot be deformed into a single point, so that there is no restriction on the value of η (or equivalently θ). In particular, we have $\theta = 0 (\mathrm{mod}\, 2\pi)$ for bosons and $\theta = \pi (\mathrm{mod}\, 2\pi)$ for fermions. *Any* other value of θ corresponds to *anyons* or particles obeying fractional statistics [3, 4].

In addition to a path-dependent, complex exchange phase, there is another difference between anyons and the "conventional" particles. In a many-anyon system, the phase acquired by exchanging two anyons will also depend on the number of other anyons enclosed by the exchange loop. Each enclosed anyon contributes an extra, non-trivial phase $(\eta^2)^k$ where k is the number of times it is encircled by the exchange loop.

Anyons as particle-flux tube composites

In view of the complexity of a path-dependent exchange phase, it is no wonder that even the problem of noninteracting anyons cannot be easily solved. In contrast to bosons and fermions, it is not possible to write the wave function as a symmetrized or antisymmetrized linear combination of single-particle wave functions. Instead, one has to use multivalued wave functions, in order to deal with the complicated boundary conditions arising from the path-dependent behaviour. One example is to

write [5]

$$\Psi(\{z_i\},\{z_i^*\}) = \prod_{i<j} \frac{(z_i - z_j)^\alpha}{|z_i - z_j|^\alpha} \Phi(\{z_i\},\{z_i^*\}), \tag{1.1.3}$$

where we have introduced complex coordinates $z_i = x_i + \mathrm{i}y_i$. The function Φ is single-valued and might be either symmetric (boson representation) or antisymmetric (fermion representation) in its arguments. The corresponding value of θ is $\pi\alpha$ and $\pi(\alpha+1)$ for the boson and fermion representations, respectively. The function Ψ in Eq. (1.1.3) has a complicated structure, extending over various branch-cuts of the first factor on the r.h.s. of Eq. (1.1.3).

There is an alternative picture of anyons where instead of treating the statistics as a boundary condition, we treat it as an interaction between bosons or fermions with single-valued wave functions and ordinary permutation relations. The advantage of this approach is that we do not have to keep track of all possible exchange paths, for the particles now obey the usual boson or fermion statistics. In this picture [4], each anyon is thought of as a composite particle consisting of a boson or fermion of charge e, pierced with a fictitious flux tube carrying a flux Φ (Fig. 1.2). The statistical phase is now viewed as the Aharonov-Bohm phase arising from the adiabatic exchange of composite particles, and is given by $\eta = \exp(\mathrm{i}\theta)$ where $\theta = \pi e\Phi/h$ for bosons and $\theta = \pi + \pi e\Phi/h$ for fermions. Since the ratio $e\Phi/h$ can take any value, the composite particles are anyons.

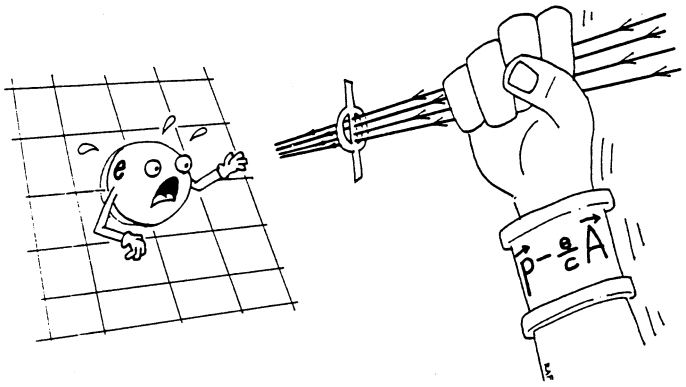

Fig. 1.2. The making of an anyon: a charge in two dimensions is pierced by a flux tube. The resultings particles have fractional statistics. (From Ref. [6].)

The fictitious flux tubes give rise to a strong long-range vector-potential interaction between the particles. Formally, the vector-potential interaction enters the Hamiltonian by substituting Eq. (1.1.3) into the free-particle Hamiltonian $\mathcal{H}_0 =$

$(-\hbar^2/2m)\sum_i \nabla_i^2$, and applying a singular gauge transformation. Although the interacting problem is quite complicated, the particles are now ordinary bosons and fermions so that one can apply the standard approximations of the many-body physics.

Do anyons exist?

We have seen that in two dimensions, the notion of quantum statistics can be nontrivially generalized to include anyons. But do anyons exist? Well, not as fundamental particles, since we live in a three-dimensional world. Yet, there are many examples of condensed-matter systems realized in the laboratory, which are effectively two-dimensional. Just as any physical system, these condensed-matter systems are also made of ordinary bosons and fermions. Nevertheless, the *excitations* of these systems might be of a quite different nature. A similar situation arises in an electron gas: whereas the fundamental particles are fermions, the system supports phonon excitations which obey Bose statistics. There are two phenomena in which anyons are believed to play a role. The first phenomenon is the fractional quantum Hall effect discussed in Sec. 2. It is now well established that the quasiparticle excitations in the fractional quantum Hall effect are anyons. The role of the anyons in the second phenomenon, the high-temperature superconductivity, is more controversial. Experiment have failed to confirm the existence of anyons in the two-dimensional planes of high-temperature superconductors.

Anyon superconductivity

Laughlin [7] has suggested that the charged excitations in the high-temperature superconductors obey fractional statistics. To see how fractional statistics implies superconductivity, consider a gas of anyons each consisting of a fermion of charge e carrying a flux tube containing the flux $\Phi = h/ep$, where p is an integer. The phase arising from the exchange of two anyons is $\exp(\mathrm{i}\theta)$ where $\theta = \pi + \pi e\Phi/h = \pi(1+1/p)$. Laughlin's insight was that composites of p anyons behave as if they were bosons: the exchange phase of two such composites equals $[\exp(\mathrm{i}\theta)]^{p^2} = \exp[\mathrm{i}\pi(p^2+p)] = 1$, where we have used that p^2+p is always an even integer. Therefore, composites of p anyons can macroscopically occupy a p-particle state, and form a charge-p superfluid. A superfluid is characterized by a gap in the single-particle excitation spectrum, and an undamped linearly dispersing longitudinal collective mode. Furthermore, since the composites are charged, the system becomes superconductive, showing for instance a Meissner effect. Laughlin has in particular considered the case $p = 2$, as a possible explanation of the high-temperature superconductivity.

In chapter 2, we investigate the mean-field (Hartree) theory [8]-[11] of anyon superconductors. In the mean-field theory, the fictitious flux tubes are smeared out,

yielding a fictitious perpendicular magnetic field

$$\mathbf{B}^{\mathrm{f}}(\mathbf{r}) = \frac{h}{pe} n(\mathbf{r}) \hat{\mathbf{z}}, \tag{1.1.4}$$

proportional to the particle density $n(\mathbf{r})$ (in the x-y plane). In the ground state $n(\mathbf{r})$ is uniform so that the problem is reduced to that of noninteracting fermions in a constant magnetic field. In a magnetic field, the kinetic energy of the motion of the particles is quantized in the highly degenerate Landau levels, separated by the energy $\hbar\omega_{\mathrm{c}}$ where $\omega_{\mathrm{c}} = eB^{\mathrm{f}}/m$ is the cyclotron frequency. Because of the relation (1.1.4), a gas of anyons precisely fills p Landau levels and the system possesses a single-particle excitation gap, a feature of superfluidity. We shall study the linear response of an anyon gas to an external electromagnetic field, using the time-dependent mean-field (Hartree) approximation and show that a gas of anyons exhibits the perfect conductivity and the Meissner effect, both characteristic of a superconductor.

1.2 The fractional quantum Hall effect

The quantum Hall effect

The quantum Hall effect (QHE) [12, 13] was discovered in 1980 by Klaus von Klitzing, for which he received the 1985 Noble prize in physics. This phenomenon occurs in a two-dimensional electron gas (2DEG) subject to a strong, perpendicular magnetic field [14, 15]. A simplified version of the experimental setup is shown in Fig. 1.3. A rectangular shaped sample with length L and width W, is placed in a perpendicular magnetic field $B\hat{\mathbf{z}}$. A constant current I is led through the sample, and the longitudinal (V_{L}) and Hall (V_{H}) voltage differences are measured. In an ideal sample, the current density $\mathbf{j}$ is uniform (given by I/W), and directed along the long edge of the sample. The electric field $\mathbf{E}$ is also uniform with components in both the x and y directions. The electric field and the current density are related by

$$\mathbf{j} = \sigma\mathbf{E},\ \mathbf{E} = \rho\mathbf{j}, \tag{1.2.1}$$

where σ and $\rho(=\sigma^{-1})$ are the conductivity and the resistivity tensors, respectively. By measuring V_{L} and V_{H}, one can determine the components of the resistivity tensor from the relations $\rho_{xx} = \rho_{yy} = (W/L)V_{\mathrm{L}}/I$, $\rho_{xy} = -\rho_{yx} = V_{\mathrm{H}}/I$. The conductivity tensor is found by inverting ρ.

In general, both the longitudinal resistivity ρ_{xx}, and the Hall resistivity ρ_{xy} depend on the material parameters. The semiclassical theory of conductivity, for instance, yields [16]

$$\rho_{xx} = \frac{1}{\sigma_0},\ \rho_{xy} = \frac{B}{en}, \tag{1.2.2}$$

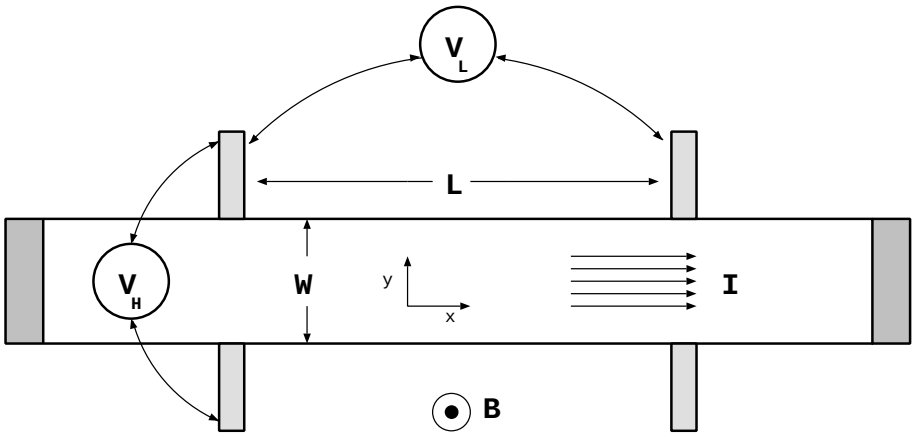

Fig. 1.3. The experimental setup for measuring the quantum Hall effect. A rectangular shaped sample with length L and width W is placed in a perpendicular magnetic field. Connections are made on the sides of the sample. A constant current I is led through the sample and the voltage differences $V_{\rm L}$ and $V_{\rm H}$ are measured. (From Ref. [14].)

where σ_0 is the Drude conductivity, $-e$ is the charge of an electron, and n is the electron density. The Drude conductivity is simply

$$\sigma_0 = \frac{ne^2\tau_0}{m}, \tag{1.2.3}$$

where τ_0 is the mean free time, and m is the effective mass of the electrons which differs from the electron mass $m_{\rm e}$. In the semiclassical theory, the quantum effects only modify the effective mass m and the mean free time τ_0. Both parameters are material dependent.

The semiclassical description is quite accurate under normal conditions. However, at very low temperatures, a completely different picture arises. Figure 1.4 shows the measured values of ρ_{xx} and ρ_{xy} plotted as a function of the magnetic field. Instead of ρ_{xy} following a straight line, as predicted by the semiclassical theory, a series of steps are found. On each step both the longitudinal conductivity and resistivity vanish, and the Hall conductivity and resistivity take the constant values

$$\sigma_{xy} = \rho_{xy}^{-1} = \nu\frac{e^2}{h}, \tag{1.2.4}$$

where ν (called the filling factor) is always a rational number with an odd denominator. Note that Eq. (1.2.4) only involves the fundamental constants e and h; there is no dependence on the material.

The current theoretical picture of the QHE can be summarized as follows [14, 15].

(i) The QHE occurs whenever a gap opens in the excitation spectrum of the 2DEG, implying incompressibility. The incompressibility is indicated by a jump in the chemical potential $\mu = \partial E(N)/\partial N$, corresponding to a cusp in the ground-state energy $E(N)$ as a function of the particle number N. This happens at special values

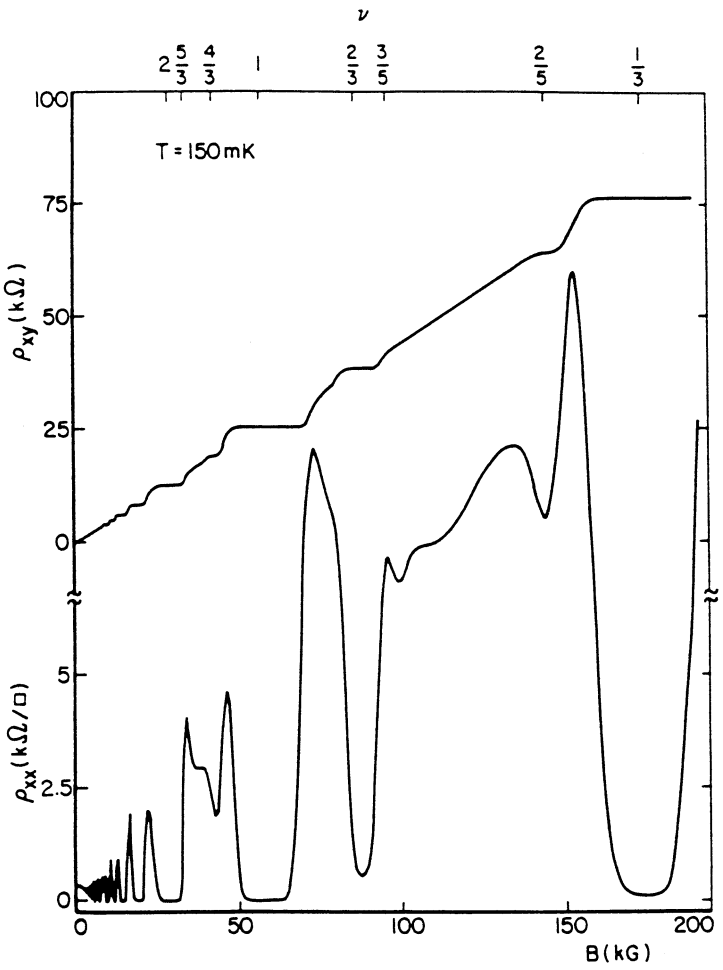

Fig. 1.4. The longitudinal (ρ_{xx}) and Hall (ρ_{xy}) resistivities as a function of the magnetic field field B, in a high-quality sample. The temperature is 150mK. Steps are formed around rational values of the filling factor $\nu = nh/eB$. On each step ρ_{xx} vanishes and ρ_{xy} becomes constant. (From Ref. [14].)

of the electron density given by $n_\nu = \nu eB/h$ where ν is a rational number. The vanishing of ρ_{xx} and the resulting dissipationless flow of current, is a manifestation of the excitation gap of the 2DEG.

(ii) Around the "magic" densities n_ν, steps are formed, on which the Hall conductivity σ_{xy} remains constant and equals $en_\nu/B = \nu e^2/h$. The Hall resistivity $\rho_{xy} = B/en_\nu$ equals the semiclassical value [Eq. (1.2.2)] at $n = n_\nu$.

(iii) The formation of the steps cannot be explained without taking into account the disorder. An ideally "clean" system does not exhibit QHE.

The integer QHE

The first filling factors which where experimentally observed were the integers $\nu = 1, 2, \ldots$ [12]. It was very soon understood that the incompressibility of the 2DEG at the integer values of ν, is essentially a property of noninteracting electrons: it is a result of the quantization of the kinetic energy of motion of the electrons in a magnetic field. The kinetic energy of motion in a magnetic field is quantized in the highly degenerate Landau levels, separated by a distance $\hbar\omega_{\rm c}$, where $\omega_{\rm c} = eB/m$ is the cyclotron frequency. The degeneracy of each Landau level is $D = eBA/h$ where A is the area of the system.

According to the Pauli principle, each single-particle state can only be occupied by a single electron. (We neglect the spin degrees of freedom of the electrons.) At zero temperature, the states with the lowest energies are occupied. Now consider a system of N noninteracting electrons. By definition, the chemical potential $\mu(N)$ is the energy needed to add an extra electron to the system. Therefore, for the noninteracting system at zero temperature, $\mu(N)$ is the energy of the lowest lying unoccupied state, and equals the energy of the highest, partially filled Landau level. As N is increased, the chemical potential remains constant, until the highest Landau level becomes completely filled. When this happens, an excitation gap opens and the chemical potential jumps by an amount of $\hbar\omega_{\rm c}$. Therefore, the noninteracting 2DEG becomes incompressible when a number of Landau levels are completely filled, *i.e.* when the filling factor $\nu = nh/eB = N/D$ becomes an integer.

The fractional QHE

The experimentally observed filling factors are not restricted to the integers. Soon after the discovery of the integer QHE, other fractions such as $\frac{1}{3}, \frac{2}{5}, \ldots$, were observed [13]. From a phenomenological point of view it is difficult to distinguish the fractional QHE from its integer counterpart. Yet, the underlying physics is completely different. In contrast to the integer QHE, the incompressibility in the fractional QHE is caused by the electron-electron interactions. At fractional filling factors, the electrons in a partially filled Landau level are condensed into a strongly correlated liquid.

The established theory of the fractional QHE is based on Laughlin's variational

wave function [17]:

$$\Psi = \prod_{i<j}(z_i - z_j)^{2k+1} \exp\left(-\sum_i \frac{|z_i|^2}{4\ell_0^2}\right), \tag{1.2.5}$$

where $\ell_0 = (\hbar/eB)^{1/2}$ is the magnetic length, and k is an integer. Laughlin's wave function accurately describes the fractional QHE in a uniform, unbounded 2DEG at the filling factor $\nu = \frac{1}{2k+1}$. An interesting feature of the wave function (1.2.5) is that its elementary excitations are quasiparticles and quasiholes with fractional charge and statistics [14, 15]. Laughlin's wave function is known to be the exact, incompressible ground state for an interaction potential of vanishing range [18, 19]; for other, more general interaction potentials its accuracy has been confirmed by numerical studies.

The generalization of Laughlin's theory to filling factors other than $\nu = \frac{1}{2k+1}$ was suggested by the hierarchy picture of Haldane [20] and Halperin [21]. In this picture, the filling factors $\nu = \frac{1}{2k+1}$ form the first level of the hierarchy of the fractional QHE states. The second level of the hierarchy is constructed by the condensation of the quasiparticles (or quasiholes) of the $\nu = \frac{1}{2k+1}$ states, into new Laughlin states. For instance, the state at $\nu = \frac{2}{5}$ is formed when the quasiparticles of the $\nu = \frac{1}{3}$ state condense into a new $\frac{1}{3}$ Laughlin state. By continuing the hierarchical construction, and invoking the particle-hole symmetry [22], one can recover all of the possible filling factors.

Jain's theory of the fractional QHE

Although the theoretical explanations of the integer and the fractional QHE's are quite different from each other, the similarity in the phenomenology motivates a unifying approach to both phenomena. The first step in this direction was taken by Jain [23]. He suggested that the fractional QHE can be viewed as the integer QHE of electron-flux-tube composites. Jain's ideas can be summarized as follows.

(i) The incompressibility in the integer QHE is enforced by the Fermi statistics of the electrons (Pauli's principle) and is not sensitive to the electron-electron interactions.

(ii) The role of the electron-electron interactions in the incompressible fractional QHE liquid is to bind a fraction of the external flux to the electrons, forming composite particles each consisting of an electron of charge e, bound to a flux tube of strength $\Phi = 2k\Phi_0$ where k is an integer and $\Phi_0 = h/e$ is the flux quantum. Consequently, the composite particles move in an effective magnetic field which is smaller than the true external magnetic field. The statistical phase arising from the exchange of two such composite particles is (see Sec. 1) $\eta = \exp(\mathrm{i}\pi + \mathrm{i}\pi e\Phi/h) = -1$, so that the composite particles will again obey Fermi statistics.

(iii) Being fermions, the composite particles are subject to the same incompressibility mechaniasm as that of the ordinary electrons in the integer QHE. The fractional QHE occurs when the gas of composite particles fills a number of Landau levels in the new, effective magnetic field.

Jain gave a prescription for constructing the fractional QHE states. He proposed the Ansatz [23]

$$\psi_\nu = \mathcal{P} \prod_{i<j} (z_i - z_j)^{2k} \psi_p, \tag{1.2.6}$$

for the fractional QHE state ψ_ν at the filling factor

$$\nu = \frac{p}{2kp+1}, \tag{1.2.7}$$

where k and p are integers, $\mathcal{P}$ is the lowest Landau level projection operator, and ψ_p is the integer QHE wave function at the filling factor p. The second factor on the r.h.s. of Eq. (1.2.6) attaches $2k$ flux quanta to each electron. The different levels of the hierarchy of the fractional QHE states are obtained by substituting different values for p. Equating $p = 1$, $k = 1, 2, \ldots$, in Eq. (1.2.7), one recovers the filling factors $\nu = \frac{1}{3}, \frac{1}{5}, \ldots$ belonging to the first level of the hierarchy. Equating $p = 2, k = 1, 2, \ldots$, results in the second level of the hierarchy $\nu = \frac{2}{5}, \frac{2}{9}, \ldots$, and so on. Jain's wave functions agree very well with exact numerical studies carried out for small systems.

Adiabatic principle of Greiter and Wilczek

Despite the attractiveness of Jain's idea to consider the fractional QHE as the integer QHE of composite particles, his method of construction of the fractional QHE states is rather heuristic. The adiabatic principle of Greiter and Wilczek [24] is in a way an attempt to put Jain's approach on a more physically and mathematically sound basis. Greiter and Wilczek have proposed that the incompressible states of the fractional QHE can be obtained by *adiabatically* attaching flux tubes to the electrons in the incompressible integer QHE states.

To understand the adiabatic principle of Greiter and Wilczek [24], consider a 2DEG filling exactly p Landau levels. The system has an excitation gap and shows the integer QHE at $\nu = p$. If it were possible to continuously reduce the filling factor (or the density) of the 2DEG, while retaining the excitation gap, we could have reached incompressible states at fractional filling factors.

It is well-known that when the Hamiltonian of the system depends on an external parameter, the excitation gap does not collapse if the external parameter is changed adiabatically. In order to introduce such a parameter into the Hamiltonian, Greiter and Wilczek considered a gas of electrons bound to fictitious flux tubes each carrying $-\lambda$ flux quanta h/e (Fig. 1.5). In Sec. 1.1 we saw that the resulting objects obey fractional statistics. The flux tubes induce a fictitious long-range vector-potential interaction between the electrons whose strength λ is used as the adiabatic parameter. Let's assume that at $\lambda = 0$ the ground state is the integer QHE state at $\nu = p$ with the density $n_0 = ph/eB$. The vector-potential interaction is now switched on by increasing λ adiabatically. To see how the density of the system changes with λ, we apply the law's of classical electrodynamics. As λ is increased adiabatically,

negative flux is introduced into the system. According to Faraday's law, the system tries to keep the total magnetic flux constant. Equating the total flux per particle $-\lambda h/e + B/n$ to its initial value $B/n_0 = h/ep$, yields the filling factor

$$\nu = \frac{nh}{eB} = \frac{p}{\lambda p + 1}. \tag{1.2.8}$$

Since the excitation gap is not destroyed by the adiabatic attachment of flux, a system of anyons is incompressible and therefore shows fractional QHE at the filling factors given by Eq. (1.2.8). But what about electrons? When λ reaches an even integer $2k$ with $k = 1, 2, \ldots$, the composite particles once again obey Fermi statistics. The vector-potential interaction can now be gauged away by a singular gauge transformation, and we are left with an incompressible state of electrons. The filling factor is found by substituting $\lambda = 2k$ in Eq. (1.2.8), after which we recover Jain's hierarchy formula (1.2.7).

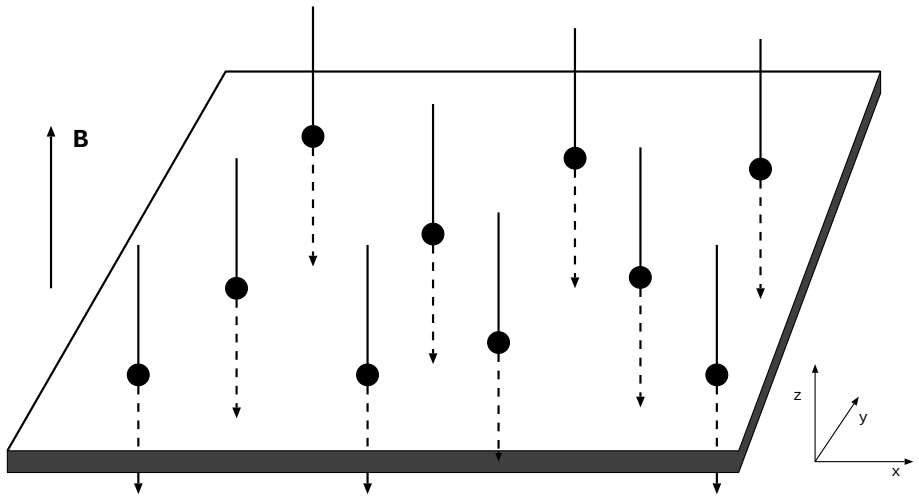

Fig. 1.5. Schematic illustration of the adiabatic mapping. The incompressible states of the integer QHE are mapped onto the incompressible states of the fractional QHE by attaching negative flux tubes to the electrons adiabatically. After binding an even number of flux quanta to each electron, the flux tubes can be removed instantaneously by a gauge transformation.

The adiabatic principle of Greiter and Wilczek is a strong theoretical tool for studying the subtle relationships between the integer and the fractional QHE states. In chapter 3 we shall use the adiabatic principle to investigate the resemblance in the energy spectra of the noninteracting fermions on the one hand, and the interacting bosons and fermions on the other hand.

Vector-mean-field theory of the fractional QHE

Although the microscopic theories of Laughlin [17] and Jain [23] are quite successful in describing the fractional QHE in an unbounded, uniform 2DEG, there is no generalization of these theories to confined or nonuniform systems. Furthermore, even in a

uniform system, the complicated nature of the microscopic wave functions of Laughlin and Jain makes it difficult to extract the physics of the fractional QHE. What we need is an effective theory which contains the essential physics of the problem, and can be easily applied to confined or nonuniform systems. Early mean-field treatments [25]-[28] of the electron-electron interaction, however, failed to explain the incompressibility of the 2DEG at fractional filling factors. The Hartree-Fock ground-state energy is just a smooth function of the filling factor (or electron density). There is no cusp indicating the incompressibility of the 2DEG. Somehow a mean-field (Hartree-Fock) treatment of the electron-electron interaction neglects the subtle correlations responsible for the incompressibility of the 2DEG at fractional filling factors.

It is, however, possible to formulate an alternative mean-field theory based on the adiabatic principle of Greiter and Wilczek. The adiabatic principle is a prescription for constructing the fractional QHE states by starting from the integer QHE states. However, it cannot be carried out unless suitable approximations are made. The mean-field (Hartree) treatment of the fictitious vector-potential interaction yields a vector-mean-field theory of the fractional QHE. The vector-mean-field theory is similar to the mean-field theory of the anyon superconductivity discussed at the end of the previous section. In this approximation the flux tubes attached to the electrons are smeared out, yielding a fictitious magnetic field proportional to the electron density. In chapter 4 we show that the vector-mean-field theory reproduces the known bulk properties of the unbounded, uniform fractional QHE states, such as the excitation gap, and the fractional charge and statistics of the quasiparticles and quasiholes. (These bulk properties are also well described by the Chern-Simon field theories of Refs. [29]-[33].) We will then consider the application of the vector-mean-field theory to a simple confined geometry, a quantum dot with parabolic confinement.

1.3 Scaling theory of conduction and random matrix theory

Random matrix theory

Random matrix theory (RMT) was developed in the 50's and 60's by Wigner, Dyson, and Mehta, in order to explain the statistical distribution of the excitation energies (resonances) of the heavy nuclei (for a review see Ref. [34]). In a typical slow-neutron scattering experiment, the energy of the incident neutron in not sharply defined. As a result, the incident neutron interacts not just with one, but with a number of neighboring energy levels, so that the average properties of the latter become important. Obviously, any statement regarding the distribution of the energy levels requires the solution of the Schrödinger equation for the nucleus under consideration. However, with the exception of certain effective Hamiltonians describing the ground state and its low-lying excitations, not much was known yet in the early sixties about the exact Hamiltonian of a nucleus.

The crucial step in formulating a statistical theory of energy levels was taken by Wigner [35]. He considered each nucleus as a member of a large ensemble of nuclei,

each with its own specific, but unknown Hamiltonian. If the number of members of the ensemble is large, then one expects the properties of each member to be well described by the statistical averages over the whole ensemble. Therefore, one has to answer the following question: given an ensemble of random Hamiltonians $\mathcal{H}$, what is the statistical distribution of the energy eigenvalues $\{E_i\}$? For simplicity we assume that the space of the physical states has a finite dimension N, and consider an ensemble of random $N \times N$ hermitian matrices.

The main hypothesis of RMT is that the probability density $P(\mathcal{H})$ of any Hamiltonian $\mathcal{H}$ is of the form

$$P(\mathcal{H}) = \prod_{i=1}^{N} p(E_i), \tag{1.3.1}$$

where $p(E)$ depends on the system under consideration and has to be determined from the available (experimental) information, such as the density of the states. The key idea is that at the level of the Hamiltonians, the energy eigenvalues are *uncorrelated* [35]. Because $P(\mathcal{H})$ is independent of the eigenvectors of $\mathcal{H}$, they can be integrated out, resulting in the new probability density

$$\begin{aligned} P(\{E_i\}) &= J(\{E_i\}) \prod_{i=1}^{N} p(E_i), \\ J(\{E_i\}) &= \prod_{i<j} |E_i - E_j|^{\beta}. \end{aligned} \tag{1.3.2}$$

The function $J(\{E_i\})$ is the jacobian of the transformation from the space of hermitian matrices to the space of eigenvalues. The basic assumption of RMT is that the only correlations between the energy eigenvalues are due to the jacobian [35]. The parameter β is not just any number: it is determined by the symmetries of the system and can only take the values $1, 2$, and 4, as shown by Dyson [36]. $\beta = 1$ in systems with time-reversal symmetry, $\beta = 2$ in systems where time-reversal symmetry is broken, and $\beta = 4$ in systems with spin-orbit scattering in the presence of time-reversal symmetry.

Application of RMT to conductivity

The central question of RMT was how to determine the probability distribution of eigenvalues from an ensemble of random Hamiltonians. A similar question arises when studying the conductivity of a disordered conductors. Consider a wire of length L and width W. The transversal motion of the electrons in the wire is quantized, and depending on the Fermi energy, a number N of waveguide modes contribute to the current. The scattering matrix $\mathbf{S}$ relates the ingoing and outgoing modes on both sides of the sample. This is a unitary $2N \times 2N$ matrix of the form

$$\mathbf{S} = \begin{pmatrix} \mathbf{r} & \mathbf{t}' \\ \mathbf{t} & \mathbf{r}' \end{pmatrix}, \tag{1.3.3}$$

where $\mathbf{r}, \mathbf{t}, \mathbf{t}'$, and $\mathbf{r}'$ are $N \times N$ matrices. The conductance G of the sample is given by the Landauer formula

$$G = \frac{2e^2}{h} \sum_{i=1}^{N} T_i, \tag{1.3.4}$$

where $\{T_i\}$ (called transmission eigenvalues) are the eigenvalues of the $N \times N$ matrix $\mathbf{t}\mathbf{t}^\dagger$.

The scattering matrix and its submatrices can only be calculated if we have detailed knowledge of the impurities and their distribution. However, just as in the case of energy levels, we can consider an ensemble of conductors similar in shape, but each with its own scattering matrix. Now the question is [37], given an ensemble of random scattering matrices, what can be said about the statistical distribution of the transmission eigenvalues $\{T_i\}$? Proceeding as in Eqs. (1.3.1) and (1.3.2), Muttalib, Pichard, and Stone [38, 39] arrived at the probability density $P(\{T_i\})$ of N transmission eigenvalues $\{T_i\}$ in the form

$$\begin{aligned} P(\{T_i\}) &= J(\{T_i\}) \prod_{i=1}^{N} p(T_i), \\ J(\{T_i\}) &= \prod_{i<j} |T_i^{-1} - T_j^{-1}|^\beta, \end{aligned} \tag{1.3.5}$$

where again $p(T)$ has to be determined independently. Note that in contrast to Eq. (1.3.2), not the $\{T_i\}$ themselves, but their reciprocals appear in the jacobian. This is because we are not dealing with the eigenvalues of $\mathbf{S}$ itself, but of the matrix $\mathbf{t}\mathbf{t}^\dagger$, so that the jacobian is different. Muttalib *et al.* presented a maximum-entropy argument, supported by numerical simulation, to argue that Eq. (1.3.5) was highly accurate and possibly exact for wire geometries ($L \gg W$).

The probability density (1.3.5) can be used to calculate the distribution of the conductance in the ensemble of wires. Of particular interest, however, are the sample to sample conductance fluctuations $\langle \delta G^2 \rangle$ where $\delta G = G - \langle G \rangle$. Using a completely different approach, Al'tshuler [41], and Lee and Stone [42] showed that in the diffusive regime where $L \ll N\ell$ (ℓ is the elastic mean free path), the conductance fluctuations are independent from the sample size or the strength of the disorder. This phenomenon is called "universal conductance fluctuations" (UCF). Their calculation, which uses diagrammatic perturbation theory, yields $\langle \delta G^2 \rangle = (2/15)\beta^{-1}(2e^2/h)^2$. To see whether RMT reproduces the UCF, Beenakker [40] has applied a generalized version of a theorem due to Dyson and Mehta [43] to this problem. The Dyson-Mehta theorem directly relates the fluctuations of any quantity of the form $A(\{T_i\}) = \sum_i a(T_i)$ (linear statistic), to the jacobian. The theorem yields $\langle \delta G^2 \rangle = (1/8)\beta^{-1}(2e^2/h)^2$ for the UCF [40], which is slightly different from the result of Al'tshuler, Lee, and Stone. The implication is that the central hypothesis of RMT (all correlations are accounted for by the jacobian) is not exactly true, but is an approximation. To test the accuracy of RMT we need the exact form of the eigenvalue

correlation. The latter, however, cannot be obtained by diagrammatic perturbation theory. We therefore choose an alternative approach based on a scaling equation for the transmission eigenvalues.

Scaling equation for the transmission eigenvalues

The scaling equation for the transmission eigenvalues governs the evolution of the probability density $P(\{T_i\}; L)$ as the length L of the sample increases. It was derived by Dorokhov [44], and independently by Mello, Pereyra, and Kumar [45] (we shall call it the DMPK equation). The DMPK equation is a diffusion or Fokker-Planck equation for N fictitious classical particles with a logarithmic repulsion. Until recently, the only exact solution known was that for $N = 1$ [46, 47]. For $N > 1$ only asymptotic solutions were known [48]-[50]. These asymptotic solutions, however, are not suitable for a determination of the exact form of the correlation between transmission eigenvalues.

In chapter 5 we present an exact solution of the DMPK equation for $\beta = 2$ and an arbitrary large N. The solution is based on a Sutherland type transformation which maps the DMPK equation onto an imaginary-time Schrödinger equation for N interacting fermions in one dimension [51]. The interaction vanishes for $\beta = 2$ and the resulting free-fermion problem is solved exactly. The exact solution enables us to calculate the exact form of the eigenvalue correlation, which is then compared to the predictions of RMT.

References

[1] M.V. Berry, Proc. Roy. Soc. Londen Ser. A **392**, 45 (1984).

[2] L.S. Schulman, *Techniques and Applications of Path Integration* (Wiley, New York, 1981).

[3] J.M. Leinaas and J. Myrheim, Nuovo Cimento **37**B, 1 (1977).

[4] F. Wilczek, Phys. Rev. Lett. **48**, 1144 (1982); Phys. Rev. Lett. **49**, 957 (1982).

[5] Y.S. Wu, Phys. Rev. Lett. **52**, 2103 (1984); Phys. Rev. Lett. **53**, 111 (1984).

[6] A. Shapere and F. Wilczek, Eds. , *Geometrical Phases in Physics* (World Scientific, Singapore, 1989).

[7] R.B. Laughlin, Science **242**, 525 (1988); Phys. Rev. Lett. **60**, 2677 (1988).

[8] C.B. Hanna, R.B. Laughlin, and A.L. Fetter, Phys. Rev. B **40**, 8745 (1989).

[9] A.L. Fetter, C.B. Hanna, and R.B. Laughlin, Phys. Rev. B **39**, 9679 (1989).

[10] C. Gros, S.M. Girvin, G.S. Canright, and M.D. Johnson, Phys. Rev. B **43**, 5883 (1991).

[11] A.L. Fetter and C.B. Hanna, Phys. Rev. B **45**, 2335 (1992).

[12] K. von Klitzing, G. Dorda, and M. Pepper, Phys. Rev. Lett. **45**, 494 (1980).

[13] C.D. Tsui, H.L. Störmer, and A.C. Gossard, Phys. Rev. Lett. **48**, 1559 (1982).

[14] *The Quantum Hall Effect*, eds. R.E. Prange and S.M. Girvin (Springer, New York, 1987).

[15] *The Fractional Quantum Hall Effect*, by T. Chakraborty and P. Pietiläinen (Springer, Berlin, 1988).

[16] N.W. Ashcroft and N.D. Mermin, *Solid State Physics* (Holt, New York, 1976).

[17] R.B. Laughlin, Phys. Rev. Lett. **50**, 1395 (1983).

[18] S.A. Trugman and S. Kivelson, Phys. Rev. B **31**, 5280 (1985).

[19] S. Kivelson and V.L. Pokrovsky, Phys. Rev. B **40**, 1373 (1989).

[20] F.D.M. Haldane, Phys. Rev. Lett. **51**, 605 (1983).

[21] B.I. Halperin, Phys. Rev. Lett. **52**, 1583 (1984); Phys. Rev. Lett. **52**, 2390 (1984).

[22] S.M. Girvin, Phys. Rev. B **29**, 6012 (1984).

[23] J.K. Jain, Phys. Rev. Lett. **63**, 199 (1989); Phys. Rev. B **40**, 8079 (1989);Adv. in Phys. **41**, 105 (1992).

[24] M. Greiter and F. Wilczek, Mod. Phys. Lett. B **4**, 1063 (1990); Nucl. Phys. B **370**, 577 (1992).

[25] H. Fukuyama, P.M. Platzman, and P.W. Anderson, Phys. Rev. B **19**, 5211 (1979).

[26] D. Yoshioka, Phys. Rev. B **27**, 3637 (1983).

[27] D. Yoshioka and P.A. Lee, Phys. Rev. B **27**, 4986 (1983).

[28] K. Maki and X. Zotos, Phys. Rev. B **28**, 4349 (1983).

[29] S.C. Zhang, T.H. Hansson, and S. Kivelson, Phys. Rev. Lett. **62**, 82 (1989).

[30] N. Read, Phys. Rev. Lett. **62**, 86 (1989).

[31] A. Lopez and E. Fradkin, Phys. Rev. B **44**, 5246 (1991).

[32] S.G. Ovchinnikov, Pis'ma Zh. Eksp. Teor. Fiz. **54**, 579 (1991) [JETP Lett. **54**, 583 (1991)].

[33] A. Perez Martinez and A. Cabo, Mod. Phys. Lett. B **5**, 1703 (1991).

[34] M.L. Mehta, *Random Matrices*, 2nd ed. (Academic, New York, 1991).

[35] E.P. Wigner, SIAM Review **9**, 1 (1967).

[36] F.J. Dyson, J. Math. Phys. **3**, 1199 (1962).

[37] Y. Imry, Europhys. Lett. **1**, 249 (1986).

[38] K.A. Muttalib, J.-L. Pichard, and A.D. Stone, Phys. Rev. Lett. **59**, 2475 (1987).

[39] A.D. Stone, P.A. Mello, K.A. Muttalib, and J.-L. Pichard, in *Mesoscopic Phenomena in Solids*, ed. by B.L. Al'tshuler, P.A. Lee, and R.A. Webb (North-Holland, Amsterdam, 1991).

[40] C.W.J. Beenakker, Phys. Rev. Lett. **70**, 1155 (1993); Phys. Rev. B **47**, 15763 (1993).

[41] B.L. Al'tshuler, Pis'ma Zh. Eksp. Teor. Fiz. **41**, 530 (1985) [JETP Lett. **41**, 648 (1985)].

[42] P.A. Lee and A.D. Stone, Phys. Rev. Lett. **55**, 1622 (1985); P.A. Lee, A.D. Stone, and H. Fukuyama, Phys. Rev. B **35**, 1039 (1987).

[43] F.J. Dyson and M.L. Mehta, J. Math. Phys. **4**, 701 (1963).

[44] O.N. Dorokhov, Pis'ma Zh. Eksp. Teor. Fiz. **36**, 259 (1982) [JETP Lett. **36**, 318 (1982)].

[45] P.A. Mello, P. Pereyra, and N. Kumar, Ann. Phys. **181**, 290 (1988).

[46] V.I. Mel'nikov, Fiz. Tverd. Tela **23**, 782 (1981) [Sov. Phys. Solid State **23**, 444 (1981)].

[47] P.A. Mello, J. Math. Phys. **27**, 2876 (1986).

[48] J.-L. Pichard, in *Quantum Coherence in Mesoscopic Systems*, edited by B. Kramer, NATO ASI Series B254 (Plenum, New York, 1991).

[49] P.A. Mello, Phys. Rev. Lett. **60**, 1089 (1988).

[50] P.A. Mello and A.D. Stone, Phys. Rev. B **44**, 3559 (1991).

[51] B. Sutherland, Phys. Rev. A **5**, 1372 (1972).

Chapter 2

Superconductivity in the mean-field anyon gas

2.1 Introduction

The introduction of particles with fractional statistics (*anyons*[1]) into condensed matter physics has led to a number of interesting applications. Among these, of particular importance is the suggestion that high-temperature superconductivity might originate from these (quasi-)particles.[2] Indeed, it appears now to be well established that a two-dimensional ideal gas of non-interacting anyons has a superconducting ground state.[3–11]

Recently, Leggett has addressed the more limited, but highly interesting question whether the anyon gas is superconducting *when solved in the mean-field approximation*.[12] In that approximation the anyon gas is replaced by a gas of fermions, subject to a perpendicular magnetic field $\mathbf{B}^{\mathrm{f}}(\mathbf{r}) = (h/pe)n(\mathbf{r})\hat{\mathbf{z}}$ proportional to the particle density $n(\mathbf{r})$ (in the x–y plane). The strength of this fictitious (or "statistical") magnetic field adjusts itself in such a way to variations in the density, that p Landau levels are kept fully occupied. (The value $p = 2$ is expected to be relevant for high-temperature superconductivity.[2]) The single-particle eigenstates of the mean-field Hamiltonian are extended along equipotentials of the electrostatic potential. Leggett uses the insensitivity of these eigenstates to variations in the boundary conditions (in a Corbino-disk geometry), to argue that the mean-field anyon gas is an *insulator*—rather than a superconductor.

In the present paper we reexamine the mean-field theory of the anyon gas. We show that the mean-field Hamiltonian contains, in addition to the fictitious magnetic field $\mathbf{B}^{\mathrm{f}}$ mentioned above, also a fictitious *electric* field $\mathbf{E}^{\mathrm{f}}(\mathbf{r}) = (h/pe^2)\hat{\mathbf{z}} \times \mathbf{j}(\mathbf{r})$ proportional to the current density $\mathbf{j}(\mathbf{r})$. This electric field arises because in the original Hamiltonian the anyons are composed of fermions bound to a flux tube, of strength h/pe and of infinitesimal cross section. In the mean-field approximation, the flux tubes are smeared out, and one obtains the fictitious magnetic field $\mathbf{B}^{\mathrm{f}}$ proportional to n. However, the flux tubes remain bound to the particles. When a flux tube at $\mathbf{r}_a$ moves with the velocity $\mathbf{v}_a$, it induces an electric field $\mathbf{E}(\mathbf{r}) = -\mathbf{v}_a \times \mathbf{b}(\mathbf{r} - \mathbf{r}_a)$, where $\mathbf{b}$ is the magnetic field of the flux tube. As we will show below, the fictitious electric field transforms the mean-field anyon gas from an insulator into

a superconductor. We consider the case of an ideal (impurity-free) anyon gas in detail, but will argue that the superconductivity persists in the presence of disorder (by using results from the integer quantum Hall effect).

2.2 Anyon gas in the Hartree approximation

The anyon Hamiltonian in the fermion-gauge representation is given by

$$\mathcal{H} = \sum_i \frac{1}{2m} \left(\mathbf{p}_i - e\mathbf{A}_i\right)^2, \tag{2.2.1}$$

$$\mathbf{A}_i = \sum_{j\neq i} \mathbf{a}(\mathbf{r}_{ij}),\ \mathbf{a}(\mathbf{r}) = \frac{h}{pe}\frac{\hat{\mathbf{z}}\times\mathbf{r}}{2\pi r^2}. \tag{2.2.2}$$

The Hartree-Fock equations are obtained by approximating the ground state Ψ of the many-body Hamiltonian (2.2.1) by a Slater determinant of single-particle wave functions $\{\psi_i\}$, and minimizing the energy $E_{\rm HF} =< \Psi_{\rm HF}|\mathcal{H}|\Psi_{\rm HF} >$. Disregarding the exchange terms, we obtain in a straightforward manner the single-particle mean-field (Hartree) Hamiltonian for anyons,

$$\mathcal{H}^{\rm H} = \frac{1}{2m}\left(\mathbf{p} - e\mathbf{A}^{\rm f}\right)^2 + e\Phi^{\rm f}. \tag{2.2.3}$$

The fictitious electromagnetic potentials $\Phi^{\rm f}$ and $\mathbf{A}^{\rm f}$ are related to the particle density n and charge current density $\mathbf{j}$ by

$$\mathbf{A}^{\rm f}(\mathbf{r},t) = \int d\mathbf{r}'\, \mathbf{a}(\mathbf{r}-\mathbf{r}')\, n(\mathbf{r}',t), \tag{2.2.4}$$

$$e\Phi^{\rm f}(\mathbf{r},t) = \int d\mathbf{r}'\, \mathbf{a}(\mathbf{r}-\mathbf{r}')\cdot\mathbf{j}(\mathbf{r}',t). \tag{2.2.5}$$

The corresponding fictitious electric and magnetic fields take the form

$$\mathbf{B}^{\rm f}(\mathbf{r},t) = \nabla\times\mathbf{A}^{\rm f} = \frac{h}{pe} n(\mathbf{r},t)\hat{\mathbf{z}}, \tag{2.2.6}$$

$$\mathbf{E}^{\rm f}(\mathbf{r},t) = -\partial_t\mathbf{A}^{\rm f} - \nabla\Phi^{\rm f} = \frac{h}{pe^2}\hat{\mathbf{z}}\times\mathbf{j}(\mathbf{r},t). \tag{2.2.7}$$

The wave functions $\{\psi_i\}$ are determined by solving the Schrödinger equation $\mathcal{H}^{\rm H}\psi_i = E_i\psi_i$ together with Eqs. (2.2.4) and (2.2.5) self-consistently.

The term $e\Phi^{\rm f}$ in Eq. (2.2.3) accounts for the fictitious electric field induced by the moving flux tubes. Such a term is required by Galileian invariance, but was omitted in a previous mean-field theory of the anyon gas.[11] Other approaches to the problem,[3–10] being Galileian invariant, include this term implicitly. Since the extra term $e\Phi^{\rm f}$ is proportional to the current density [see Eq. (2.2.5)], it may presumably be disregarded in calculations of the density response.[11] However, it plays a crucial role in the current response (*i.e.* in the conductivity), as we now show.

2.3 Electromagnetic response of an anyon gas

When an external electromagnetic field $(\Phi^{\rm ex}, \mathbf{A}^{\rm ex})$ is switched on, the anyon density and current distributions are modified. Therefore, the perturbation Hamiltonian $\Delta\mathcal{H}$ contains terms due to the variations $\delta\Phi^{\rm f}$ and $\delta\mathbf{A}^{\rm f}$ in the internal fictitious fields from their ground state values $\Phi^{\rm gr}$ and $\mathbf{A}^{\rm gr}$. To first order in the perturbation, one obtains

$$\mathcal{H}^{\rm H} = \mathcal{H}_0 + \Delta\mathcal{H}, \tag{2.3.1}$$

$$\mathcal{H}_0 = \frac{1}{2m}\left(\mathbf{p} - e\mathbf{A}^{\rm gr}\right)^2 + e\Phi^{\rm gr}, \tag{2.3.2}$$

$$\Delta\mathcal{H} = -\frac{e}{m}\left(\mathbf{p} - e\mathbf{A}^{\rm gr}\right)\cdot\left(\mathbf{A}^{\rm ex} + \delta\mathbf{A}^{\rm f}\right) + e\left(\Phi^{\rm ex} + \delta\Phi^{\rm f}\right). \tag{2.3.3}$$

A straightforward application of the Kubo formalism,[13] yields in the long wavelength limit ($\mathbf{k} = 0$) the current density response

$$\delta\mathbf{j}(\omega) = \boldsymbol{\sigma}_0(\omega)\cdot\left[\mathbf{E}^{\rm ex}(\omega) + \delta\mathbf{E}^{\rm f}(\omega)\right], \tag{2.3.4}$$

where $\mathbf{E}^{\rm ex} = {\rm i}\omega\mathbf{A}^{\rm ex} - \nabla\Phi^{\rm ex}$. The conductivity tensor $\boldsymbol{\sigma}_0$ is associated with the Hamiltonian $\mathcal{H}_0$ with unperturbed potentials $\Phi^{\rm gr}$ and $\mathbf{A}^{\rm gr}$. To obtain the true conductivity tensor $\boldsymbol{\sigma}$, one still needs to eliminate $\delta\mathbf{E}^{\rm f}$ from Eq. (2.3.4) by applying the self-consistency relation (2.2.7), which we write in the form

$$\delta\mathbf{E}^{\rm f} = -\frac{h}{pe^2}\boldsymbol{\epsilon}\cdot\delta\mathbf{j}. \tag{2.3.5}$$

Here, $\boldsymbol{\epsilon}$ is the antisymmetric tensor of rank two ($\epsilon_{xx} = \epsilon_{yy} = 0, \epsilon_{xy} = -\epsilon_{yx} = 1$). The solution to Eqs. (2.3.4) and (2.3.5) is

$$\delta\mathbf{j}(\omega) = \boldsymbol{\sigma}(\omega)\cdot\mathbf{E}^{\rm ex}(\omega), \tag{2.3.6}$$

$$\boldsymbol{\sigma}(\omega) = \left[\boldsymbol{\rho}_0(\omega) + \frac{h}{pe^2}\boldsymbol{\epsilon}\right]^{-1},\ \boldsymbol{\rho}_0 \equiv \boldsymbol{\sigma}_0^{-1}. \tag{2.3.7}$$

Now we use that $\mathcal{H}_0$ describes a fermion gas with p fully filled Landau levels. This implies that $\boldsymbol{\rho}_0$ equals the integer quantum Hall effect resistivity tensor at filling factor p, *i.e.*

$$(\rho_0)_{xx} = (\rho_0)_{yy} = -{\rm i}\omega\frac{m}{e^2 n_0},$$
$$(\rho_0)_{xy} = -(\rho_0)_{yx} = -\frac{h}{pe^2}, \tag{2.3.8}$$

where n_0 is the bulk density. Upon substitution of the expression for $\boldsymbol{\rho}_0$ into Eq. (2.3.7), one obtains

$$\sigma_{\alpha\beta} = -\frac{1}{{\rm i}\omega}\frac{e^2 n_0}{m}\delta_{\alpha\beta}. \tag{2.3.9}$$

The anyon gas is thus a perfect conductor in the limit $\omega \to 0$. We now take the curl of Eq. (2.3.6) and substitute Eq. (2.3.9) to arrive at the London equation

$$\nabla \times \delta\mathbf{j} = -\frac{e^2 n_0}{m}\mathbf{B}^{\rm ex}. \tag{2.3.10}$$

So far we have considered the electromagnetic response for $\mathbf{k} = 0$ in the limit $\omega \to 0$. The existence of the Meissner effect depends on whether Eq. (2.3.10) is valid for $\omega = 0$, in the subsequent limit $\mathbf{k} \to 0$.[14] As we will now show, this is indeed the case.

To demonstrate that Eq. (2.3.10) holds regardless of the order of the limits $\mathbf{k} \to 0$ and $\omega \to 0$, we consider the general form of the linear response for density and current density in the Fourier space,

$$\begin{aligned} &\delta\mathcal{J}_\mu(\mathbf{k},\omega) = K_{\mu\nu}(\mathbf{k},\omega)\mathcal{A}_\nu(\mathbf{k},\omega), \\ &\mathcal{J} = (en, \mathbf{j}), \mathcal{A} = (\Phi, -\mathbf{A}). \end{aligned} \tag{2.3.11}$$

The response function $K_{\mu\nu}$ is defined in the space-time representation as

$$\begin{aligned} K_{\mu\nu}(\mathbf{r},t;\mathbf{r}',t') &= (\mathrm{i}\hbar)^{-1} < \Psi| \left[\mathcal{J}_\mu(\mathbf{r},t), \mathcal{J}_\nu(\mathbf{r}',t')\right] |\Psi > \theta(t-t') \\ &\quad + \frac{n_0}{m}(1-\delta_{\mu 0})\delta_{\mu\nu}. \end{aligned} \tag{2.3.12}$$

The response function satisfies the continuity relations $\partial_\mu K_{\mu\nu} = \partial'_\nu K_{\mu\nu} = 0$. As shown in the Appendix, the elements of the tensor $K_{\mu\nu}$ can all be expressed in terms of four coefficients $\chi_0, \xi_0, \eta_0, \zeta_0$, according to

$$K_{00}(\mathbf{k},\omega) = -k^2\chi_0(\mathbf{k},\omega), \tag{2.3.13}$$

$$K_{0j}(\mathbf{k},\omega) = -\omega\chi_0(\mathbf{k},\omega)k_j + \mathrm{i}\xi_0(\mathbf{k},\omega)\epsilon_{jn}k_n, \tag{2.3.14}$$

$$K_{i0}(\mathbf{k},\omega) = -\omega\chi_0(\mathbf{k},\omega)k_i + \mathrm{i}\eta_0(\mathbf{k},\omega)\epsilon_{im}k_m, \tag{2.3.15}$$

$$\begin{aligned} K_{ij}(\mathbf{k},\omega) &= -\frac{\omega^2}{k^2}\chi_0(\mathbf{k},\omega)k_ik_j + \frac{\mathrm{i}\omega}{k^2}\eta_0(\mathbf{k},\omega)\epsilon_{im}k_mk_j + \frac{\mathrm{i}\omega}{k^2}\xi_0(\mathbf{k},\omega)k_i\epsilon_{jn}k_n \\ &\quad + \frac{1}{k^2}\zeta_0(\mathbf{k},\omega)\epsilon_{im}k_m\epsilon_{jn}k_n. \end{aligned} \tag{2.3.16}$$

Here, roman indices denote the carthesian components x, y. The physical meaning of these coefficients becomes more apparent if we rewrite the response equation (2.3.11) in terms of the density δn and the vorticity $\delta\Omega \equiv \hat{\mathbf{z}} \cdot (\mathrm{i}\mathbf{k} \times \delta\mathbf{j})$. (The component of $\delta\mathbf{j}$ along $\mathbf{k}$ is not an independent variable, as it is constrained by the continuity equation $\mathrm{i}\mathbf{k} \cdot \delta\mathbf{j} = \mathrm{i}\omega e\delta n$.) The resulting equations are [1]

$$e\delta n(\mathbf{k},\omega) = -\chi_0(\mathbf{k},\omega)k^2\Phi(\mathbf{k},\omega) + \xi_0(\mathbf{k},\omega)B(\mathbf{k},\omega), \tag{2.3.17}$$

$$\delta\Omega(\mathbf{k},\omega) = \eta_0(\mathbf{k},\omega)k^2\Phi(\mathbf{k},\omega) - \zeta_0(\mathbf{k},\omega)B(\mathbf{k},\omega). \tag{2.3.18}$$

[1] The static limit ($\omega = 0$) of the coefficient ζ_0 describes the current (or vorticity) induced in a fermion gas by a spatially varying time-independent magnetic field. Such a current is not usually considered in theories of the quantum Hall effect, where a uniform magnetic field is assumed, but is known in plasma physics as the Alfvén drift [see J. D. Jackson, *Classical Electrodynamics* (Wiley, New York, 1975), sec. 12.5].

The potential Φ and the magnetic field B contain an external part and a fictitious part, given according to Eqs. (5) and (6) by

$$\Phi = \Phi^{\rm ex} + \delta\Phi^{\rm f} = \Phi^{\rm ex} - \frac{h}{pe^2k^2}\delta\Omega, \tag{2.3.19}$$

$$B = B^{\rm ex} + \delta B^{\rm f} = B^{\rm ex} + \frac{h}{pe}\delta n. \tag{2.3.20}$$

In Eq. (2.3.19) we used the result $\mathbf{a}(\mathbf{k}) = (h/pek^2)\mathrm{i}\mathbf{k}\times\hat{\mathbf{z}}$ for the Fourier transform of the flux tube vector potential. We now solve Eqs. (2.3.17)–(2.3.20) for the case $\Phi^{\rm ex} = 0$, and find

$$\delta\Omega(\mathbf{k},\omega) = -\zeta(\mathbf{k},\omega)B^{\rm ex}(\mathbf{k},\omega), \tag{2.3.21}$$

$$\zeta \equiv \Big[\Big(1-(h/pe^2)\xi_0\Big)\Big(1+(h/pe^2)\eta_0\Big) + (h/pe^2)^2\chi_0\zeta_0\Big]^{-1}\zeta_0. \tag{2.3.22}$$

The Meissner effect is obtained if $\zeta(\mathbf{k},0) > 0$ in the limit $\mathbf{k}\to 0$. We now calculate this limit and show that it is the same as $\lim_{\omega\to 0}\zeta(0,\omega)$, thereby proving the analyticity of the response function.

By direct evaluation of Eq. (2.3.12), for the case of an ideal (impurity-free) two-dimensional electron gas at the filling factor p, one obtains the following relations:

$$\chi_0(0,\omega) = \chi_0(0,0) + \mathcal{O}(\omega^2), \chi_0(\mathbf{k},0) = \chi_0(0,0) + \mathcal{O}(k^2), \tag{2.3.23}$$

$$\xi_0(0,\omega) = \frac{pe^2}{h} + \mathcal{O}(\omega^2), \xi_0(\mathbf{k},0) = \frac{pe^2}{h} + \mathcal{O}(k^2), \tag{2.3.24}$$

$$\eta_0(0,\omega) = -\frac{pe^2}{h} + \mathcal{O}(\omega^2), \eta_0(\mathbf{k},0) = -\frac{pe^2}{h} + \mathcal{O}(k^2), \tag{2.3.25}$$

$$\zeta_0(0,\omega) = \mathcal{O}(\omega^2), \zeta_0(\mathbf{k},0) = \mathcal{O}(k^2). \tag{2.3.26}$$

In Eq. (2.3.23), the constant $\chi_0(0,0)$ is given by

$$\chi_0(0,0) = \frac{mp^2e^2}{n_0h^2}. \tag{2.3.27}$$

Substitution of these relations into Eq. (2.3.22) yields

$$\lim_{\mathbf{k}\to 0}\zeta(\mathbf{k},0) = \lim_{\omega\to 0}\zeta(0,\omega) = \Lambda^{-2}, \tag{2.3.28}$$

$$\Lambda \equiv \frac{h}{pe^2}\left[\chi_0(0,0)\right]^{1/2} = \left(\frac{m}{e^2n_0}\right)^{1/2}. \tag{2.3.29}$$

We conclude that $\zeta(\mathbf{k},\omega)$ is analytic at $(\mathbf{k},\omega) = (0,0)$, so that the anyon gas shows the perfect conductivity and the Meissner effect in accordance with the London equation (2.3.10). This completes our demonstration of superconductivity of the anyon gas in the mean-field approximation.

We conclude this chapter with a discussion of the symmetry of the conductivity tensor, and of the influence of impurities. Since the anyon Hamiltonian (2.2.1) is

not invariant under time reversal, it is possible in principle to have a non-symmetric conductivity tensor. In the foregoing analysis we have seen that although $\boldsymbol{\sigma}_0$ is not a symmetric tensor, the true conductivity $\boldsymbol{\sigma}$ is symmetrical. We believe that the symmetry of $\boldsymbol{\sigma}$, derived here at $T = 0$ in the mean-field approximation, holds also at higher temperatures and particularly in the normal state. A heuristic way to see this is to replace $\boldsymbol{\rho}_0$ by the classical resistivity

$$\begin{aligned}(\boldsymbol{\rho}_0)_{xx} &= (\boldsymbol{\rho}_0)_{yy} = \frac{m}{e^2 n_0 \tau}, \\ (\boldsymbol{\rho}_0)_{xy} &= -(\boldsymbol{\rho}_0)_{yx} = -\frac{h}{pe^2},\end{aligned} \tag{2.3.30}$$

where τ is a relaxation time. Substitution of this expression into Eq. (2.3.7) leads to the Drude conductivity tensor, *i.e.* a symmetrical $\boldsymbol{\sigma}$. The question of the symmetry of $\boldsymbol{\sigma}$ in the normal state is relevant for the recent experimental search by Gijs *et al.*[15] for a spontaneous Hall effect in zero magnetic field. In this experiment a symmetrical conductivity tensor was found within the experimental resolution. In our description of the anyon gas the Hall electric field originating from the fictitious magnetic field is fully compensated by the fictitious electric field induced by the moving flux tubes. An explanation in different terms has recently been put forward by Wiegmann.[8]

The demonstration of superconductivity given above can be generalized to include a uniform distribution of impurities. The key step in this generalization is to show that Eqs. (2.3.23)–(2.3.26) remain valid. This can be shown if the gap in the density of states for the integer quantum Hall effect Hamiltonian $\mathcal{H}_0$ is not closed by the impurities. The presence of the excitation gap then implies that the response coefficients $\chi_0, \xi_0, \eta_0, \zeta_0$ are analytical at $(\mathbf{k}, \omega) = (0, 0)$, and hence Eqs. (2.3.23) and (2.3.26) result. (Whether a *mobility* gap is sufficient for the analyticity is not clear to us.) Eqs. (31) and (32) are enforced by the quantum Hall effect, since $\zeta_0(0,0) = -\eta_0(0,0) = [\sigma_0(0)]_{xy} = pe^2/h$ regardless of the presence of impurities. Note that the impurities will modify the penetration depth $\Lambda = (h/pe^2)[\chi_0(0,0)]^{1/2}$, through their effect on the susceptibility $K_{00} = -k^2\chi_0$.

A Response function in two dimensions

The general form of the linear response for the density n and current density $\mathbf{j}$ in the Fourier space is

$$\delta\mathcal{J}_\mu(\mathbf{k},\omega) = K_{\mu\nu}(\mathbf{k},\omega)\mathcal{A}_\nu(\mathbf{k},\omega), \tag{A.1}$$

where $\mathcal{J} = (en, \mathbf{j}), \mathcal{A} = (\Phi, -\mathbf{A})$, and the response function $K_{\mu\nu}$ is defined in the space-time representation as

$$\begin{aligned} K_{\mu\nu}(\mathbf{r},t;\mathbf{r}',t') &= (\mathrm{i}\hbar)^{-1} < \Psi|\left[\mathcal{J}_\mu(\mathbf{r},t), \mathcal{J}_\nu(\mathbf{r}',t')\right]|\Psi > \theta(t-t') \\ &\quad + \frac{n_0}{m}(1-\delta_{\mu 0})\delta_{\mu\nu}. \end{aligned} \tag{A.2}$$

The matrix $K_{\mu\nu}(\mathbf{k},\omega)$ can be decomposed using the vectors $\mathbf{k}$ and $\hat{\mathbf{z}}\times\mathbf{k}$:

$$K_{00}(\mathbf{k},\omega) = \quad a(\mathbf{k},\omega), \tag{A.3}$$

$$K_{0j}(\mathbf{k},\omega) = \quad b^{(1)}(\mathbf{k},\omega)k_j + b^{(2)}(\mathbf{k},\omega)\epsilon_{jn}k_n, \tag{A.4}$$

$$K_{i0}(\mathbf{k},\omega) = \quad c^{(1)}(\mathbf{k},\omega)k_i + c^{(2)}(\mathbf{k},\omega)\epsilon_{im}k_m, \tag{A.5}$$

$$\begin{aligned} K_{ij}(\mathbf{k},\omega) = \quad & d^{(1)}(\mathbf{k},\omega)k_ik_j + d^{(2)}(\mathbf{k},\omega)\epsilon_{im}k_mk_j + d^{(3)}(\mathbf{k},\omega)k_i\epsilon_{jn}k_n + \\ & d^{(4)}(\mathbf{k},\omega)\epsilon_{im}k_m\epsilon_{jn}k_n, \end{aligned} \tag{A.6}$$

where roman indices denote the carthesian components, and we have used $(\hat{\mathbf{z}}\times\mathbf{k})_i = -\epsilon_{im}k_m$ where ϵ is the antisymmetric tensor of rank two ($\epsilon_{11} = \epsilon_{22} = 0, \epsilon_{12} = -\epsilon_{21} = 1$). In the space-time representation $K_{\mu\nu}$ satisfies the continuity relation $\partial_\mu K_{\mu\nu} = \partial'_\nu K_{\mu\nu} = 0$. The corresponding relation in the Fourier space is

$$\omega K_{0\nu} - k_i K_{i\nu} = \omega K_{\mu 0} - k_j K_{\mu j} = 0. \tag{A.7}$$

Imposing the condition (A.7) on $K_{\mu\nu}$ in Eqs. (A.3)-(A.6) yields the following relations:

$$\frac{k^2}{\omega}b^{(1)} = \frac{k^2}{\omega}c^{(1)} = \frac{k^4}{\omega^2}d^{(1)} = a,\ \frac{k^2}{\omega}d^{(2)} = c^{(2)},\ \frac{k^2}{\omega}d^{(3)} = b^{(2)}. \tag{A.8}$$

We recast Eqs. (A.3)-(A.6) in a simpler form by defining four new coefficients χ, ξ, η, ζ, according to

$$a = -k^2\chi,\ b^{(2)} = \mathrm{i}\xi,\ c^{(2)} = \mathrm{i}\eta,\ d^{(4)} = \frac{1}{k^2}\zeta. \tag{A.9}$$

The resulting equations are

$$K_{00}(\mathbf{k},\omega) = \quad -k^2\chi(\mathbf{k},\omega), \tag{A.10}$$

$$K_{0j}(\mathbf{k},\omega) = \quad -\omega\chi(\mathbf{k},\omega)k_j + \mathrm{i}\xi(\mathbf{k},\omega)\epsilon_{jn}k_n, \tag{A.11}$$

$$K_{i0}(\mathbf{k},\omega) = \quad -\omega\chi(\mathbf{k},\omega)k_i + \mathrm{i}\eta(\mathbf{k},\omega)\epsilon_{im}k_m, \tag{A.12}$$

$$\begin{aligned} K_{ij}(\mathbf{k},\omega) = \quad & -\frac{\omega^2}{k^2}\chi(\mathbf{k},\omega)k_ik_j + \frac{\mathrm{i}\omega}{k^2}\eta(\mathbf{k},\omega)\epsilon_{im}k_mk_j + \frac{\mathrm{i}\omega}{k^2}\xi(\mathbf{k},\omega)k_i\epsilon_{jn}k_n + \\ & \frac{1}{k^2}\zeta(\mathbf{k},\omega)\epsilon_{im}k_m\epsilon_{jn}k_n. \end{aligned} \tag{A.13}$$

Let us now return to Eq. (A.1) and express $\delta n, \delta \mathbf{j}$ in terms of χ, ξ, η, ζ, by substituting Eqs. (A.10)-(A.13). Bearing in mind that $\mathrm{i}\epsilon_{im}k_m A_i(\mathbf{k},\omega) = -B(\mathbf{k},\omega)$ where $B(\mathbf{k},\omega)$ is the magnetic field in the z-direction, and choosing the Coulomb gauge for the vector potential $[k_i A_i(\mathbf{k},\omega) = 0]$, we have

$$e\delta n(\mathbf{k},\omega) = -\chi(\mathbf{k},\omega)k^2\Phi(\mathbf{k},\omega) + \xi(\mathbf{k},\omega)B(\mathbf{k},\omega), \tag{A.14}$$

and

$$\begin{aligned}\delta j_i(\mathbf{k},\omega) = \quad & \omega k_i \chi(\mathbf{k},\omega)\Phi(\mathbf{k},\omega) + \mathrm{i}\epsilon_{im}k_m\eta(\mathbf{k},\omega)\Phi(\mathbf{k},\omega) + \frac{\omega k_i}{k^2}\xi(\mathbf{k},\omega)B(\mathbf{k},\omega) - \\ & \frac{\mathrm{i}\epsilon_{im}k_m}{k^2}\zeta(\mathbf{k},\omega)B(\mathbf{k},\omega).\end{aligned} \tag{A.15}$$

Multiplying Eq. (A.15) by $-\mathrm{i}\epsilon_{im}k_m$ yields

$$\delta\Omega(\mathbf{k},\omega) = \eta(\mathbf{k},\omega)k^2\Phi(\mathbf{k},\omega) - \zeta(\mathbf{k},\omega)B(\mathbf{k},\omega), \tag{A.16}$$

where $\Omega \equiv -\mathrm{i}\epsilon_{im}k_m j_i$ is the vorticity. Eqs. (A.14) and (A.16) completely describe the electromagnetic response of a 2D system to an external electromagnetic field. Note that the only relevant quantities are δn and $\delta\Omega$. The latter is proportional to the component of $\delta\mathbf{j}$ along $\epsilon_{im}k_m$. The component of $\delta\mathbf{j}$ along $\mathbf{k}$ is not an independent variable, as it is constrained by the continuity equation $\mathrm{i}\mathbf{k}\cdot\delta\mathbf{j} = \mathrm{i}\omega\delta n$.

References

[1] F. Wilczek, Phys. Rev. Lett. **49**, 957 (1982).

[2] R.B. Laughlin, Phys. Rev. Lett. **60**, 2677 (1988).

[3] A.L. Fetter, C.B. Hanna, and R.B. Laughlin, Phys. Rev. B **39**, 9679 (1989); C.B. Hanna, R.B. Laughlin, and A.L. Fetter, Phys. Rev. B **40**, 8745 (1989).

[4] Y.H. Chen, F. Wilczek, E. Witten, and B.I. Halperin, Int. J. Mod. Phys. B **3**, 1001 (1989).

[5] X.G. Wen and A. Zee, Phys. Rev. B **41**, 240 (1990).

[6] Y. Hosotani and S. Chakravarty, Phys. Rev. B **42**, 342 (1990).

[7] E. Fradkin, Phys. Rev. B **42**, 570 (1990).

[8] P.B. Wiegmann, Phys. Rev. Lett. **65**, 2070 (1990).

[9] Y.C. Kao and M.F. Yang, Mod. Phys. Lett. B **4**, 1023 (1990).

[10] T. Banks and J.D. Lykken, Nucl. Phys. B **336**, 500 (1990).

[11] L. Zhang, M. Ma, and F.C. Zhang, Phys. Rev. B **42**, 7894 (1990).

[12] A.J. Leggett, *The Mean-Field Anyon Gas: Superconductor or "Superdiamagnetic Insulator"?* (University of Minnesota, preprint No. TPI-MINN-90/36-T).

[13] R. Kubo, M. Toda, and N. Hashitsume, *Statistical Physics II* (Springer, Berlin, 1985), Sec. 4.

[14] G. Rickayzen, *Theory of Superconductivity* (Wiley, New York, 1965), Sec. 2.

[15] M.A.M. Gijs, A. M. Gerrits, and C.W.J. Beenakker, Phys. Rev. B **42**, 10789 (1990).

Chapter 3

Quasi-Landau level structure in the fractional quantum Hall effect

1 Introduction

In contrast to the integer quantum Hall effect (QHE) which is a property of noninteracting electrons, the fractional QHE is a genuine many-body effect caused by strong correlations between electrons. The common feature of the two phenomena is the appearance of an excitation gap responsible for incompressibility of the two-dimensional electron system at certain electron densities. However, whereas in the integer QHE the excitation gap is a result of the Landau-level quantization of the kinetic energy, in the fractional QHE it originates from interactions between electrons in the lowest Landau level.

Nevertheless, almost indistinguishable phenomenologies have motivated the search for a common theoretical framework for understanding both effects [1, 2, 3]. It was pointed out by Jain [1] that the fractional QHE might be thought of as the integer QHE for composite particles consisting of an electron carrying an even number of flux quanta. Starting from the integer QHE at filling factor p, he constructed trial wave functions for the fractional QHE at filling factors $\nu = p/(2kp+1)$. In the same spirit, Greiter and Wilczek [2, 3] proposed an adiabatic mapping for constructing the fractional QHE states. The adiabatic mapping is based on the introduction of a fictitious long-range vector-potential interaction between the electrons. It is suggested that the incompressible states of the integer QHE evolve continuously into the incompressible states of the fractional QHE by adiabatically switching on the vector-potential interaction, *i.e.* by attaching flux quanta to the electrons adiabatically. The adiabatic mapping is exact in principle but cannot be carried out in practice unless suitable approximations are made. One possibility is the *vector-mean-field theory* which treats the vector-potential interaction in mean-field approximation (see chapter 4).

These unifying theories raise the question how the single-particle energy gap of the integer QHE is transformed into the many-body gap of the fractional QHE. In the present paper we argue that a short-range interaction induces a quasi-Landau level structure on the angular momentum dependence of the ground-state energy of

fermions in the lowest Landau level. We believe that this induction is the origin of the incompressibility in the fractional QHE. The argument is based on the adiabatic principle of Greiter and Wilczek, and exact results obtained from small-system calculations. The analysis provides a new understanding of how the excitation gap changes its origin during the adiabatic evolution.

We start the discussion in Sec. 2 by numerically calculating the ground-state energy of a small system. It turns out that for a few electrons in the lowest Landau level with a short-range interaction, the dependence of the ground-state energy on the filling factor ν (or, equivalently, on the angular momentum) in the interval $1 \geq \nu \geq \frac{1}{3}$ is strikingly similar to that of noninteracting electrons in the interval $\nu \geq 1$. This is the *quasi-Landau level structure* referred to above. We will also investigate numerically the seemingly unrelated problem of hard-core bosons in the lowest Landau level. Remarkably, once more a quasi-noninteracting ground-state energy spectrum is found. The connection between the hard-core boson problem on the one hand, and the noninteracting and interacting fermion problems on the other hand, is discussed in terms of the adiabatic principle of Greiter and Wilczek [2, 3], which is reviewed in Sec. 3. The adiabatic principle assumes that the initial single-particle excitation gap does not collapse during the adiabatic evolution, and becomes a many-body gap induced by the electron-electron interaction in the final state. We will show in Sec. 4 that for noninteracting electrons the single-particle gap has vanished by the time a single negative flux quantum has been adiabatically attached to each electron. In order to prevent the complete collapse of the excitation gap, one has to include the scalar-potential interaction between the electrons. We then proceed to analyse the adiabatic mapping near the critical point where each electron is bound to a single negative flux quantum. Since at this point the vector-potential interaction can be gauged away, leaving a gas of noninteracting bosons, the critical point is referred to as the *boson point*.

The main technical result of this paper, presented in Sec. 4 and the Appendix, is that near the boson point the vector-potential interaction between fermions is equivalent to a hard-core repulsion between bosons in the lowest Landau level. More precisely, in the high magnetic field limit, the ground-state energies of the two systems are identical up to and including the first order in a small negative number ε, where each electron carries $1 + \varepsilon$ flux quanta. This equivalence near the boson point of noninteracting electrons and hard-core bosons, together with the fact that the boson point is adiabatically connected to the integer QHE, explains the hard-core-boson to integer QHE correspondence found numerically in Sec. 2. Beyond the boson point, *i.e.* for more than one attached flux quantum, the hard-core interaction vanishes. Nevertheless, the small system results discussed in Sec. 2 suggest the possibility of a smooth transition from hard-core bosons to fermions with a short-range interaction. We have, however, no analytical proof. For completeness, we present in Sec. 5 a short discussion of the relation between edge excitations in integer and fractional QHE. The discussion will be concluded in Sec. 6.

2 Results for small systems

We consider a noninteracting two-dimensional electron gas (2DEG) in the x-y plane, subject to a magnetic field $B\hat{\mathbf{z}}$ with $\hat{\mathbf{z}}$ the unit vector in the z-direction. The Hamiltonian is

$$\mathcal{H}_0 = \sum_i \frac{1}{2m} \left[-\mathrm{i}\hbar\nabla_i + e\mathbf{A}(\mathbf{r}_i)\right]^2, \tag{2.1}$$

where $\mathbf{A}(\mathbf{r})$ is the vector potential associated with $B\hat{\mathbf{z}}\,(=\nabla\times\mathbf{A})$. It is instructive to investigate the behavior of the N-electron ground-state energy as a function of the total angular momentum M. Figure 3.1 shows the ground-state energy E_0 for $N = 5$ and 6 in the interval $\frac{1}{2}N(N-1) \geq M \geq -\frac{1}{2}N(N-1)$. If we define an equivalent filling factor by $\nu = N(N-1)/2|M|$, the above interval corresponds to $\nu \geq 1$. For large N the plateaus in Fig. 3.1 evolve into the sequence of Landau levels associated with quantization of the kinetic energy in the magnetic field.

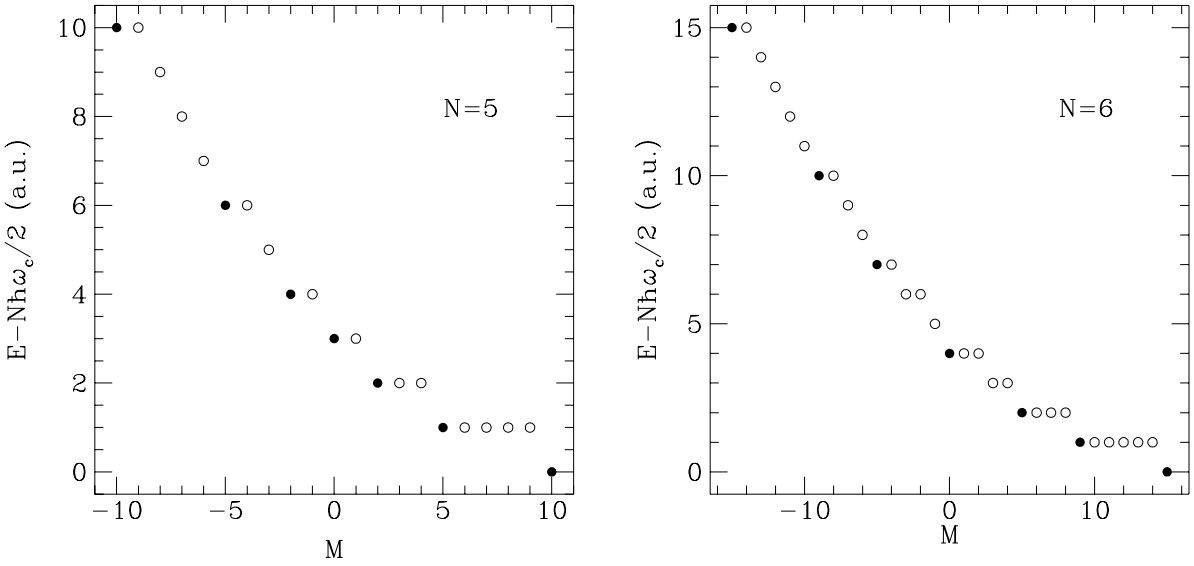

Fig. 3.1. Ground-state energy $E_0 - \frac{1}{2}N\hbar\omega_\mathrm{c}$ of N noninteracting electrons, as a function of total angular momentum M for $N = 5$ and $N = 6$. The angular momentum interval shown corresponds to the filling factors $\nu \geq 1$. Nondegenerate and degenerate states are represented by filled and open symbols, respectively.

Next, consider an interacting 2DEG with the Hamiltonian

$$\mathcal{H} = \mathcal{H}_0 + \mathcal{H}_\mathrm{int},\ \mathcal{H}_\mathrm{int} = \sum_{i<j} u(\mathbf{r}_i - \mathbf{r}_j), \tag{2.2}$$

where $u(\mathbf{r})$ is the electron-electron interaction potential. We are interested in the high magnetic field limit where the interaction part $\mathcal{H}_\mathrm{int}$ can be treated as a perturbation

to the kinetic part $\mathcal{H}_0$. Consider the angular momentum values $\frac{3}{2}N(N-1) \geq M \geq \frac{1}{2}N(N-1)$, corresponding to $1 \geq \nu \geq \frac{1}{3}$. Because all electrons now lie in the lowest Landau level, the unperturbed ground-state energies are degenerate, equal to $E_0 = \frac{1}{2}N\hbar\omega_c$ independent of M. Here $\omega_c = eB/m$ is the cyclotron frequency. We calculate the ground-state energy of the full Hamiltonian $\mathcal{H}$ in first order degenerate perturbation theory. This is equivalent to diagonalizing $\mathcal{H}_{\rm int}$ (or $\mathcal{H}$) in the lowest Landau level. Figure 3.2 shows the results of the degenerate perturbation theory for 5 and 6 electrons with the repulsive hard-core interaction $u(\mathbf{r}) = -\nabla^2\delta(\mathbf{r})$. Comparison with Fig. 3.1 reveals a striking similarity: apart from a shift equal to $N(N-1)$ in M and a different energy scale, the two spectra are almost identical. Note that it is now the electron-electron interaction and not the Landau-level quantization which governs the M-dependence of the ground-state energy. We find that a short-range interaction induces a quasi-Landau level structure on the angular momentum dependence of the ground-state energy of fermions in the lowest Landau level.

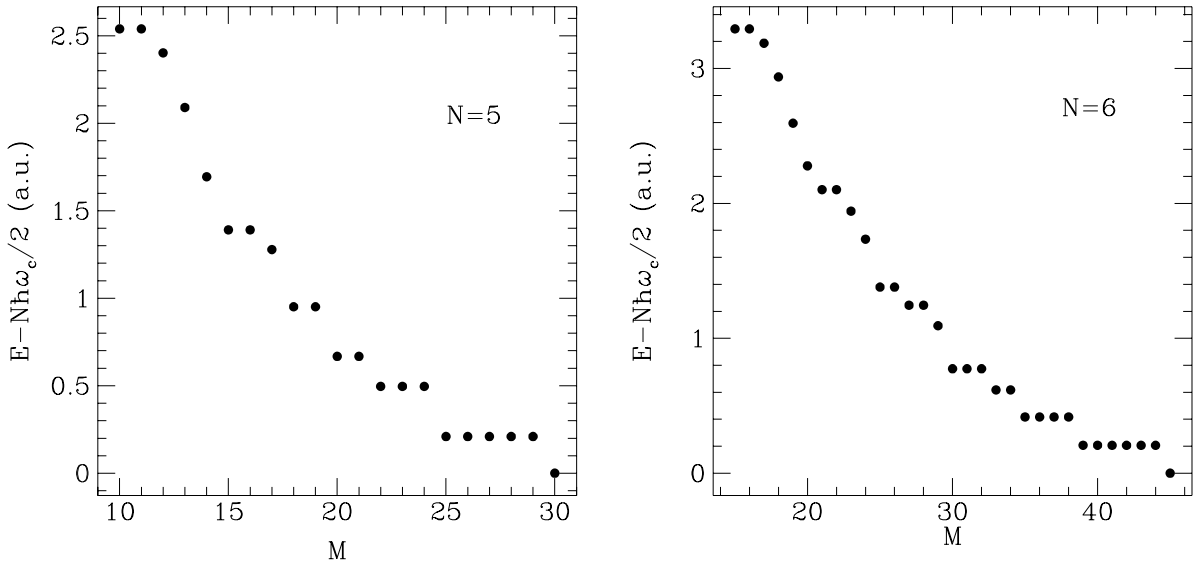

Fig. 3.2. Ground-state energy $E - \frac{1}{2}N\hbar\omega_c$ of N electrons in the lowest Landau level with a $-\nabla^2\delta(\mathbf{r})$ interaction, as a function of total angular momentum M for $N = 5$ and $N = 6$. The angular momentum interval shown corresponds to filling factors $1 \geq \nu \geq \frac{1}{3}$.

Let us now consider the seemingly unrelated problem of interacting bosons in a magnetic field. The Hamiltonian is still given by Eq. (2.2), but now its eigenstates have to be symmetric under particle exchange. We are interested in the angular momentum interval $N(N-1) \geq M \geq 0$. Since there is no restriction on the number of bosons occupying a single state, the condition $M \geq 0$ is satisfied by all boson states lying entirely in the lowest Landau level. Therefore, as in the previous case, the unperturbed ground-state energies are degenerate with the energy $E_0 = \frac{1}{2}N\hbar\omega_c$. Figure 3.3 shows the results of the degenerate perturbation theory for 5 and 6 bosons

with a hard-core repulsion $u(\mathbf{r}) = \delta(\mathbf{r})$. Remarkably enough, once more an almost noninteracting ground-state energy structure emerges from the calculations (compare Fig. 3.3 with Fig. 3.1). These numerical findings formed the motivation for the analytical work prescribed in the next sections; there we shall show that the hard-core boson gas forms the critical point in the transition from noninteracting to interacting fermions.

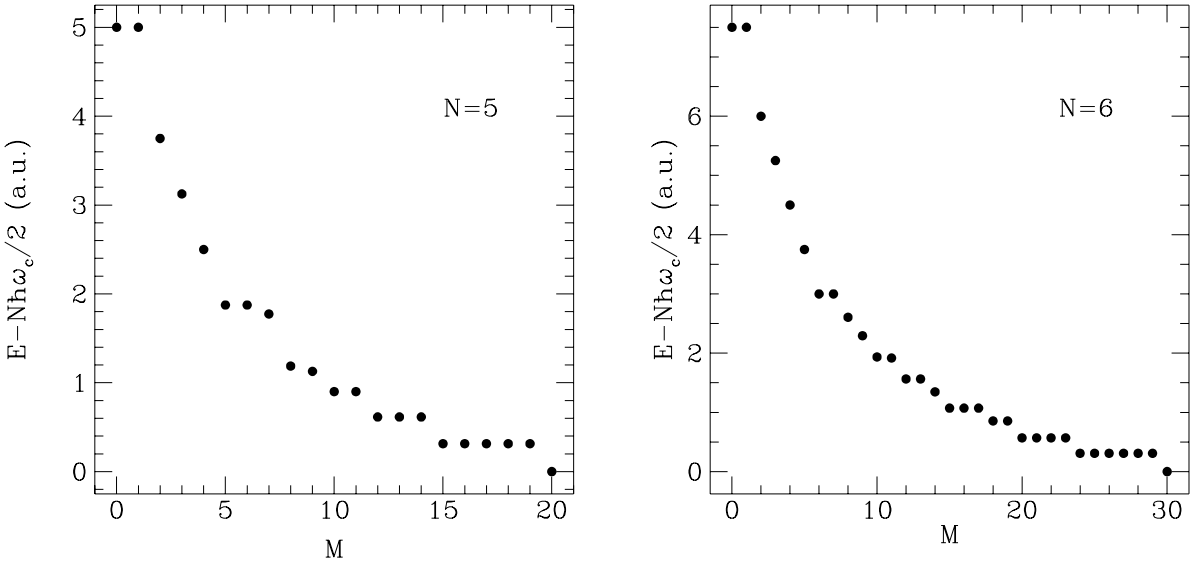

Fig. 3.3. Ground-state energy $E - \frac{1}{2}N\hbar\omega_{\rm c}$ of N bosons in the lowest Landau level with a $\delta(\mathbf{r})$ interaction, as a function of total angular momentum M for $N = 5$ and $N = 6$.

3 Adiabatic principle

Our discussion is based on the adiabatic principle of Greiter and Wilczek [2, 3]. The adiabatic principle is formulated in terms of a new Hamiltonian

$$\begin{aligned}\mathcal{H}(\lambda) &= \mathcal{H}_0(\lambda) + \mathcal{H}_{\rm int},\\ \mathcal{H}_0(\lambda) &= \sum_i \frac{1}{2m}\left[-\mathrm{i}\hbar\nabla_i + e\mathbf{A}(\mathbf{r}_i) - e\lambda\sum_{j(\neq i)}\mathbf{a}(\mathbf{r}_i - \mathbf{r}_j)\right]^2,\end{aligned} \tag{3.1}$$

which contains an extra vector-potential interaction. The vector potential $\mathbf{a}(\mathbf{r})$ is the field of a flux tube of strength h/e in the z-direction, located at the origin:

$$\mathbf{a}(\mathbf{r}) = \frac{h}{e}\,\frac{\hat{\mathbf{z}}\times\mathbf{r}}{2\pi r^2},\ \nabla\times\mathbf{a}(\mathbf{r}) = \frac{h}{e}\,\delta(\mathbf{r})\,\hat{\mathbf{z}}. \tag{3.2}$$

The Hamiltonian $\mathcal{H}(\lambda)$ is thus obtained from $\mathcal{H} = \mathcal{H}(0)$ by binding flux tubes of strength $-\lambda h/e$ to each electron.

One can now define an adiabatic mapping of the set of eigenstates of the original Hamiltonian $\mathcal{H}$ onto itself as follows. Starting from an eigenstate $\Psi \equiv \Psi(0)$ of $\mathcal{H}$, one switches on the vector-potential interaction adiabatically by increasing λ very slowly from 0 to an even positive integer $2k$. The eigenstates and eigenvalues evolve according to

$$\mathcal{H}(\lambda)\Psi(\lambda) = E(\lambda)\Psi(\lambda). \tag{3.3}$$

After $\Psi(0)$ has evolved adiabatically into $\Psi(2k)$, the vector-potential interaction in $\mathcal{H}(2k)$ is eliminated by the unitary gauge transformation

$$\begin{aligned} &\mathcal{H}(2k) \rightarrow \mathcal{G}(2k)\mathcal{H}(2k)\mathcal{G}^{\dagger}(2k) = \mathcal{H}(0), \\ &\Psi(2k) \rightarrow \mathcal{G}(2k)\Psi(2k) = \tilde{\Psi}, \end{aligned} \tag{3.4}$$

where we have defined

$$\mathcal{G}(2k) = \prod_{i<j} \frac{(z_i - z_j)^{2k}}{|z_i - z_j|^{2k}},\ z_i = x_i - \mathrm{i}y_i. \tag{3.5}$$

The initial state Ψ is therefore mapped onto $\tilde{\Psi}$, a new, exact eigenstate of $\mathcal{H}$. Note that, although the transformation $\mathcal{G}(\lambda)$ can be applied for every value of λ, the resulting wave function $\mathcal{G}(\lambda)\Psi(\lambda)$ is single-valued only if λ is an integer. Furthermore, the requirement of antisymmetry restricts λ to even values. In the spirit of Jain's theory of the fractional QHE [1], Greiter and Wilczek [2] propose that the incompressible states in the fractional QHE can be obtained by an adiabatic mapping of the incompressible states in the integer QHE. As an explicit demonstration of this adiabatic principle, they have shown [3] that the $\nu = 1$ integer QHE state is mapped onto the $\nu = \frac{1}{2k+1}$ fractional QHE state, after binding $-2k$ flux quanta to each electron adiabatically.

In this paper we will use the notion of adiabatic mapping to argue that the incompressibility in the fractional QHE can be viewed as the consequence of a quasi-Landau level structure induced by the short-range interaction between the electrons in the lowest Landau level. The analysis is carried out for the initial states with angular momentum in the interval $\frac{1}{2}N(N-1) \geq M \geq -\frac{1}{2}N(N-1)$ corresponding to $\nu \geq 1$. For simplicity, we restrict ourselves to $k = 1$. From the adiabaticity of the process and Eq. (3.4) it follows that the angular momenta and the corresponding filling factors of the final states satisfy $\frac{3}{2}N(N-1) \geq M \geq \frac{1}{2}N(N-1)$ and $1 \geq \nu \geq \frac{1}{3}$, respectively.

4 Adiabatic mapping near the boson point

The adiabatic mapping is a prescription for constructing exact states of the fractional QHE by starting from the states of the integer QHE. Adiabaticity requires that the excitation gap does not collapse during the evolution. Somewhere along

the mapping, the initial kinetic energy gap $\hbar\omega_c$ becomes an interaction-induced gap separating the final fractional QHE state from low-lying excitations. We will argue that this metamorphosis occurs near the point where each electron carries a single flux quantum.

Consider eigenstates Ψ of $\mathcal{H}$ with angular momenta satisfying $\frac{1}{2}N(N-1) \geq M \geq -\frac{1}{2}N(N-1)$. In this interval the behaviour of the ground-state energy is mainly determined by the unperturbed Hamiltonian $\mathcal{H}_0$. The interaction causes a small shift (compared to $\hbar\omega_c$) in the non-degenerate levels, and lifts the degeneracy of the degenerate levels, creating narrow subbands of close energy levels. However, these effects of the interaction are not essential for the incompressibility. Therefore, instead of applying the adiabatic mapping to the eigenstates of the full Hamiltonian $\mathcal{H}$, let us start from unperturbed eigenstates Ψ_0 of $\mathcal{H}_0$. After increasing λ adiabatically from 0 to 1 in the equation

$$\mathcal{H}_0(\lambda)\Psi_0(\lambda) = E_0(\lambda)\Psi_0(\lambda), \tag{4.1}$$

we apply the gauge transformation

$$\begin{aligned} &\mathcal{H}_0(1) \to \mathcal{G}(1)\mathcal{H}_0(1)\mathcal{G}^\dagger(1) = \mathcal{H}_0(0) \equiv \mathcal{H}_0, \\ &\Psi_0(1) \to \mathcal{G}(1)\Psi_0(1) = \Phi_0. \end{aligned} \tag{4.2}$$

Note that the transformed wave function

$$\Phi_0 = \prod_{i<j} \frac{z_i - z_j}{|z_i - z_j|}\Psi_0(1), \tag{4.3}$$

is symmetric under particle exchange. The original system of fermions with the Hamiltonian $\mathcal{H}_0(1)$ is therefore transformed into a system of noninteracting bosons with the Hamiltonian $\mathcal{H}_0(0) \equiv \mathcal{H}_0$. Thus the adiabatic mapping carries noninteracting fermion states in the angular momentum interval $\frac{1}{2}N(N-1) \geq M \geq -\frac{1}{2}N(N-1)$, into noninteracting boson states in the interval $N(N-1) \geq M \geq 0$. However, whereas the ground-state energies of the initial fermion states depend on M as a result of occupation of higher Landau levels, the ground-state energies of the noninteracting boson states are all degenerate, equal to $E_0 = \frac{1}{2}N\hbar\omega_c$ (cf. Sec. 2). Evidently, the kinetic energy gap separating initial fermion ground states has disappeared completely when each electron carries one flux quantum.

We believe that the collapse of the kinetic energy gap occurs precisely at the boson point ($\lambda = 1$). This is certainly true in the special cases where the mapping can be carried out exactly. [1] The implication is that the transition of the kinetic energy gap to the interaction gap for the full Hamiltonian $\mathcal{H}$ takes place at the boson point. One would therefore expect that by analyzing the adiabatic mapping near $\lambda = 1$, the

[1] Cases where the adiabatic mapping can be carried out exactly are the two-body problem in general, and the N-body problem with the initial state given by $\prod_{i<j}(z_i - z_j)\exp(-\sum_i |z_i^2|/4\ell_0^2)$ or $\prod_{i<j}(z_i^* - z_j^*)\exp(-\sum_i |z_i^2|/4\ell_0^2)$. [See Refs. [3] and [4].]

relation between the initial integer QHE states at $\lambda = 0$ and the final fractional QHE states at $\lambda = 2$ might be clarified.

In the rest of this section we present an investigation of the adiabatic mapping near the boson point. Starting once again from eigenstates Ψ_0 of $\mathcal{H}_0$, we increase λ this time from 0 to $1 + \varepsilon$ where ε is a small number. Next we apply the gauge transformation

$$\begin{aligned} &\mathcal{H}_0(1+\varepsilon) \to \mathcal{G}(1)\mathcal{H}_0(1+\varepsilon)\mathcal{G}^\dagger(1) = \mathcal{H}_0(\varepsilon), \\ &\Psi_0(1+\varepsilon) \to \mathcal{G}(1)\Psi_0(1+\varepsilon) = \Phi_0(\varepsilon). \end{aligned} \tag{4.4}$$

The Hamiltonian $\mathcal{H}_0(\varepsilon)$ now describes a system of bosons each carrying a flux tube of strength $-\varepsilon h/e$.

Our central technical result is that up to a similarity transformation, the lowest Landau level projection of $\mathcal{H}_0(\varepsilon)$ for negative ε, is identical to the lowest Landau level projection of another Hamiltonian:

$$\mathcal{H}_{\rm B}(\varepsilon) = \sum_i \frac{1}{2m}\left[-{\rm i}\hbar\nabla_i + e\mathbf{A}(\mathbf{r}_i)\right]^2 - \varepsilon\hbar\omega_{\rm c}\sum_{i<j}\delta(\mathbf{r}_i - \mathbf{r}_j). \tag{4.5}$$

The Hamiltonian $\mathcal{H}_{\rm B}(\varepsilon)$ describes a system of bosons moving in a magnetic field $B\hat{\mathbf{z}}$, with a hard-core repulsion $-\varepsilon\hbar\omega_{\rm c}\delta(\mathbf{r})$ (note that $\varepsilon < 0$). More precisely we have

$$\mathcal{P}T^{-1}(\varepsilon)\mathcal{H}_0(\varepsilon)T(\varepsilon)\mathcal{P} = \mathcal{P}\mathcal{H}_{\rm B}(\varepsilon)\mathcal{P}, \tag{4.6}$$

where $\mathcal{P}$ is the lowest Landau level projection operator and

$$T(\varepsilon) = \prod_{i<j}|z_i - z_j|^{-\varepsilon}. \tag{4.7}$$

The derivation is presented in the Appendix. As discussed in Sec. 2, the ground-state energy spectrum of $\mathcal{H}_{\rm B}(\varepsilon)$ in first order degenerate perturbation theory is identical to the spectrum of the projected Hamiltonian $\mathcal{P}\mathcal{H}_{\rm B}(\varepsilon)\mathcal{P}$. The same holds for $T^{-1}(\varepsilon)\mathcal{H}_0(\varepsilon)T(\varepsilon)$. Since a similarity transformation does not change the eigenvalues, we conclude that

$$E_0(\varepsilon, M) = E_{\rm B}(\varepsilon, M) + \mathcal{O}(\varepsilon^2), \tag{4.8}$$

where $E_0(\varepsilon, M)$ and $E_{\rm B}(\varepsilon, M)$ denote the ground-state energies of $\mathcal{H}_0(\varepsilon)$ and $\mathcal{H}_{\rm B}(\varepsilon)$, respectively, for the angular momentum M.

The above discussion leads us to the following conclusion. As λ is increased from 0 to 1, the ground states of the noninteracting Hamiltonian $\mathcal{H}_0$ are smoothly transformed into the ground states of a system of bosons lying entirely in the lowest Landau level with a repulsive $\delta(\mathbf{r})$ interaction. Conversely, in the lowest Landau level, a hard-core repulsion between bosons is equivalent to a vector-potential interaction between fermions if the number of flux quanta bound to an electron is slightly less than one. In view of the above, one would expect a close correspondence between the initial

noninteracting fermion states and the interacting boson states in the lowest Landau level, since they are connected by an adiabatic mapping. This correspondence should be reflected in the dependence of the ground-state energy on the angular momentum. This is indeed what we observe in Figs. 3.1 and 3.3.

We now return to the similarity which motivated this analysis, *i.e.* the resemblance of the spectrum of noninteracting fermions (Fig. 3.1) to that of fermions with a short-range repulsive interaction (Fig. 3.2). Beyond the boson point ($\lambda \geq 1, \varepsilon \geq 0$), the hard-core repulsion generated by the vector-potential interaction vanishes, as shown in the Appendix. To prevent the collapse of the excitation gap we have to include the ordinary interaction $\mathcal{H}_{\rm int}$, which we did not need for $\lambda < 1$. The similarity between Figs. 3.2 and 3.3 suggests the possibility of a smooth transition from bosons with a $\delta(\mathbf{r})$ interaction to fermions with a $-\nabla^2\delta(\mathbf{r})$ interaction, in such a way that the energy gap does not close. We might consider an interaction potential which varies smoothly from $\delta(\mathbf{r})$ at $\lambda = 1$ (boson point) to $-\nabla^2\delta(\mathbf{r})$ at $\lambda = 2$ (fermion point). An example of such a potential is $u(\mathbf{r}, \varepsilon) = r^{-2|\varepsilon|}\delta(\mathbf{r})$. In the space of lowest Landau level wave functions, $u(\mathbf{r}, \varepsilon)$ interpolates between $\delta(\mathbf{r})$ and $-\nabla^2\delta(\mathbf{r})$ as ε is increased from 0 to 1. Apart from the exactly soluble two-body problem, so far the persistence of the energy gap has only been proven for the $\frac{1}{3}$ state [3].

5 Edge excitations

The numerical and analytical results presented above emphasize the close link between ground-state energy spectra of interacting bosons and fermions in the lowest Landau level on the one hand, and noninteracting fermions on the other hand. A question which arises naturally is whether these ideas can be generalized to excited states as well. For completeness, this question is addressed in Fig. 3.4. Similar results were obtained previously in Refs. [5] and [6].

Figure 3.4a shows the excitation spectrum for 6 bosons with a $\delta(\mathbf{r})$ interaction as a function of the angular momentum M. For 6 electrons with a $-\nabla^2\delta(\mathbf{r})$ interaction, the excitation spectrum is shown in Fig. 3.4b. In both cases one can distinguish a set of low-lying energy levels separated from a band of higher excitations. The low-lying energy levels correspond to the edge states. For every value of M we have also indicated for the noninteracting system, the degeneracy of the ground state adiabatically connected to the states in Fig. 3.4. When the degeneracy is small, we observe that this number is identical to the number of edge states in the interacting system. For higher degeneracies, some of the edge excitations are absorbed into the band of higher excitations, and the one-to-one correspondence breaks down.

6 Conclusions

The numerical results obtained from small-system calculations suggest that a short-range interaction induces a quasi-Landau level structure in the ground-state energy

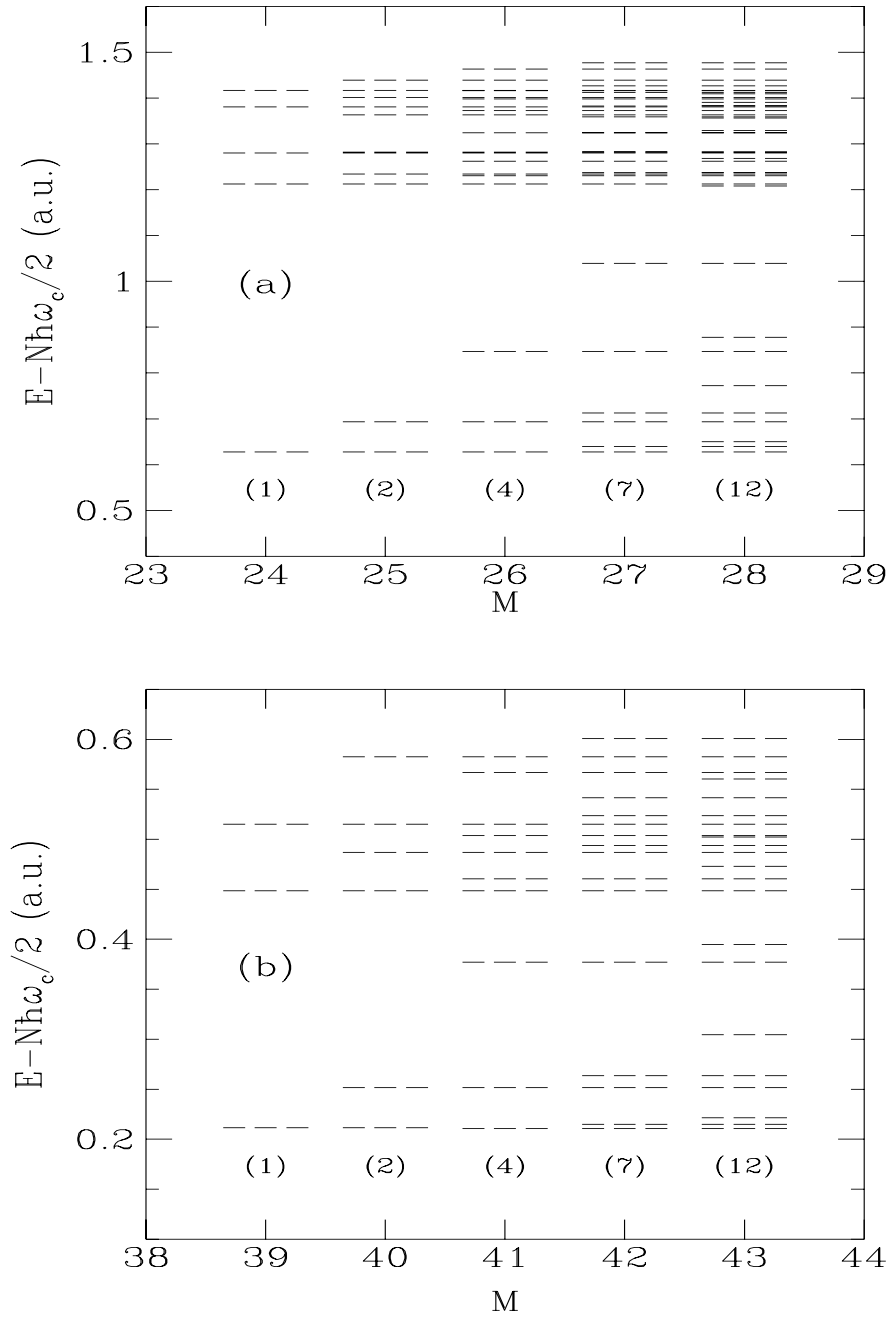

Fig. 3.4. The energy spectrum $E - \frac{1}{2}N\hbar\omega_{\rm c}$ of 6 bosons with a $\delta(\mathbf{r})$ interaction (Fig. 3.4a), and 6 fermions with a $-\nabla^2\delta(\mathbf{r})$ interaction (Fig. 3.4b) in the lowest Landau level, as a function of total angular momentum M. The nearly twofold and threefold degenerate levels are marked by $<$ and $\prec$, respectively. The numbers in the parentheses indicate the degeneracy of the noninteracting ground state, adiabatically connected to the interacting states.

of electrons in the lowest Landau level. We have employed the adiabatic principle of Greiter and Wilczek to explain this correspondence between the integer and fractional QHE.

We have argued that the initial single-particle gap collapses at the point where a single negative flux quantum is attached to each electron. If the number of attached flux quanta is slightly less than one, the vector-potential interaction between electrons becomes equivalent to a hard-core repulsion between bosons in the lowest Landau level. Therefore as the vector-potential interaction is switched on adiabatically, the initial noninteracting ground states are smoothly transformed into the ground states of a hard-core boson gas. This correspondence is verified by exact results for a small number of bosons. It is important to note that the vector-potential interaction is identical to a hard-core repulsion only after a lowest Landau level projection, *i.e.* both interactions have the same pseudo-potential expansion in the lowest Landau level. A gas of bosons with a true hard-core interaction does not show any cusps in the energy spectrum as a result of mixing of higher Landau levels [7], and therefore cannot reproduce the almost noninteracting energy spectrum of Fig. 3.3.

The hard-core boson gas is halfway between the initial noninteracting and the final interacting electron systems. To prevent the collapse of the excitation gap when crossing the boson point, we have to include the ordinary electron-electron interaction. Although we have no general proof, our numerical results suggest that the interacting boson ground states can be smoothly transformed into the final interacting fermion ground states by varying the interaction potential during the adiabatic evolution.

It should be remarked that recent work by Dev and Jain [6] suggests that the correspondence between the integer and fractional QHE states is not restricted to the ground-state energy spectrum. These authors have found that the low-lying excitations in the fractional QHE form well-defined energy bands which correspond to the low-lying excitations of the noninteracting system. The excitations of the fractional QHE are constructed by attaching $2k$ flux quanta ($k = 1, 2, \ldots$) to each electron in the initial noninteracting integer QHE state, *i.e.* by multiplying the initial wave function by $\prod_{i<j}(z_i - z_j)^{2k}$. The equivalence between this approach and that of standard hierarchy theory [8, 9] has recently been shown by Yang and Su [10].

A Vector-potential interaction near the boson point

In this appendix we prove Eq. (4.6), which states that the vector-potential interaction is equivalent to a hard-core repulsion near the boson point, in the space of lowest Landau level wave functions. We will also show that beyond the boson point the hard-core repulsion vanishes, leading to the collapse of the excitation gap.

Consider the Hamiltonian

$$\mathcal{H}_0(\varepsilon) = \sum_i \frac{1}{2m}\left[-\mathrm{i}\hbar\nabla_i + e\mathbf{A}(\mathbf{r}_i) - e\varepsilon \sum_{j(\neq i)} \mathbf{a}(\mathbf{r}_i - \mathbf{r}_j)\right]^2, \tag{A.1}$$

describing a system of bosons with a vector-potential interaction. We are interested in eigenfunctions and eigenvalues of $\mathcal{H}_0(\varepsilon)$ near $\varepsilon = 0$. Following Refs. [11, 12], we construct the model Hamiltonian

$$\mathcal{H}_{\mathrm{M}}(\varepsilon) = \mathcal{H}_0(\varepsilon) + \frac{2\pi\hbar^2\varepsilon}{m}\sum_{i<j}\delta(\mathbf{r}_i - \mathbf{r}_j). \tag{A.2}$$

If an eigenfunction of $\mathcal{H}_{\mathrm{M}}(\varepsilon)$ vanishes upon bringing two particles together, then it has to be an eigenfunction of $\mathcal{H}_0(\varepsilon)$ as well. Therefore by requiring the eigenfunctions to vanish when particles coincide, $\mathcal{H}_{\mathrm{M}}(\varepsilon)$ and $\mathcal{H}_0(\varepsilon)$ become equivalent. Using complex coordinates, $\mathcal{H}_{\mathrm{M}}(\varepsilon)$ is written in the form

$$\mathcal{H}_{\mathrm{M}}(\varepsilon) = \hbar\omega_{\mathrm{c}}\sum_i\left[a_i^\dagger(\varepsilon)a_i(\varepsilon) + \frac{1}{2}\right], \tag{A.3}$$

$$a_i(\varepsilon) \equiv \frac{1}{\sqrt{2}}\left(2\ell_0\frac{\partial}{\partial z_i^*} + \frac{1}{2\ell_0}z_i - \varepsilon\ell_0\sum_{j(\neq i)}\frac{1}{z_i^* - z_j^*}\right),$$

$$a_i^\dagger(\varepsilon) \equiv \frac{1}{\sqrt{2}}\left(-2\ell_0\frac{\partial}{\partial z_i} + \frac{1}{2\ell_0}z_i^* - \varepsilon\ell_0\sum_{j(\neq i)}\frac{1}{z_i - z_j}\right), \tag{A.4}$$

where $\ell_0 = (\hbar/eB)^{1/2}$.

We first consider the case $\varepsilon < 0$. We apply the nonunitary transformation

$$\begin{aligned}&\mathcal{H}_{\mathrm{M}}(\varepsilon) \to T^{-1}(\varepsilon)\mathcal{H}_{\mathrm{M}}(\varepsilon)T(\varepsilon) = \mathcal{H}'_{\mathrm{M}}(\varepsilon),\\ &\Phi(\varepsilon) \to T^{-1}(\varepsilon)\Phi(\varepsilon) = \Phi'(\varepsilon),\end{aligned} \tag{A.5}$$

in which

$$T(\varepsilon) = \prod_{i<j}|z_i - z_j|^{-\varepsilon}. \tag{A.6}$$

If $\Phi'(\varepsilon)$ is not singular, then $\Phi(\varepsilon) = T(\varepsilon)\Phi'(\varepsilon)$ vanishes as two particles approach each other, so that the requirement mentioned above is satisfied. Upon substitution of Eqs. (A.3),(A.4), and (A.6) into Eq. (A.5) one finds

$$\mathcal{H}'_{\mathrm{M}}(\varepsilon) = \hbar\omega_{\mathrm{c}}\sum_i(a_i^\dagger a_i + \frac{1}{2}) - \varepsilon\hbar\omega_{\mathrm{c}}\ell_0\sqrt{2}\sum_{i<j}\frac{a_i^\dagger - a_j^\dagger}{z_i^* - z_j^*}, \tag{A.7}$$

where $a_i^\dagger \equiv a_i^\dagger(0)$ and $a_i \equiv a_i(0)$ are the Landau level raising and lowering operators, respectively.

Our next step is to obtain the lowest Landau level projection $\mathcal{P}\mathcal{H}'_{\rm M}(\varepsilon)\mathcal{P}$ of $\mathcal{H}'_{\rm M}(\varepsilon)$. The space of many-body states is then restricted to wave functions of the form

$$\mathcal{P}\Phi' = f_{\rm S}(z_1,\ldots,z_N)\exp\left(-\sum_{i=1}^{N}|z_i|^2/4\ell_0^2\right), \tag{A.8}$$

where $f_{\rm S}$ is a symmetric polynomial. We find for functions of this form

$$\mathcal{H}'_{\rm M}(\varepsilon)\mathcal{P}\Phi' = \exp\left(-\sum_{i=1}^{N}|z_i|^2/4\ell_0^2\right)\left[\frac{1}{2}N\hbar\omega_{\rm c} - \varepsilon\hbar\omega_{\rm c}\sum_{i<j}S_{ij}\right]f_{\rm S}, \tag{A.9}$$

$$S_{ij} = 1 - 2\ell_0^2\frac{1}{z_i^* - z_j^*}\left(\frac{\partial}{\partial z_i} - \frac{\partial}{\partial z_j}\right). \tag{A.10}$$

The wave function (A.9) does not lie entirely within the lowest Landau level, since the operators S_{ij} introduce higher Landau-level components. To project $S_{ij}f_{\rm S}$ onto the lowest Landau level we proceed as follows. The polynomial $f_{\rm S}$, being symmetric, can always be expanded as

$$f_{\rm S} = \sum_{m,n=0}^{\infty}(z_i - z_j)^{2m}(z_i + z_j)^n\, g_{mn}, \tag{A.11}$$

where g_{mn} are symmetric polynomials in $N-2$ complex variables z_k, $k \neq i,j$. The operator S_{ij} only works on the factor $(z_i - z_j)^{2m}$. The lowest Landau level projection operator in the relative coordinate $\xi = z_i - z_j$ can be written as

$$\mathcal{P}_{ij} = \int {\rm d}\xi' \exp\left(-|\xi'|^2/4\ell_0^2\right)\sum_{k=0}^{\infty}\frac{1}{4\pi\ell_0^2 k!}\left(\frac{\xi\xi'^*}{4\ell_0^2}\right)^k. \tag{A.12}$$

Using the definitions of S_{ij} and $\mathcal{P}_{ij}$ we find

$$\mathcal{P}_{ij}S_{ij}\,(z_i - z_j)^{2m} = \delta_{m,0}\,(z_i - z_j)^{2m}, \tag{A.13}$$

where $\delta_{m,n}$ is the Kronecker delta. Therefore, $\mathcal{P}_{ij}S_{ij}$ projects every symmetric lowest Landau level wave function onto its component with zero relative angular momentum with respect to particles i and j. The lowest Landau level projection of $\mathcal{H}'_{\rm M}(\varepsilon)$ can finally be written as

$$\mathcal{P}\mathcal{H}'_{\rm M}(\varepsilon)\mathcal{P} = \frac{1}{2}N\hbar\omega_{\rm c} - \varepsilon\hbar\omega_{\rm c}\sum_{i<j}\mathcal{P}_{ij}S_{ij}. \tag{A.14}$$

So much for the vector-potential interaction. We now turn to a system of bosons with a hard-core repulsion. The Hamiltonian is

$$\mathcal{H}_{\rm B}(\eta) = \sum_i \frac{1}{2m}\left[-{\rm i}\hbar\nabla_i + e\mathbf{A}(\mathbf{r}_i)\right]^2 + \eta\sum_{i<j}\delta(\mathbf{r}_i - \mathbf{r}_j), \tag{A.15}$$

where $\eta > 0$ determines the strength of the interaction. We need the lowest Landau level projection $\mathcal{P}\mathcal{H}_{\rm B}(\eta)\mathcal{P}$ of $\mathcal{H}_{\rm B}(\eta)$. Therefore, as above, we let $\mathcal{H}_{\rm B}(\eta)$ operate on wave functions of the form (A.8). Projection of the kinetic energy term yields the constant term $\frac{1}{2}N\hbar\omega_{\rm c}$. To project the interaction term we consider the product $\mathcal{P}_{ij}\delta(\mathbf{r}_i - \mathbf{r}_j)\mathcal{P}\Phi'$. The polynomial part of $\mathcal{P}\Phi'$ is once again expanded in powers of $z_i - z_j$ and $z_i + z_j$ as in Eq. (A.11). Using the definition of $\mathcal{P}_{ij}$ we find

$$\mathcal{P}_{ij}\delta(\mathbf{r}_i - \mathbf{r}_j)(z_i - z_j)^{2m} = \frac{1}{4\pi\ell_0^2}\delta_{m,0}(z_i - z_j)^{2m}. \tag{A.16}$$

The projected boson Hamiltonian can finally be written as

$$\mathcal{P}\mathcal{H}_{\rm B}(\eta)\mathcal{P} = \frac{1}{2}N\hbar\omega_{\rm c} + \frac{\eta}{4\pi\ell_0^2}\sum_{i<j}\mathcal{P}_{ij}S_{ij}. \tag{A.17}$$

To prove Eq. (4.6) we equate $\eta = -4\pi\hbar^2\varepsilon/m$. The two operators (A.14) and (A.17) then become identical.

So far we have investigated the model Hamiltonian $\mathcal{H}_{\rm M}$ for negative ε. We now consider positive values of ε. Returning to Eq. (A.3) we apply a new transformation similar to Eq. (A.5) with

$$T(\varepsilon) = \prod_{i<j}|z_i - z_j|^{\varepsilon}. \tag{A.18}$$

The transformed Hamiltonian is

$$\mathcal{H}'_{\rm M}(\varepsilon) = \hbar\omega_{\rm c}\sum_i(a_i^\dagger a_i + \frac{1}{2}) + \varepsilon\hbar\omega_{\rm c}\ell_0\sqrt{2}\sum_{i<j}\frac{a_i - a_j}{z_i - z_j}. \tag{A.19}$$

Obviously, every lowest Landau level wave function of the form (A.8) is an eigenfunction of this Hamiltonian with the energy $\frac{1}{2}N\hbar\omega_{\rm c}$. As a result, the hard-core interaction found for $\varepsilon < 0$ vanishes completely and the energy gap collapses.

References

[1] J.K. Jain, Phys. Rev. Lett. **63**, 199 (1989); Adv. in Phys. **41**, 105 (1992).

[2] M. Greiter and F. Wilczek, Mod. Phys. Lett. B **4**, 1063 (1990).

[3] M. Greiter and F. Wilczek, Nucl. Phys. B **370**, 577 (1992).

[4] G. Dunne, A. Lerda, S. Sciuto, and C.A. Trugenberger, Nucl. Phys. B **370**, 601 (1992).

[5] D.H. Lee and X.G. Wen, Phys. Rev. Lett. **66**, 1765 (1991).

[6] G. Dev and J.K. Jain, Phys. Rev. Lett. **69**, 2843 (1992).

[7] F.C. Zhang, M. Ma, Y. Zhu, and J.K. Jain, Phys. Rev. B **46**, 2632 (1992).

[8] F.D.M. Haldane, Phys. Rev. Lett. **51**, 605 (1983).

[9] B.I. Halperin, Phys. Rev. Lett. **52**, 1583 (1984).

[10] J. Yang and W.P. Su, Phys. Rev. Lett. **68**, 2382 (1992).

[11] S.M. Girvin, A.H. MacDonald, M.P.A. Fisher, S.-J. Rey and J.P. Sethna, Phys. Rev. Lett. **65**, 1671 (1990).

[12] R. Jackiw and S.-Y. Pi, Phys. Rev. Lett. **64**, 2969 (1990).

Chapter 4

Vector-mean-field theory of the fractional quantum Hall effect

1 Introduction

The quantum Hall effect (QHE) is the manifestation of the incompressibility of a two-dimensional electron gas (2DEG) in a strong perpendicular magnetic field. The integer QHE occurs at the integer values of the filling factor $\nu = nh/eB = 2\pi\ell_0^2 n$ where $\ell_0 = (\hbar/eB)^{1/2}$ is the magnetic length and n is the electron density. The integer QHE is essentially a phenomenon of noninteracting electrons: it is a result of the quantization of the kinetic energy of cyclotron orbits. The fractional QHE, on the other hand, requires electron-electron interactions.

The fractional QHE in an unbounded, uniform 2DEG is described accurately by Laughlin's variational wave functions [1]. The theory explains the incompressibility of the ground state at the filling factors $\nu = \frac{1}{2k+1}$ with k integer. Laughlin's wave function is known to be the exact, nondegenerate ground state for repulsive interactions of vanishing range [2, 3]. In the hierarchy scheme [4, 5], other fractional filling factors are obtained by constructing Laughlin states from the quasiparticle and quasihole excitations of the fundamental states.

There is no generalization of Laughlin's variational theory to confined or nonuniform systems. The fact that it is now possible experimentally to study the fractional QHE in a nanostructured 2DEG calls for a mean-field theory which can explain the novel effects occuring in such "mesoscopic" systems. However, early mean-field (Hartree-Fock) calculations failed to explain the incompressibility of the 2DEG at fractional filling factors [6]-[9]. The Hartree-Fock ground-state energy is just a smooth function of the electron density, without any cusps to indicate incompressibility. Somehow the subtle correlations responsible for the incompressibility of the 2DEG at noninteger ν are lost in a conventional mean-field treatment.

In this chapter we propose an alternative mean-field theory based on the adiabatic principle of Greiter and Wilczek [10, 11]. The adiabatic principle is formulated in terms of a fictitious long-range vector potential interaction between the electrons. Motivated by Jain's theory of the fractional QHE [12], Greiter and Wilczek pro-

pose that the incompressible states of the integer QHE evolve continuously into the incompressible states of the fractional QHE by adiabatically switching on the vector-potential interaction, *i.e.* by attaching flux tubes to each electron adiabatically.

The adiabatic mapping is exact in principle, but in practice cannot be carried out without approximations. By treating the vector-potential interaction in mean-field we obtain a "vector-mean-field theory" [13] of the fractional QHE, a name borrowed [14] from anyon superconductivity [15, 16], where the fractional statistics is mediated by a similar vector-potential interaction. In this mean-field approximation the flux tubes attached to the electrons are smeared out, yielding a fictitious magnetic field proportional to the electron density. In addition, a fictitious electric field is generated by the motion of the flux tubes bound to the electrons [17].

Vector-mean-field theory can be readily applied to confined or non-uniform systems. However, as a test we will first show that the theory reproduces the known bulk properties of the correlated fractional QHE states, such as fractional charge and statistics of the quasiparticle excitations, and we will calculate the excitation energies. These bulk properties are also well described by the Chern-Simon field theories of Refs. [18]-[22], although, as far as we are aware, this is the first time that a mean-field theory is used to actually calculate the excitation gap.

We will then focus on a simple confined geometry, a quantum dot with parabolic confinement. For a few electrons in the dot we compare the mean-field theory with an exact diagonalization of the Hamiltonian. We shall see that the mean-field theory reproduces quite well the "magic" filling factors at which the exact ground-state energy shows a cusp. We then turn to the problem of resonant tunneling through a quantum dot in the fractional QHE regime. As discovered by Wen [23] and Kinaret *et al.* [24], the probability for resonant tunneling through the dot is suppressed algebraically as the number of the electrons in the dot is increased (orthogonality catastrophe). Our mean-field theory yields a similar orthogonality catastrophe. This demonstrates that, unlike conventional Hartree-Fock theory, the vector-mean-field theory does not produce a Fermi liquid.

This chapter is organized as follows. In Sec. 2 we review the adiabatic principle of Greiter and Wilczek. Our mean-field approximation is discussed in Sec. 3. In Sec. 4 we apply the vector-mean-field theory to the unbounded, uniform 2DEG. The mean-field equations are solved analytically and closed expressions are found for the ground state energy. We then apply the theory to the quasiparticle excitations. Although the mean-field equations do not allow an analytic solution in this case, the charge and statistics of the quasiparticles can be determined by an asymptotic analysis. We then proceed to numerically calculate the quasiparticle energies and the excitation gap for several filling factors. In Sec. 5 we consider a quantum dot with a parabolic confinement. The results of the mean-field theory are compared with the exact results for a small number N of electrons. We calculate the tunneling probability through the dot and show that it vanishes in the limit $N \to \infty$. We conclude in Sec. 6. Most technical details are relegated to the appendices. The derivation of the mean-field equations is given in App. A. Appendix B contains the solution of the Schrödinger

equation for an electron in a magnetic field with a flux tube at the origin. The solution is used to determine the charge of the quasiparticles in Sec. 4. The mean-field equations in a rotationally symmetric geometry (a quantum dot) are presented in App. C. We give a brief discussion of the numerical method in App. D. Finally, App. E contains the details of the calculation of the probability for tunneling through a quantum dot discussed in Sec. 5.

2 Adiabatic principle

The adiabatic principle of Greiter and Wilczek [10, 11] was reviewed in Sec. 3. For the sake of completeness, we present here a brief discussion. [1] We consider a two-dimensional electron gas in the x-y plane, subject to a magnetic field $B\hat{\mathbf{z}}$ with $\hat{\mathbf{z}}$ the unit vector in the z-direction. The Hamiltonian is

$$\mathcal{H} = \sum_i \frac{1}{2m} \left[-\mathrm{i}\hbar\nabla_i + e\mathbf{A}(\mathbf{r}_i)\right]^2 + \sum_{i<j} u(\mathbf{r}_i - \mathbf{r}_j) + \sum_i V(\mathbf{r}_i), \tag{2.1}$$

where $\mathbf{A}(\mathbf{r})$ is the vector potential associated with $B\hat{\mathbf{z}}$ ($= \nabla \times \mathbf{A}$), $u(\mathbf{r})$ is the electron-electron interaction potential, and $V(\mathbf{r})$ is the electrostatic potential from impurities or an external confinement. The adiabatic principle of Greiter and Wilczek [10, 11] is formulated in terms of a new Hamiltonian

$$\begin{aligned} \mathcal{H}_\lambda = \quad & \sum_i \frac{1}{2m} \left[-\mathrm{i}\hbar\nabla_i + e\mathbf{A}(\mathbf{r}_i) - e\lambda \sum_{j(\neq i)} \mathbf{a}(\mathbf{r}_i - \mathbf{r}_j)\right]^2 + \\ & \sum_{i<j} u(\mathbf{r}_i - \mathbf{r}_j) + \sum_i V(\mathbf{r}_i), \end{aligned} \tag{2.2}$$

which contains an extra vector-potential interaction. The vector potential $\mathbf{a}(\mathbf{r})$ is the field of a flux tube of strength h/e in the z-direction, located at the origin:

$$\begin{aligned} \mathbf{a}(\mathbf{r}) &= \frac{h}{e} \frac{\hat{\mathbf{z}} \times \mathbf{r}}{2\pi r^2}, \\ \nabla \times \mathbf{a}(\mathbf{r}) &= \frac{h}{e}\, \delta(\mathbf{r})\hat{\mathbf{z}}. \end{aligned} \tag{2.3}$$

The Hamiltonian $\mathcal{H}_\lambda$ is thus obtained from $\mathcal{H} = \mathcal{H}_0$ by binding flux tubes of strength $-\lambda h/e$ to each electron (cf. Fig. 1.5).

One can now define an adiabatic mapping of the set of eigenstates of the original Hamiltonian $\mathcal{H} = \mathcal{H}_0$ onto itself as follows. Starting from an eigenstate $\Psi \equiv \Psi_0$ of $\mathcal{H}$, one switches on the vector-potential interaction adiabatically by increasing λ very slowly from 0 to an even positive integer $2k$. The eigenstates and eigenvalues evolve according to

$$\mathcal{H}_\lambda \Psi_\lambda = E_\lambda \Psi_\lambda. \tag{2.4}$$

[1] The notation used here is slightly different from that of chapter 3. The dependence of various operators and functions on the strength of the attached flux λ, is denoted here by subscripts.

After Ψ_0 has evolved adiabatically into Ψ_{2k}, the vector potential interaction in $\mathcal{H}_{2k}$ is eliminated by applying the unitary gauge transformation

$$\begin{aligned} \mathcal{H}_{2k} &\to \mathcal{G}_{2k}\mathcal{H}_{2k}\mathcal{G}_{2k}^{\dagger} = \mathcal{H}_0, \\ \Psi_{2k} &\to \mathcal{G}_{2k}\Psi_{2k} = \tilde{\Psi}, \end{aligned} \tag{2.5}$$

where we have defined

$$\mathcal{G}_{2k} = \prod_{i<j} \frac{(z_i - z_j)^{2k}}{|z_i - z_j|^{2k}}. \tag{2.6}$$

Here $z_i = x_i - \mathrm{i}y_i$ is the complex-plane representation of $\mathbf{r}_i$. The initial state Ψ is therefore mapped onto $\tilde{\Psi} = \mathcal{G}_{2k}\Psi_{2k}$, a new, exact eigenstate of $\mathcal{H}$. The adiabatic principle of Greiter and Wilczek says that the incompressible states of the fractional QHE can be obtained by an adiabatic mapping of the incompressible states of the integer QHE.

The adiabatic mapping is a prescription for constructing exact states of the fractional QHE by starting from the states of integer QHE. However, with the exception of several special cases, the adiabatic mapping cannot be carried out in practice unless suitable approximations are made. In the next section we introduce the *vector-mean-field theory* of the fractional QHE [13], which is based on a mean-field approximation of the adiabatic mapping.

3 Vector-mean-field theory

The mean-field approximation to the adiabatic mapping is suggested by the vector-mean-field theory of anyon superconductivity [14]-[16]. In this approximation the flux tubes are smeared out, yielding a fictitious magnetic field $\mathbf{B}^{\mathrm{f}}$ proportional to the electron density. In addition, a fictitious electric field $\mathbf{E}^{\mathrm{f}}$ is generated by the motion of the flux tubes bound to the electrons [17]. Formally, the mean-field equations are obtained by approximating the eigenstates Ψ_λ of the many-body Hamiltonian (2.2) by a Slater determinant:

$$\Psi_\lambda^{\mathrm{MF}} = \frac{1}{\sqrt{N!}} \sum_\sigma \mathrm{sgn}(\sigma)\, \phi_{\lambda,\sigma(1)}(\mathbf{r}_1) \cdots \phi_{\lambda,\sigma(N)}(\mathbf{r}_N). \tag{3.1}$$

Here N is the number of electrons, σ denotes a permutation with sign $\mathrm{sgn}(\sigma)$, and $\phi_{\lambda,i}$, $i = 1, \ldots, N$ are single-particle wave functions. The mean-field (Hartree) equations are obtained by minimizing the energy functional $E_\lambda^{\mathrm{MF}} = \langle \Psi_\lambda^{\mathrm{MF}} | \mathcal{H}_\lambda | \Psi_\lambda^{\mathrm{MF}} \rangle$, with neglect of exchange terms. The details of the derivation are presented in App. A. The single-particle mean-field Hamiltonian is

$$\mathcal{H}_\lambda^{\mathrm{MF}} = \frac{1}{2m} \left[-\mathrm{i}\hbar\nabla + e\mathbf{A}(\mathbf{r}) - e\lambda\mathbf{A}^{\mathrm{f}}(\mathbf{r}) \right]^2 + e\lambda\Phi^{\mathrm{f}}(\mathbf{r}) + U(\mathbf{r}) + V(\mathbf{r}), \tag{3.2}$$

where the fictitious potentials $\mathbf{A}^{\mathrm{f}}$ and Φ^{f} are given by

$$\mathbf{A}^{\mathrm{f}}(\mathbf{r}) = \int d\mathbf{r}'\, \mathbf{a}(\mathbf{r}-\mathbf{r}')n(\mathbf{r}'), \tag{3.3}$$

$$\Phi^{\mathrm{f}}(\mathbf{r}) = \int d\mathbf{r}'\, \mathbf{a}(\mathbf{r}-\mathbf{r}')\cdot\mathbf{j}(\mathbf{r}'), \tag{3.4}$$

and the ordinary Hartree potential is given by

$$U(\mathbf{r}) = \int d\mathbf{r}'\, u(\mathbf{r}-\mathbf{r}')n(\mathbf{r}'). \tag{3.5}$$

The electron density $n(\mathbf{r})$ and current density $\mathbf{j}(\mathbf{r})$ are

$$n(\mathbf{r}) = \sum_{i=1}^{N} \phi^*_{\lambda,i}(\mathbf{r})\phi_{\lambda,i}(\mathbf{r}), \tag{3.6}$$

$$\mathbf{j}(\mathbf{r}) = \frac{1}{m}\mathrm{Im}\sum_{i=1}^{N} \phi^*_{\lambda,i}(\mathbf{r})\left[-\mathrm{i}\hbar\nabla + e\mathbf{A}(\mathbf{r}) - e\lambda\mathbf{A}^{\mathrm{f}}(\mathbf{r})\right]\phi_{\lambda,i}(\mathbf{r}). \tag{3.7}$$

The wave functions $\phi_{\lambda,i}$ satisfy the eigenvalue equation

$$\mathcal{H}^{\mathrm{MF}}_{\lambda}\phi_{\lambda,i} = \epsilon_{\lambda,i}\,\phi_{\lambda,i}. \tag{3.8}$$

The mapping is now carried out by starting from an initial set of self-consistent single-particle eigenstates $\phi_{0,i}$ of $\mathcal{H}^{\mathrm{MF}}_0$, and increasing λ from 0 to $2k$ adiabatically. The single-particle eigenstates $\phi_{\lambda,i}$ and eigenvalues $\varepsilon_{\lambda,i}$ evolve according to Eq. (3.8). A further simplification results if the potential $u(\mathbf{r})$ is also switched on adiabatically by replacing it with $(\lambda/2k)u(\mathbf{r})$. Then, $\mathcal{H}^{\mathrm{MF}}_0$ describes a system of noninteracting electrons, so that the initial single-particle states $\phi_{0,i}$ can be determined exactly. After reaching $\lambda = 2k$, we apply the gauge transformation (2.5) to the Slater determinant (3.1), and find the final state

$$\tilde{\Psi}^{\mathrm{MF}} = \frac{1}{\sqrt{N!}}\prod_{i<j}\frac{(z_i-z_j)^{2k}}{|z_i-z_j|^{2k}}\sum_{\sigma}\mathrm{sgn}(\sigma)\,\phi_{2k,\sigma(1)}(\mathbf{r}_1)\cdots\phi_{2k,\sigma(N)}(\mathbf{r}_N). \tag{3.9}$$

In general, the wave function (3.9) does not lie entirely in the lowest Landau level. In order to dispose of the higher Landau level components in the high magnetic field limit ($B\to\infty$), one might consider a projection of $\tilde{\Psi}^{\mathrm{MF}}$ onto the lowest Landau level. This, however, makes the theory less tractable: a lowest Landau level projection is not straightforward at all because of the gauge transformation (2.5). In what follows, we will use unprojected wave functions to compute the electron density $n(\mathbf{r})$ and the pair distribution function

$$P(\mathbf{r}_1,\mathbf{r}_2) = N(N-1)\int d\mathbf{r}_3\cdots d\mathbf{r}_N \left|\tilde{\Psi}^{\mathrm{MF}}(\mathbf{r}_1,\mathbf{r}_2,\mathbf{r}_3,\cdots,\mathbf{r}_N)\right|^2, \tag{3.10}$$

but we evaluate the kinetic energy within the lowest Landau level. The energy of the final state then becomes $E^{\rm MF} = \frac{1}{2}N\hbar\omega_{\rm c} + \int d\mathbf{r}\, n(\mathbf{r})V(\mathbf{r}) + E_{\rm ee}$ where the electron-electron interaction energy $E_{\rm ee}$ is

$$E_{\rm ee} = \frac{1}{2}\int d\mathbf{r}_1 d\mathbf{r}_2\, P(\mathbf{r}_1,\mathbf{r}_2)u(\mathbf{r}_1-\mathbf{r}_2), \tag{3.11}$$

and $\omega_{\rm c} = eB/m$ is the cyclotron frequency. In order to express $P(\mathbf{r}_1,\mathbf{r}_2)$ in terms of single-particle wave functions, we substitute Eq. (3.9) into Eq. (3.10), and use the unitarity of the gauge transformation (2.5). The resulting pair distribution function is

$$P(\mathbf{r}_1,\mathbf{r}_2) = n(\mathbf{r}_1)n(\mathbf{r}_2) - |D(\mathbf{r}_1,\mathbf{r}_2)|^2\,, \tag{3.12}$$

$$D(\mathbf{r}_1,\mathbf{r}_2) = \sum_{i=1}^{N}\phi_{2k,i}(\mathbf{r}_1)\phi^*_{2k,i}(\mathbf{r}_2). \tag{3.13}$$

4 Application to unbounded systems

In this section we apply the vector-mean-field theory to the fractional QHE in an unbounded homogeneous system, and compare the results obtained with those in the literature. We shall show that the mean-field Eqs. (3.2)-(3.8) can be solved analytically in this case. The solution is presented in Sec. 4.1. To determine whether the mean-field ground-state shows the fractional QHE, we will study its excitations in Sec. 4.2. We shall see that the adiabatic mapping in its simplest formulation only generates filling factors $\nu < \frac{1}{2}$. In Sec. 4.3 we generalize the adiabatic principle to ground states with $\nu > \frac{1}{2}$.

4.1 Ground state

Starting from a noninteracting integer QHE state consisting of p filled Landau levels, the adiabatic mapping is carried out by switching on both scalar- and vector-potential interactions in the Hamiltonian (3.2). The solution is particularly simple if $u(\mathbf{r})$ is the Coulomb potential e^2/r, and $V(\mathbf{r})$ is the potential of a neutralizing background of positive charges with density $\rho = n$. In this case, the electron density remains uniform, and the current density vanishes during the adiabatic evolution. This leads to a uniform fictitious magnetic field $\mathbf{B}^{\rm f} = \nabla\times\mathbf{A}^{\rm f} = (h/e)n\,\hat{\mathbf{z}}$ and a vanishing fictitious potential $\Phi^{\rm f}(\mathbf{r}) \equiv 0$.

The total single-particle potential $U(\mathbf{r})+V(\mathbf{r})$ is now just a constant, and does not affect the eigenfunctions $\phi_{\lambda,i}(\mathbf{r})$ of $\mathcal{H}^{\rm MF}_\lambda$. Therefore, $\mathcal{H}^{\rm MF}_\lambda$ describes particles moving in a uniform, effective magnetic field

$$B^{\rm eff} = B - \frac{\lambda h}{e}n. \tag{4.1}$$

Since the mapping is adiabatic, no transitions occur between different Landau levels during the evolution: we retain p fully filled Landau levels, but now in the effective magnetic field $B^{\rm eff}$. Equating $B^{\rm eff} = hn/ep$, we find

$$n = \frac{p}{\lambda p + 1}\,\frac{eB}{h}, \tag{4.2}$$

$$B^{\rm eff} = \frac{1}{\lambda p + 1}\,B. \tag{4.3}$$

After letting $\lambda \to 2k$, one recovers Jain's formula [12] for the hierarchy of fractional QHE filling factors

$$\nu = \frac{hn}{eB} = \frac{p}{2kp+1}. \tag{4.4}$$

Substituting $p = 1$, $k = 1, 2, 3, \ldots$, one obtains the fundamental filling factors $\nu = \frac{1}{3}, \frac{1}{5}, \frac{1}{7}, \ldots$. Other filling factors can be obtained by starting from more than one filled Landau levels. For instance for $p = 2, k = 1, 2, 3, \ldots$, we get $\nu = \frac{2}{5}, \frac{2}{9}, \frac{2}{13}, \ldots$. Note that the filling factors obtained from Eq. (4.4) are restricted to $\nu < \frac{1}{2}$. In Sec. 4.3 we generalize the adiabatic mapping to filling factors $\nu > \frac{1}{2}$.

In order to calculate the interaction energy in the final state we need the pair distribution function defined in terms of the eigenfunctions of $\mathcal{H}^{\rm MF}_{2k}$ in Eq. (3.12). In the symmetric gauge $\mathbf{A} = \frac{1}{2}B\hat{\mathbf{z}} \times \mathbf{r}$, the eigenfunctions of $\mathcal{H}^{\rm MF}_{\lambda}$ for the quantum numbers $l, m = 0, 1, 2, \ldots$ are

$$\phi_{\lambda,l,m} = \frac{(l!)^{1/2}}{(2\pi m!)^{1/2}\ell_{\rm eff}}\,\xi^{m-l}\,L_l^{m-l}(|\xi^2|)\,\exp\left(-\frac{|\xi|^2}{2}\right), \tag{4.5}$$

where $\ell_{\rm eff} = (\hbar/eB^{\rm eff})^{1/2}$ is the effective magnetic length, $\xi = z/(\ell_{\rm eff}\sqrt{2})$, and L_l^{m-l} is the generalized Laguerre polynomial. Substituting Eq. (4.5) into Eq. (3.13), we find after some algebra

$$\begin{aligned} D(\mathbf{r}_1, \mathbf{r}_2) =& \sum_{l=0}^{p-1}\sum_{m=0}^{\infty} \phi_{2k,l,m}(\mathbf{r}_1)\phi^*_{2k,l,m}(\mathbf{r}_2) \\ =& \frac{1}{2\pi\ell^2_{\rm eff}} \sum_{l=0}^{p-1} L_l\left(\frac{|z_1 - z_2|^2}{2\ell^2_{\rm eff}}\right) \exp\left[-\frac{1}{4\ell^2_{\rm eff}}(|z_1|^2 + |z_2|^2 - 2z_1 z_2^*)\right], \end{aligned} \tag{4.6}$$

where $L_l \equiv L_l^0$ is the Laguerre polynomial. After substitution of Eqs. (4.2) and (4.6) into Eq. (3.12), the pair distribution function becomes

$$(2\pi\ell^2_{\rm eff})^2\,P(\mathbf{r}_1, \mathbf{r}_2) = p^2 - \left[\sum_{l=0}^{p-1} L_l\left(\frac{|\mathbf{r}_{12}|^2}{2\ell^2_{\rm eff}}\right)\right]^2 \exp\left(-\frac{|\mathbf{r}_{12}|^2}{2\ell^2_{\rm eff}}\right), \tag{4.7}$$

with $\mathbf{r}_{12} = \mathbf{r}_1 - \mathbf{r}_2$. The total Coulomb energy of the system (including the interaction with the positive charges) is given by

$$E_{\rm c} = E_{\rm ee} - \int d\mathbf{r}_1 d\mathbf{r}_2\,\frac{e^2\rho n}{|\mathbf{r}_1 - \mathbf{r}_2|} + \frac{1}{2}\int d\mathbf{r}_1 d\mathbf{r}_2\,\frac{e^2\rho^2}{|\mathbf{r}_1 - \mathbf{r}_2|}. \tag{4.8}$$

The constant third term represents the electrostatic energy of the positive charges. Substitution of Eqs. (3.11) and (3.12) into Eq. (4.8) yields

$$E_{\rm c} = -\frac{1}{2}\int d\mathbf{r}_1 d\mathbf{r}_2 \, \frac{e^2|D(\mathbf{r}_1,\mathbf{r}_2)|^2}{|\mathbf{r}_1-\mathbf{r}_2|}. \tag{4.9}$$

After substitution of Eq. (4.6) and carrying out the integral, we end up with the mean-field Coulomb energy per electron

$$\frac{E_{\rm c}}{N} = -\left(\frac{e^2}{\ell_{\rm eff}}\right)\frac{(\pi)^{1/2}}{2^{3/2}p}\sum_{i,j=0}^{p-1}\binom{p}{i+1}\binom{p}{j+1}\frac{(-1)^{i+j}(2i+2j)!}{4^{i+j}i!j!(i+j)!}. \tag{4.10}$$

In Fig. 4.1 we have plotted $E_{\rm c}/N$ from Eq. (4.10) for the first levels of the hierarchy given by Eq. (4.4). For comparison, we have also plotted the results of exact finite system calculations, represented by the interpolation formula of Ref. [25]:

$$E_{\rm c}/N = -(\pi/8)^{1/2}\nu + a_3\,\nu^{1/2}(1-\nu)^{3/2} + a_4\,\nu(1-\nu)^2 + a_5\,\nu^{3/2}(1-\nu)^{5/2}, \tag{4.11}$$

where $a_3 = -0.782133$, $a_4 = 0.683$, and $a_5 = -0.806$. On the average, the mean-field values are too large by about 10%.

An interesting feature of Fig. 4.1 is that the mean-field correlation energy per particle has a negative second derivative with respect to ν in the regions between the fundamental filling factors $1, \frac{1}{3}, \frac{1}{5}$, etc. This implies that the chemical potential

$$\mu = \frac{\partial E^{\rm MF}}{\partial N} \tag{4.12}$$

decreases with increasing filling factor, and the compressibility

$$\kappa = \left(n^2\frac{\partial\mu}{\partial n}\right)^{-1} \tag{4.13}$$

becomes negative. The latter, however, does not imply an instability of the system [26]: the presence of the rigid background of positive charge density prevents the collapse of the electron gas.

4.2 Quasiparticles and quasiholes

The fractional QHE is characterized by an energy gap $E_{\rm g} = \epsilon_+ + \epsilon_-$, where ϵ_- and ϵ_+ are the quasiparticle and quasihole creation energies, respectively. The energy gap is required for the incompressibility of the ground state. The quasiparticles and quasiholes in the fractional QHE are unusual in having fractional charge and statistics [27, 28]. In this section we show that the vector-mean-field theory reproduces the fractional charge and statistics of the quasiparticles and quasiholes, and yields a non-zero energy gap $E_{\rm g}$.

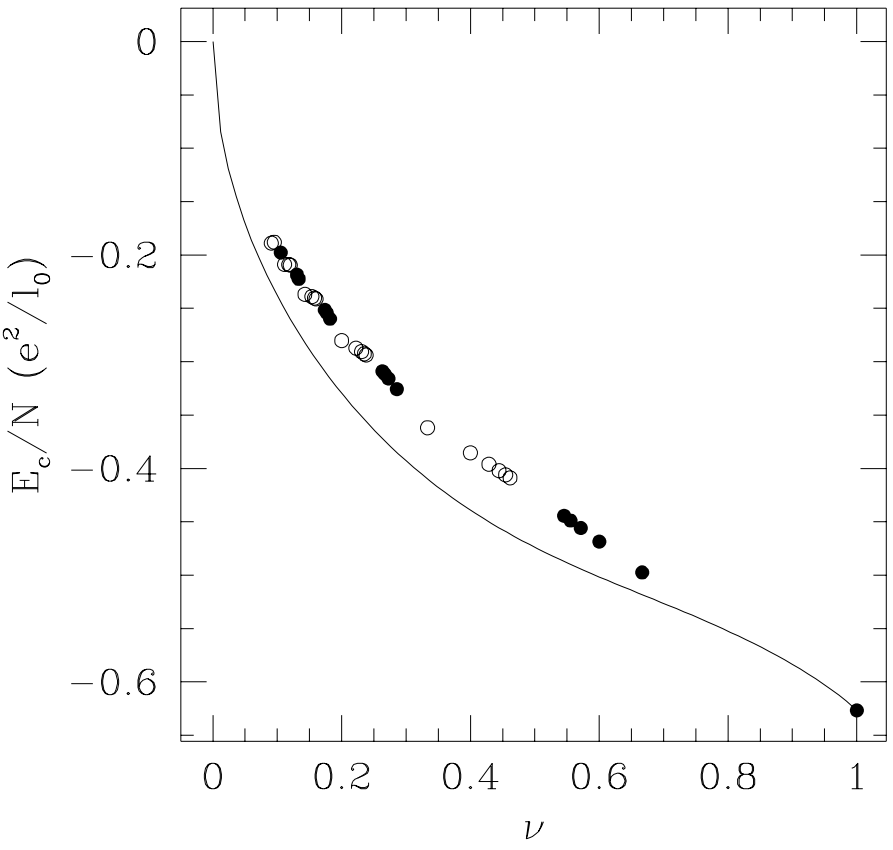

Fig. 4.1. Mean-field Coulomb energy per electron E_c/N in units of e^2/ℓ_0 as a function of the filling factor ν. Open circles represent the filling factors given by the hierarchy formula (4.4). The filling factors given by the hierarchy formula (4.37) are shown as filled circles. The solid line represents the interpolation formula of Ref. [25], which is based on exact finite system calculations.

Originally, the adiabatic principle has been formulated as a statement relating the incompressible integer and fractional QHE ground states [10, 11]. Here we apply the same principle to the excitations. We assume that the adiabatic mapping carries the lowest particle and hole excitations of the integer QHE into the quasiparticle and quasihole excitations of the fractional QHE. The lowest charged excitations of the integer QHE at filling factor p have an electron in the $(p+1)$-th Landau level or a hole in the p-th Landau level. Although the self-consistent mean-field equations do not allow an analytic solution for the excited state, it is possible to find an asymptotic solution at large distances from a quasiparticle or quasihole. As we shall see below, this solution is sufficient to calculate the charge of the excitations. Using a semi-classical argument, we next determine the statistics of the excitations. Calculation of the excitation energies requires the full (numerical) solution to the self-consistent mean-field equations. We shall present a short discussion of the method of solution and compare the results obtained with those in the literature.

Charge

Consider an integer QHE excited state consisting of p filled Landau levels plus an extra electron in the $(p+1)$-th Landau level near the origin. To carry out the mapping, we switch on the vector-potential interaction by increasing λ from 0 to $2k$ adiabatically. In contrast to the uniform case, the effective magnetic field $B^{\rm eff}(\mathbf{r}) = B-(\lambda h/e)n(\mathbf{r})$ is now inhomogeneous, varying rapidly near the origin where we have an excess density due to the extra electron. The excess density, however, decays exponentially fast so that, far away from the origin, the electron density and the effective magnetic field become uniform. Hence, for $r \to \infty$ Eqs. (4.2) and (4.3) are valid again:

$$n_\infty \equiv \lim_{r\to\infty} n(\mathbf{r}) = \frac{p}{\lambda p+1}\,\frac{eB}{h}, \tag{4.14}$$

$$B^{\rm eff}_\infty \equiv \lim_{r\to\infty} B^{\rm eff}(\mathbf{r}) = \frac{1}{\lambda p+1}\,B. \tag{4.15}$$

Using Eqs. (3.3) and (4.14), the total vector potential can be written identically as

$$\mathbf{A}(\mathbf{r}) - \lambda\mathbf{A}^{\rm f}(\mathbf{r}) = \mathbf{A}^{\rm eff}_\infty(\mathbf{r}) - \lambda\int d\mathbf{r}'\,\mathbf{a}(\mathbf{r}-\mathbf{r}')\,[n(\mathbf{r}')-n_\infty]\,, \tag{4.16}$$

where we have defined

$$\mathbf{A}^{\rm eff}_\infty(\mathbf{r}) = \frac{1}{2}B^{\rm eff}_\infty\,\hat{\mathbf{z}}\times\mathbf{r}. \tag{4.17}$$

The second term on the right hand side of Eq. (4.16) is an additional fictitious vector potential induced by the excitation. Since the excess density $n(\mathbf{r})-n_\infty$ is localized near the origin, we have as $r\to\infty$,

$$\int d\mathbf{r}'\,\mathbf{a}(\mathbf{r}-\mathbf{r}')\,[n(\mathbf{r}')-n_\infty] \to \frac{e^*}{e}\,\mathbf{a}(\mathbf{r}), \tag{4.18}$$

where

$$-e^* \equiv -e \int d\mathbf{r}\ [n(\mathbf{r}) - n_\infty]\,, \tag{4.19}$$

is by definition the charge of the quasiparticle ($e > 0$). Hence, in addition to a uniform effective magnetic field $B_\infty^{\rm eff}$, the electrons far away from the origin see a flux tube with the strength $\Phi = -\lambda h e^*/e^2$, localized near $\mathbf{r} = 0$.

We can now write down the eigenfunctions $\phi^-_{\lambda,l,m}$ of the mean-field Hamiltonian (3.2) in the limit of large r (see App. B):

$$\phi^-_{\lambda,l,m} = \frac{(l!)^{1/2}|\xi|^\delta\, \xi^{m-l}}{[2\pi\Gamma(m+\delta+1)]^{1/2}\ell_{\rm eff}}\, L_l^{m+\delta-l}(|\xi|^2) \exp\left(-\frac{|\xi|^2}{2}\right), \tag{4.20}$$

where $\delta = -e\Phi/h = \lambda e^*/e$, $\ell_{\rm eff} = (\hbar/eB_\infty^{\rm eff})^{1/2}$, and $\xi = z/(\ell_{\rm eff}\sqrt{2})$.

Compared to the single-particle wave functions (4.5) of the uniform ground state, the wave functions (4.20) are shifted towards the boundary: the average area enclosed by each single-particle state is increased by an amount of

$$\langle \phi^-_{\lambda,l,m}|\pi r^2|\phi^-_{\lambda,l,m}\rangle - \langle \phi_{\lambda,l,m}|\pi r^2|\phi_{\lambda,l,m}\rangle = 2\pi\ell_{\rm eff}^2\delta, \tag{4.21}$$

where we have used the results of App. B. Therefore, part of the charge $-e$ of the initially added electron is screened by the uniform electron gas filling p Landau levels. The charge of the screening hole is given by $2\pi\ell_{\rm eff}^2 n_\infty \delta e = p\delta e$, where Eqs. (4.14) and (4.21) have been used. The net charge of the quasiparticle therefore equals $-e^* = -e + p\delta e$. Equating $\delta = \lambda e^*/e$ and taking the limit $\lambda \to 2k$, we finally obtain the quasiparticle charge $-e^*$ with

$$e^* = \frac{1}{2kp+1}\, e. \tag{4.22}$$

A similar analysis yields the quasihole charge $+e^*$. Since the total charge in the system is preserved, the difference $e - e^*$ is in fact transferred to the boundary. For $k = 1$, $p = 1, 2$ we recover the well known results $e^* = \frac{1}{3}e, e^* = \frac{1}{5}e$ for the $\frac{1}{3}$ and $\frac{2}{5}$ states, respectively [27, 28].

Statistics

In a quantum mechanical many-body system, the statistical angle is defined as the extra phase θ that the wave function acquires, as one particle traverses a path enclosing another particle in the clockwise direction. In two dimensions there is no limitation on the value of θ. In particular we have $\theta = 0(\mathrm{mod}4\pi)$ for bosons and $\theta = 2\pi(\mathrm{mod}4\pi)$ for fermions. Any other value of θ corresponds to particles obeying fractional statistics (anyons).

It is a fundamental result of Laughlin's theory that the charged excitations of the fractional QHE states are anyons [29]. For the fundamental filling factors $\nu = \frac{1}{2k+1}$,

the corresponding statistical angle is $\theta = (2k+1)^{-1}2\pi(\mathrm{mod}4\pi)$. In this section we show how the vector-mean-field theory reproduces this result.

In the previous section we showed that the mean-field theory reproduces the fractional charge e^* of the excitations. In the final state of the adiabatic mapping, each electron carries $-2k$ flux quanta so that the total flux carried by each quasiparticle is

$$\Phi = -\frac{2ke^*}{e}\frac{h}{e}. \tag{4.23}$$

Hence the extra phase θ^* gained by moving a quasiparticle around another quasiparticle should equal

$$\theta^* = 2\pi - \frac{e^*}{\hbar}\Phi = 2\pi + 2\pi\frac{2k}{(2kp+1)^2}, \tag{4.24}$$

where Eq. (4.22) has been used. The extra 2π accounts for the fermi statistics of the electrons: in the initial state of the adiabatic mapping the excitations are true particles or holes which obviously obey fermi statistics. For the fundamental filling factors $\nu = \frac{1}{2k+1}$ ($p = 1$) Eq. (4.24) gives $\theta^* = 2\pi + 4\pi k(2k+1)^{-2}$. This result is obviously wrong!

What has been the wrong step in the derivation of θ^*? The error lies in ignoring the gauge transformation (2.5). Being a pure phase, the gauge transformation does not alter the charge of the excitations, but it does affect their statistics. What we calculated above is not the statistical angle of the excitations of a system of electrons, but that of electron-flux-tube composites. Before calculating the statistical phase, we should therefore remove the flux tubes by applying the gauge transformation (2.5).

We will determine the statistical phase of the quasiparticles by the following semiclassical argument. Consider a fractional QHE state with two quasiparticles of charge $-e^*$. The first quasiparticle is located near the origin. The second quasiparticle is situated far away from the origin, encircling the first quasiparticle. For the second quasiparticle, the semiclassical Bohr-Sommerfeld quantization condition for periodic orbits requires that [30]

$$-e^* \oint \mathbf{A}\cdot d\mathbf{l} + \hbar\theta^* = nh, \tag{4.25}$$

where the integral is taken along the path that the second quasiparticle traverses around the origin in the clockwise direction, and n is an integer. The l.h.s. of Eq. (4.25) is the classical action. The first term is the Aharonov-Bohm contribution due to the external magnetic field. Note that the fictitious magnetic field is removed by the gauge transformation (2.5). The second term is the statistical contribution from the quasiparticle at the origin. The integral $-\oint \mathbf{A}\cdot d\mathbf{l}$ is is the total flux enclosed by the second quasiparticle. (The negative sign is due to the negative (clockwise) direction of the integral.) Hence, if Ω denotes the area enclosed by the second quasiparticle, then Eq. (4.25) gives

$$\theta^* = 2\pi n - \frac{e^*B}{\hbar}\Omega. \tag{4.26}$$

The enclosed area Ω can be determined using vector-mean-field theory. Let's assume that the initial (noninteracting) state of the adiabatic mapping consists of p filled Landau levels and two extra electrons in the $(p+1)$-th Landau level. The single-particle wave functions of the two excitations are $\phi_{0,p,m_1}(\mathbf{r})$ and $\phi_{0,p,m_2}(\mathbf{r})$ which are given by Eq. (4.5). We take m_1 to be small and $m_2 \gg m_1$, so that the first electron is located near the origin and is encircled by the second electron at a large distance. As the vector-potential interaction is switched on adiabatically, the charges of both electrons are partly screened by the electron gas filling p Landau levels, as described above. The electrons surrounding the first quasiparticle are shifted towards the boundary creating a screening hole near the origin. Also the second quasiparticle is shifted because it encloses the extra flux of the first quasiparticle. The semiclassical quantization condition for the second quasiparticle is written as

$$-e \oint \mathbf{A}^{\text{eff}} \cdot d\mathbf{l} = n'h, \tag{4.27}$$

where $\mathbf{A}^{\text{eff}}(\mathbf{r})$ is the total effective vector-potential and n' is an integer. The charge entering Eq. (4.27) is e and not e^*, because the mean-field Hamiltonian (3.2) describes electrons of charge $-e$ interacting with self-consistent fields. The electrons obey fermi statistics so that the statistical contribution $\hbar\theta^*$ appearing in Eq. (4.25) is just an integer multiple of h and can be incorporated in the r.h.s. of Eq. (4.27).

After the adiabatic mapping is carried out, the total flux enclosed by the second quasiparticle is given by

$$-\oint \mathbf{A}^{\text{eff}} \cdot d\mathbf{l} = \Phi + B_\infty^{\text{eff}}\Omega, \tag{4.28}$$

where Φ is the excess flux of the first quasiparticle given by Eq. (4.23), and B_∞^{eff} is the effective magnetic field in the uniform state given by Eq. (4.15). The enclosed area Ω can now be determined from Eq. (4.28) and the quantization condition (4.25), and substituted back into Eq. (4.26). The result for the statistical phase angle is

$$\theta^* = 2\pi(n-n') - 2\pi\frac{2k}{2kp+1}. \tag{4.29}$$

Since in the initial state ($k=0$) the excitations are fermions with $\theta^* = 2\pi(\text{mod}4\pi)$, we choose $(n-n')$ such that

$$\theta^* = 2\pi(\text{mod}\,4\pi) - 2\pi\frac{2k}{2kp+1}. \tag{4.30}$$

For the fundamental filling factors $\nu = \frac{1}{2k+1}$ corresponding to $p=1$, Eq. (4.30) reproduces the result $\theta^* = (2k+1)^{-1}2\pi(\text{mod}4\pi)$. The analysis for quasiholes is identical to that for quasiparticles, yielding $-\theta^*$ for the statistical phase angle.

Method of solution of the mean-field equations

In order to calculate the quasiparticle and quasihole energies, the mean-field equations have to be solved numerically. We give here a brief discussion of the method of solution. The method also applies to the confined geometry considered in the next section.

The calculations are carried out in a rotationally symmetric geometry, *i.e.* on a disc. We assume that the external potential is rotationally symmetric [$V(\mathbf{r}) = V(r)$] and choose the symmetric gauge for the external vector potential ($\mathbf{A} = \frac{1}{2}B\hat{\mathbf{z}} \times \mathbf{r}$). Because of the rotational symmetry, the single-particle mean-field Hamiltonian commutes with the angular momentum operator. One can therefore assign a definite angular momentum quantum number to each electron. This number does not change as the interactions are switched on since the angular momentum operator only allows integer eigenvalues, and any change in angular momentum implies a discontinuous change in the wavefunction of the corresponding electron. This contradicts the adiabaticity of the mapping. Hence, the angular momentum of each electron is an adiabatic invariant determined by the choice of the initial state. The Schrödinger equation (3.8) can then be reduced to an ordinary differential equation, which can be solved by standard techniques. The mean-field equations on a disc are given in App. C. The details of the numerical method are given in App. D.

In the conventional theory of the fractional QHE, it is assumed that the Landau level separation $\hbar\omega_{\mathrm{c}}$ is much larger than the typical Coulomb interaction energy e^2/ℓ_0. The Coulomb interaction can therefore be considered as a perturbation to the large kinetic energy of the electrons. Application of first order degenerate pertubation theory is then equivalent to diagonalization of the interaction Hamiltonian in the lowest Landau level. In solving the mean-field equations no restrictions are made to the lowest Landau level. Consistency with the standard theory requires a projection onto the lowest Landau level of the mean-field fractional QHE states. This, however, makes the theory much less tractable. Hence, we ignore the lowest Landau level projection, but instead take the ratio $e^2/\ell_0\hbar\omega_{\mathrm{c}}$ to be very small (≈ 0.1) in the calculation.

When solving the mean-field equations for the unbounded (but non-uniform) quasiparticle and quasihole states, it should be kept in mind that the calculation can only be carried out for a finite number of electrons. Although this number is much larger than the number of electrons in a typical exact finite system calculation (≈ 200 vs. ≈ 10), one still has to deal with finite size effects. In order to minimize these effects, we use the asymptotic solution obtained previously. The numerical solution is then matched to the asymptotic at a point far away from the quasiparticle or quasihole.

Excitation energy

There are various ways of defining the quasiparticle and quasihole energies. Here we use the definition of Ref. [31]. The excitation energy is defined as the energy

difference between the excited state and the ground state, after ignoring the changes at the edge of the system. The only changes which are included are those in the electron density $n(\mathbf{r})$ and pair distribution function $P(\mathbf{r},\mathbf{r}')$ in the vicinity of the quasiparticle or quasihole.

Using Eqs. (3.11) and (4.8), we have for the total Coulomb energy of the excited state:

$$E_{\rm c}^{\pm} = \frac{1}{2}\int d\mathbf{r}_1 d\mathbf{r}_2 \, \frac{e^2}{|\mathbf{r}_1-\mathbf{r}_2|}\left[\delta n^{\pm}(\mathbf{r}_1)\delta n^{\pm}(\mathbf{r}_2) - |D^{\pm}(\mathbf{r}_1,\mathbf{r}_2)|^2\right], \tag{4.31}$$

where $\delta n^{\pm}(\mathbf{r}) = n^{\pm}(\mathbf{r}) - \rho$, and

$$D^{\pm}(\mathbf{r}_1,\mathbf{r}_2) \equiv \sum_{i=1}^{N} \phi^{\pm}_{2k,i}(\mathbf{r}_1)\phi^{\pm *}_{2k,i}(\mathbf{r}_2). \tag{4.32}$$

Here $\phi^{\pm}_{2k,i}$ are eigenfunctions of $\mathcal{H}^{\rm MF}_{2k}$ in the excited state. Using Eqs. (4.9) and (4.31) the excitation energy is defined as

$$\epsilon^{\pm} \equiv E_{\rm c}^{\pm} - E_{\rm c} = \frac{1}{2}\int d\mathbf{r}_1 d\mathbf{r}_2 \, \frac{e^2\mathcal{E}(\mathbf{r}_1,\mathbf{r}_2)}{|\mathbf{r}_1-\mathbf{r}_2|}, \tag{4.33}$$

$$\mathcal{E}(\mathbf{r}_1,\mathbf{r}_2) = \delta n^{\pm}(\mathbf{r}_1)\delta n^{\pm}(\mathbf{r}_2) - |D^{\pm}(\mathbf{r}_1,\mathbf{r}_2)|^2 + |D(\mathbf{r}_1,\mathbf{r}_2)|^2. \tag{4.34}$$

The energy defined by Eq. (4.33) is known as the gross excitation energy [31]. This is the change in the energy of the system as a result of changing the number of electrons, and keeping the magnetic field and the volume of the system constant.

We have calculated the excitation energies and the electron density profiles of the quasiparticles and quasiholes for the filling factors $\nu = \frac{1}{3}$, $\frac{1}{5}$ ($k = 1, 2$, $p = 1$) and $\nu = \frac{2}{5}$ ($k = 1$, $p = 2$), belonging to the first, respectively, second level of the hierarchy. The electron density profiles of the quasihole and quasiparticle states are shown in Fig. 4.2. The quasihole state at $\nu = \frac{1}{3}$ and $\nu = \frac{1}{5}$ is obtained by adiabatically attaching two, respectively four flux quanta to each electron, starting from a completely filled lowest Landau level where a hole has been created by leaving out the electron with quantum numbers $l = 0$, $m = 0$. For the quasiparticle at $\nu = \frac{1}{3}$ and $\nu = \frac{1}{5}$ we take the initial state to consist of a completely filled lowest Landau level plus an extra electron in the second Landau level with quantum numbers $l = 1$, $m = 0$. For the quasihole at $\nu = \frac{2}{5}$ we start from two completely filled Landau levels plus a hole in the second Landau level with quantum numbers $l = 1$, $m = 0$. For the quasiparticle the mapping is started from two filled Landau levels and an extra electron in the third Landau level with quantum numbers $l = 2$, $m = 0$. For comparison we have included in Fig. 4.2a the result of an exact calculation by Morf and Halperin [32] carried out for 72 electrons. The agreement is quite good.

The mean-field excitation energies and energy gaps are given in Table 4.1. They differ from the exact finite-system calculations of Refs. [31] and [33] by 10-20% [2].

[2]The results presented in Table 4.1 are slightly different from those reported in a previous paper [13]. The difference is due to a different, more accurate numerical method used in our later calculations.

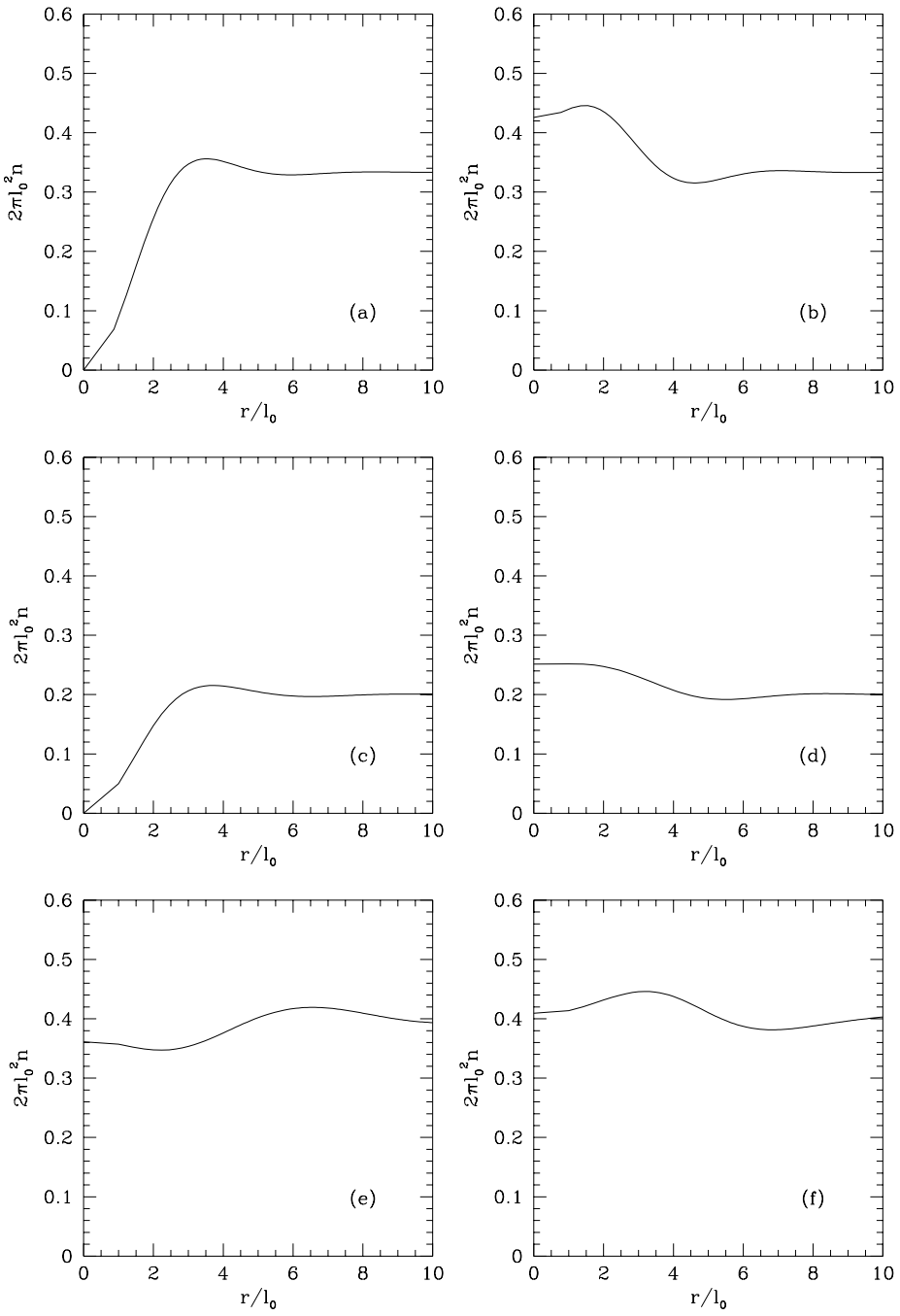

Fig. 4.2. Electron density in units of $(2\pi\ell_0^2)^{-1}$ for the $\nu = \frac{1}{3}$ quasihole (Fig. 4.2a), $\nu = \frac{1}{3}$ quasiparticle (Fig. 4.2b), $\nu = \frac{1}{5}$ quasihole (Fig. 4.2c), $\nu = \frac{1}{5}$ quasiparticle (Fig. 4.2d), $\nu = \frac{2}{5}$ quasihole (Fig. 4.2e), and $\nu = \frac{2}{5}$ quasiparticle (Fig. 4.2f). The number of electrons in the calculation is $N = 100$ for $\nu = \frac{1}{3}$ and $\nu = \frac{1}{5}$, and $N = 200$ for $\nu = \frac{2}{5}$. The numerical solution has been matched to the asymptotic solution of Sec. 4.22 at $r = 20\ell_0$ for $\nu = \frac{1}{3}$, $r = 26\ell_0$ for $\nu = \frac{1}{5}$, and $r = 18\ell_0$ for $\nu = \frac{2}{5}$. The dashed line in Fig. 4.2a represents the exact result for 72 electrons taken from Ref. [32].

Table 4.1. Comparison of the mean-field (MF) results with exact (EX) finite-system calculations. The interaction energy per particle (E_c/N), and the quasi-particle (ϵ_-), quasi-hole (ϵ_+), and excitation-gap (E_g) energies are compared for $\nu = \frac{1}{3}, \frac{1}{5}$, and $\frac{2}{5}$. The energy unit is e^2/ℓ_0. The exact results for $\nu = \frac{1}{3}$ and $\frac{2}{5}$ are taken from Ref. [33]. Those for $\nu = \frac{1}{5}$ are from Ref. [31].

	E_c/N		ϵ_-		ϵ_+		E_g	
ν	MF	EX	MF	EX	MF	EX	MF	EX
$\frac{1}{3}$	-0.362	-0.410	-0.121	-0.130	0.210	0.232	0.089	0.102
$\frac{1}{5}$	-0.280	-0.328	-0.053	-0.076	0.091	0.107	0.038	0.031
$\frac{2}{5}$	-0.385	-0.434	-0.086	-0.084	0.142	0.145	0.056	0.061

4.3 Conjugate fractional QHE states

The filling factors given by the hierarchy formula (4.4) are restricted to the intervals $\frac{1}{2k+1} \leq \nu < \frac{1}{2k}$, with $k = 1, 2, \ldots, \infty$. In particular, we have $\nu < \frac{1}{2}$. It might seem at first that this limitation of the mean-field theory can be lifted by invoking the particle-hole symmetry [34], thus creating a new family of filling factors with $\bar{\nu} = 1 - \nu$, where ν is given by Eq. (4.4). Howeve not all the filling factors at which the fractional QHE occurs can be recovered in this way. For instance the filling factors in the range $\frac{1}{3} < \nu < \frac{1}{4}$ can neither be obtained from the hierarchy formula (4.4) nor from particle-hole symmetry.

This limitation, in fact, arises because we only consider incompressible initial states consisting of several completely filled Landau levels. Can the adiabatic principle be extended to other, more general, initial states? For the moment we will simply assume that if those additional initial states exist, they evolve into final fractional QHE states satisfying the mean-field equations at $\lambda = 2k$. Hence we look for solutions of the final mean-field equations, without trying to make any statement concerning their adiabatic evolution. Instead we impose the physical condition of uniformity to select the appropriate solutions.

Our starting point is the self-consistency relation (4.1). In Sec. 4.1, we used this relation, together with the condition that p Landau levels remain filled during the adiabatic mapping, to derive the hierarchy formula (4.4). Note that the effective magnetic field B^{eff} [given by Eq. (4.3)] decreases, but remains positive as λ is increased gradually from 0 to $2k$. There is however no reason why B^{eff} should be positive if we only consider solutions at $\lambda = 2k$. The only necessary condition is that B^{eff} and n are independent of $\mathbf{r}$, since we are looking for uniform solutions. Let us take B^{eff} to be negative and assume that p Landau levels are filled in the *final* state. As a result we have $B^{\text{eff}} = -hn/ep$. Substitution of this relation into Eq. (4.1) with $\lambda = 2k$ yields

$$n = \frac{p}{2kp - 1} \frac{eB}{h}, \tag{4.35}$$

$$B^{\text{eff}} = -\frac{1}{2kp-1}\,B, \tag{4.36}$$

and a new family of filling factors given by

$$\bar{\nu} = \frac{hn}{eB} = \frac{p}{2kp-1}. \tag{4.37}$$

The single-particle eigenfunctions of $\mathcal{H}_{2k}^{\text{MF}}$ for negative B^{eff} are given by

$$\bar{\phi}_{2k,l,m} = \frac{(l!)^{1/2}}{(2\pi m!)^{1/2}\ell_{\text{eff}}}(\xi^*)^{m-l}L_l^{m-l}(|\xi|^2)\exp\left(-\frac{|\xi|^2}{2}\right), \tag{4.38}$$

where $\ell_{\text{eff}} = (-\hbar/eB^{\text{eff}})^{1/2}$ and $\xi = z/(\ell_{\text{eff}}\sqrt{2})$. Apart from a different length scale ℓ_{eff}, these wavefunctions are just complex conjugates of those given by Eq. (4.5). Therefore the pair distribution function and the Coulomb energy per electron for these new states are again given by Eqs. (4.7) and (4.10). The Coulomb energy per electron for some of these new filling factors is shown in Fig. 4.1.

The charge of the quasiparticles and quasiholes follows from an asymptotic analysis similar to the one presented in Sec. 4.2. We briefly discuss the essential steps of the derivation for a quasiparticle. Assuming once again that the quasiparticle is located near the origin, the asymptotic values of the electron density and the effective magnetic field at $\lambda = 2k$ are given by:

$$n_\infty \equiv \lim_{r\to\infty} n(\mathbf{r}) = \frac{p}{2kp-1}\,\frac{eB}{h}, \tag{4.39}$$

$$B_\infty^{\text{eff}} \equiv \lim_{r\to\infty} B^{\text{eff}}(\mathbf{r}) = -\frac{1}{2kp-1}\,B. \tag{4.40}$$

For the electrons far away from the origin, the mean-field equations are satisfied by the asymptotic solution

$$\bar{\phi}^-_{2k,l,m} = \frac{(l!)^{1/2}|\xi|^{-\delta}(\xi^*)^{m-l}}{[2\pi\Gamma(m-\delta+1)]^{1/2}\ell_{\text{eff}}}\,L^{m-\delta-l}(|\xi|^2)\exp\left(-\frac{|\xi|^2}{2}\right), \tag{4.41}$$

where $\delta = 2ke^*/e$. Here $-e^*$ is the quasiparticle charge which is by definition the total excess charge accumulated near the origin. Note that in contrast to Sec. 4.2, the electrons far away from the origin are shifted *inwards*, creating a screening *particle* of charge $-p\delta e$. This is because of the negative sign of the effective magnetic field. In Sec. 4.2 we considered the quasiparticle charge to be the charge of an electron, plus that of the screening hole. This was obvious, since the initial excited state contained an extra electron. Here, however, we do not know the nature of the initial excited state. Let us assume that initially the excess charge near the origin is a multiple (positive or negative) of e. Then, we have $-e^* = ne - p\delta e$, where n is an integer. Equating $\delta = 2ke^*/e$ yields $e^* = -n(2kp-1)^{-1}e$. For the smallest positive value of e^* we take $n = -1$, which results in

$$e^* = \frac{1}{2kp-1}e. \tag{4.42}$$

Other negative values of n represent solutions with more than one quasiparticle. The statistics of the quasiparticles follows from a semiclassical argument analogous to the one presented in Sec. 4.2. The result is

$$\theta^* = 2\pi(\mathrm{mod}\, 4\pi) - 2\pi\frac{2k}{2kp-1}. \tag{4.43}$$

5 Application to confined geometries

In this section we discuss the application of the vector-mean-field theory to a confined geometry. We consider a quantum dot with a 2D parabolic confining potential. This choice of the confining potential is particulary suitable for calculations, as will be discussed below. In Sec. 5.1 we summarize some exact results concerning interacting and noninteracting electrons with a parabolic confinement. The application of vector-mean-field theory is discussed in Sec. 5.2. Finally, in Sec. 5.3 we consider the problem of tunneling through a quantum dot in the fractional QHE regime.

5.1 Exact results

The problem of noninteracting electrons in an external magnetic field $B\hat{\mathbf{z}}$, and a 2D parabolic potential

$$V(\mathbf{r}) = \frac{1}{2}m\omega_0^2(x^2+y^2), \tag{5.1}$$

can be solved exactly [35]. The eigenstates of energy and angular momentum are

$$\phi_{l,m}(z) = \frac{(l!)^{1/2}}{(2\pi m!)^{1/2}\ell}\left(\frac{z}{\ell\sqrt{2}}\right)^{m-l} L_l^{m-l}\left(\frac{|z|^2}{2\ell^2}\right)\exp\left(-\frac{|z|^2}{4\ell^2}\right), \tag{5.2}$$

where $\ell^2 = \hbar/m\omega$, $\omega^2 = \omega_\mathrm{c}^2 + 4\omega_0^2$, $\omega_\mathrm{c} = eB/m$, and l and m are nonnegative integers. The energy eigenvalue is

$$\epsilon_{l,m} = (l+\frac{1}{2})\hbar\omega + \frac{1}{2}(m-l)(\hbar\omega - \hbar\omega_\mathrm{c}). \tag{5.3}$$

The corresponding angular momentum is $m-l$. In the lowest Landau level ($l=0$), the sum of the single-particle energies of N electrons with total angular momentum M is

$$E_\mathrm{sp}(N,M) = \frac{1}{2}N\hbar\omega + \frac{1}{2}M\hbar(\omega-\omega_\mathrm{c}). \tag{5.4}$$

Because ω_0 enters in the eigenstates (5.2) only as a scale factor (through ℓ), the problem of calculating the electron-electron interaction energy can be solved independently of the value of ω_0. More precisely, if $E_\mathrm{ee}(N,M)$ is the Coulomb interaction energy for $\omega_0 = 0$, then the total energy for $\omega_0 \neq 0$ is given by

$$E_\mathrm{tot}(N,M) = (\omega/\omega_\mathrm{c})^{1/2}E_\mathrm{ee}(N,M) + E_\mathrm{sp}(N,M). \tag{5.5}$$

The ground state for given ω_0 is obtained by choosing the value of M which minimizes $E_{\rm tot}(N, M)$.

For small N the interaction energy can be calculated exactly, by diagonalizing the Hamiltonian (2.1) in the space spanned by the lowest Landau level wave functions. The technique is described by Trugman and Kivelson [2]. Our exact results for the interaction energy $E_{\rm ee}(N, M)$ as a function of M for 5 and 6 electrons are plotted in Fig. 4.3 (open symbols). To determine the ground state value of M one has to minimize $E_{\rm ee}(N, M) + \alpha M$, with $\alpha \equiv \frac{1}{2}\hbar(\omega - \omega_{\rm c})(\omega_{\rm c}/\omega)^{1/2}$. This amounts to tilting the plot of $E_{\rm ee}$ versus M with a slope α determined by the strength of the confining potential, and finding the global minimum. The angular momentum values on the convex envelope of the plot (dashed curve in Fig. 4.3) are global minima for some range of ω_0. These are the stable incompressible states of the system, at which the interaction energy shows a cusp (squares in Fig. 4.3). Not all cusps are global minima, for example $N = 5$, $M = 22$ and $N = 6$, $M = 33$. These cusps are local minima, or "meta-stable" incompressible states [2].

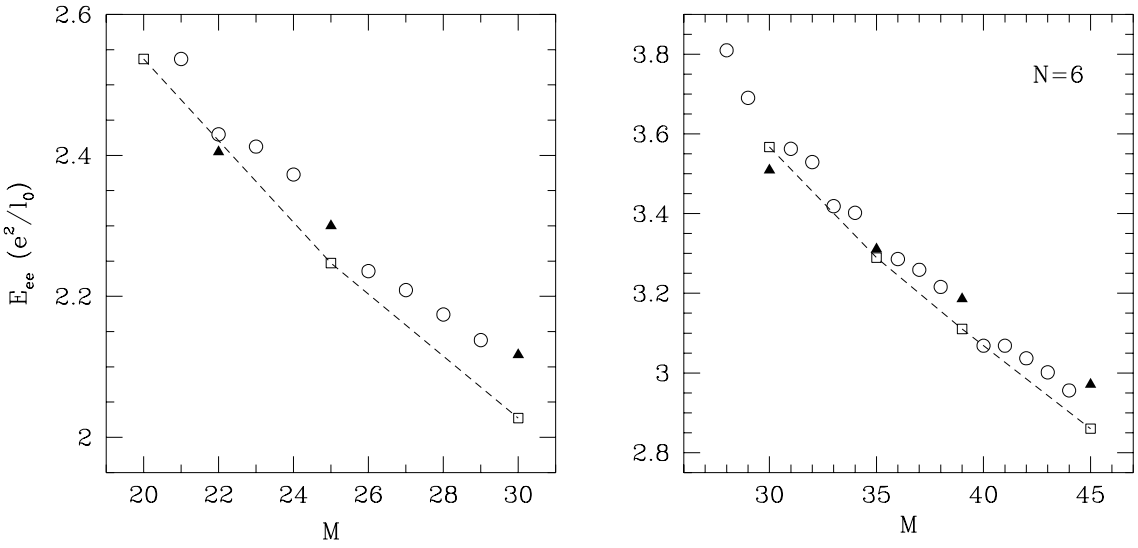

Fig. 4.3. Electron-electron interaction energy of 5 and 6 electrons as a function of the angular momentum M. The energy is in units of e^2/ℓ_0. Triangles follow from the adiabatic mapping in mean-field approximation. Squares and circles are exact results, squares representing incompressible ground states. Solid lines are a guide to the eye, dashed lines form the Maxwell construction for finding ground states (described in the text). The range $M \leq 21$ ($N = 5$) and $M \leq 29$ ($N = 6$) can not be reached by adiabatic mapping.

5.2 Results from vector-mean-field theory

We now turn to the vector-mean-field theory. As initial state of the adiabatic mapping we can choose any noninteracting incompressible state, which occupies p Landau

levels. If N_l ($l = 0, 1, 2, \ldots$) is the number of electrons in each Landau level, the initial angular momentum eigenvalue is $M_0 = \frac{1}{2}\sum_l N_l(N_l - 1 - 2l)$. Here we have used that the angular momentum eigenvalues in the l-th Landau level are $m - l$, with $m = 0, 1, 2, \ldots$. This angular momentum is conserved during the adiabatic evolution, during which the electron density is reduced by exchanging mechanical angular momentum for electromagnetic angular momentum (at constant number of electrons in the system). The final gauge transformation (2.6) increments the angular momentum by

$$\Delta M = \chi_{2k}^{-1} \sum_{i=1}^{N} \left(z_i \frac{\partial}{\partial z_i} - z_i^* \frac{\partial}{\partial z_i^*} \right) \chi_{2k} = kN(N-1), \tag{5.6}$$

so that the final angular momentum becomes

$$M = \frac{1}{2} \sum_{l=0}^{p-1} N_l(N_l - 1 - 2l) + kN(N-1). \tag{5.7}$$

To ensure that the initial state is a ground state, each Landau level should be filled up to the same Fermi level. This is achieved by ordering the single-electron energies $\epsilon_{l,m}$ given by Eq. (5.3) in ascending order and occupying the N lowest levels. The complete set of incompressible ground states turns out to consist of the set of occupation numbers which satisfy

$$\begin{aligned} &N_0 > N_1 > \ldots > N_{p-1} > 0, \\ &N_l = 0 \text{ for } l \geq p, \ \sum_{l=0}^{p-1} N_l = N. \end{aligned} \tag{5.8}$$

The occupation numbers of subsequent occupied Landau levels thus have to form a strictly descending series.

In Fig. 4.3 the triangular symbols are mean-field interaction energies for $N = 5$ and $N = 6$. The angular momentum values reached by the adiabatic mapping are dictated by Eqs. (5.7) and (5.8). For example, for $N = 5$ the smallest M results from $p = 2$, $k = 1$, $N_0 = 3$, $N_1 = 2$, yielding $M = 22$. For $N = 6$, the smallest value of M is obtained by choosing $p = 3$, $k = 1$, $N_0 = 3$, $N_1 = 2$, $N_2 = 1$, with the result $M = 30$. The existence of a smallest value of M corresponds to the restriction $\nu < \frac{1}{2}$ in the unbounded system (see Sec. 4.3). It is evident from Fig. 4.3 that all the M's reached by adiabatic mapping correspond to a cusp in the exact interaction energy, i.e. to a (possibly meta-stable) incompressible state. The adiabatic mapping thus reveals the rule for the "magic" angular momentum values of incompressibility.

For further comparison between the mean-field theory and the exact diagonalization, we show in Fig. 4.4 the density profile in the $\frac{1}{3}$ state ($N = 5$, $M = 30$). The agreement is quite reasonable, in particular the curious density peak near the edge (noted in previous exact calculations [36]) is reproduced by the mean-field wave function, albeit with a somewhat smaller amplitude.

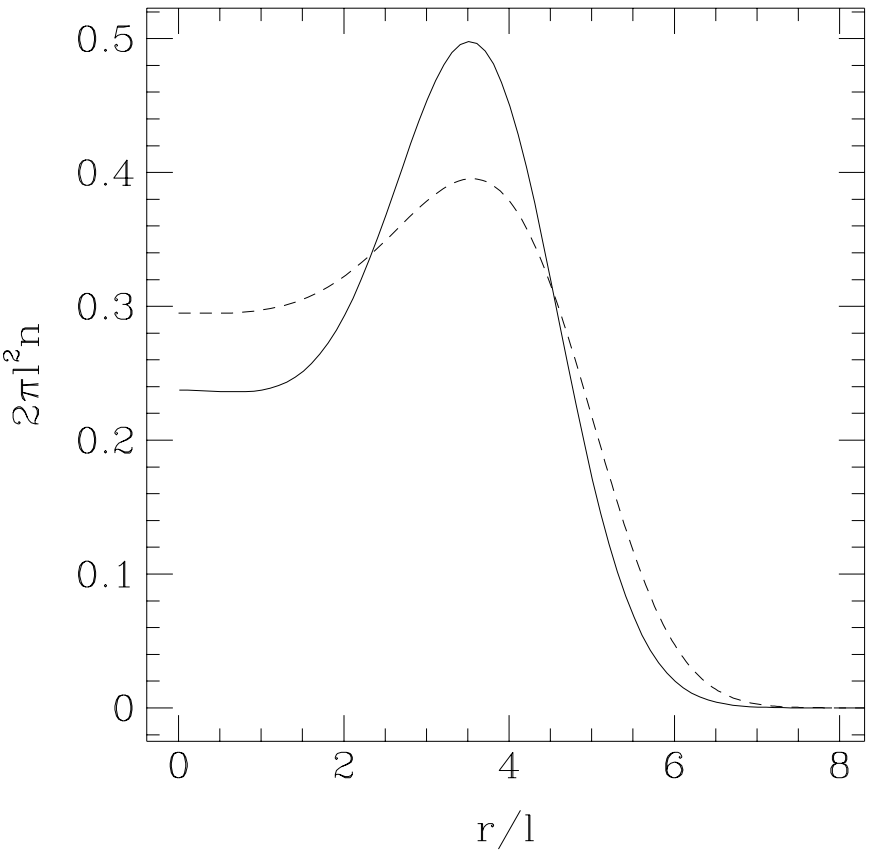

Fig. 4.4. Density profile in units of $(2\pi\ell^2)^{-1}$ in a quantum dot with a parabolic confining potential. Comparison of the exact result (solid curve) with the mean-field theory (dashed). The plot is for $N = 5$, $M = 30$, corresponding to the $\frac{1}{3}$ state in an unbounded system. The normalization length ℓ is defined in the text [below Eq. (5.2)].

5.3 Resonant tunneling

We consider a quantum dot which is weakly coupled to two electron reservoirs by tunnel barriers (cf. Fig. 4.5). A voltage difference V is applied between the two reservoirs, resulting in a current I passing through the quantum dot. The conductance G of the quantum dot is $G = I/V$ in the limit $V \to 0$. At low temperatures, the condition for resonant tunneling through the quantum dot is [37]

$$E(N) - E(N-1) = E_{\rm F}, \tag{5.9}$$

where $E(N)$ is the ground-state energy of the quantum dot for N electrons, and $E_{\rm F}$ is the Fermi energy in the reservoirs. Equation (5.9) equates the electrochemical potential in the dot and in the reservoirs. In a measurement of the conductance as a function of the density in the dot or in the reservoirs, one observes a conductance peak whenever the condition (5.9) is satisfied. At finite temperatures the peaks are observed as oscillations in the dependence of the electrochemical potential on electron density. Because the periodicity of the oscillations is regulated by the Coulomb repulsion, these oscillations are known as Coulomb-blockade oscillations [37]. A discussion of the *periodicity* of the conductance oscillations in the fractional QHE regime, based on the adiabatic mapping, was given in Ref. [38]. Here we discuss the application to the *amplitude* of the conductance oscillations.

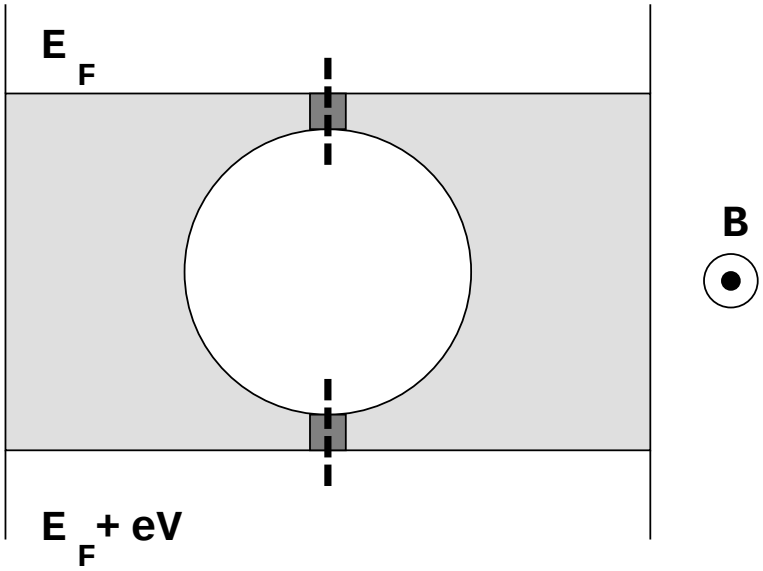

Fig. 4.5. Quantum dot geometry. A gate (shaded) isolates a disc-shaped region in a 2DEG from two reservoirs. Conduction through the dot occurs by tunneling (dashed lines), in the case of a small voltage difference between the reservoirs at Fermi energy $E_{\rm F}$.

It was shown by Meir and Wingreen [39], that if the resonances are thermally broadened, the height of a conductance peak is proportional to

$|\langle\Psi_N|c^\dagger_{\Delta M}|\Psi_{N-1}\rangle|^2$, where Ψ_N is the N-electron ground state (with angular momentum M_N) and the operator $c^\dagger_{\Delta M}$ creates an electron in the lowest Landau level with angular momentum $\Delta M = M_N - M_{N-1}$ [24]. In the integer QHE regime the overlap given by Eq. (5.10) equals unity. In contrast, in the fractional QHE, Wen and Kinaret *et al.* [23, 24] found that it vanishes as N^{-k} when $N \to \infty$ for a quantum dot at the fractional filling factor $\nu = 1/(2k+1)$. The thermally broadenend conductance peaks in the fractional states are therefore suppressed algebraically in the large-N limit. This suppression is referred to as an "orthogonality catastrophe", because its origin is the orthogonality of the ground state $|\Psi_N\rangle$ for N electrons to the state $c^\dagger_{\Delta M}|\Psi_{N-1}\rangle$ obtained when an electron tunnels into the quantum dot containing $N-1$ electrons. The condition for thermal broadening is that the thermal energy $k_{\rm B}T$ should be large compared to the intrinsic resonance width $\hbar\Gamma$, with Γ the tunneling matrix element of the barrier between dot and reservoir. While $k_{\rm B}T$ should be larger than $\hbar\Gamma$, it should be still smaller than the energy of the lowest excited state of the quantum dot. In the zero-temperature limit ($k_{\rm B}T \ll \hbar\Gamma$) the height of the conductance peaks takes on the universal value of e^2/h. In that limit the orthogonality catastrophe is expected [24] to occur in the width of the resonance, which vanishes in the limit $N \to \infty$.

To see whether the mean-field theory can reproduce the orthogonality catastrophe, we have to compute the matrix element

$$\mathcal{T}(N) = \langle\tilde\Psi^{\rm MF}_N|c^\dagger_{\Delta M}|\tilde\Psi^{\rm MF}_{N-1}\rangle, \tag{5.10}$$

where $\tilde\Psi^{\rm MF}_N$ is the N-electron mean-field ground state (3.9). We first rewrite the N-electron state $c^\dagger_{\Delta M}|\tilde\Psi^{\rm MF}_{N-1}\rangle$ as the integral

$$c^\dagger_{\Delta M}|\tilde\Psi^{\rm MF}_{N-1}\rangle = \int d\mathbf{R}\,\phi_{\Delta M}(\mathbf{R})\psi^\dagger(\mathbf{R})|\tilde\Psi^{\rm MF}_{N-1}\rangle, \tag{5.11}$$

where $\phi_{\Delta M}(\mathbf{R})$ is the wave function of an electron in the lowest Landau level with angular momentum ΔM and $\psi^\dagger(\mathbf{R})$ creates an electron at the position $\mathbf{R}$. In App. E we show that

$$\psi^\dagger(\mathbf{R})|\tilde\Psi^{\rm MF}_{N-1}\rangle = \mathcal{G}_{2k,N}|\Phi_{N,\mathbf{R}}\rangle, \tag{5.12}$$

where $\mathcal{G}_{2k,N}$ is the N-electron gauge transformation (2.6) and $\Phi_{N,\mathbf{R}}$ is a N-electron Slater determinant consisting of the localized wave function $\delta(\mathbf{r}-\mathbf{R})$, and $N-1$ wave functions of the form

$$\phi_{2k,i,\mathbf{R}}(\mathbf{r}) = \frac{(Z-z)^{-2k}}{|Z-z|^{-2k}}\,\phi_{2k,i}(\mathbf{r}). \tag{5.13}$$

The wavefunctions $\phi_{2k,i}(\mathbf{r})$ are the eigenfunctions of the mean-field Hamiltonian (3.2) and $Z = X - {\rm i}Y$ is the complex plane representation of $\mathbf{R}$. Note that $\mathbf{R}$ is just a parameter and not a particle coordinate. We substitute Eqs. (5.11) and (5.12) into

Eq. (5.10), and equate $\tilde{\Psi}_N^{\rm MF} = \mathcal{G}_{2k,N}\Psi_{2k,N}^{\rm MF}$ from Eq. (3.9). Using $\mathcal{G}_{2k,N}^\dagger\mathcal{G}_{2k,N} = 1$ we find

$$\mathcal{T}(N) = \int d\mathbf{R}\,\phi_{\Delta M}(\mathbf{R})\langle\Psi_{2k,N}^{\rm MF}|\Phi_{N,\mathbf{R}}\rangle. \tag{5.14}$$

Since $\langle\Psi_{2k,N}^{\rm MF}|\Phi_{N,\mathbf{R}}\rangle$ is just the overlap of two Slater determinants it can be shown that (see App. E)

$$\langle\Psi_{2k,N}^{\rm MF}|\Phi_{N,\mathbf{R}}\rangle = {\rm Det}\,\mathcal{M}_{i,j}(\mathbf{R}), \tag{5.15}$$

where $\mathcal{M}_{i,j}(\mathbf{R})$ is a $N\times N$ matrix with the elements

$$\begin{aligned}\mathcal{M}_{i,j}(\mathbf{R}) &= \langle\phi_{2k,i}|\phi_{2k,j,\mathbf{R}}\rangle = \int d\mathbf{r}\,\frac{(z-Z)^{-2k}}{|z-Z|^{-2k}}\,\phi_{2k,i}^*(\mathbf{r})\phi_{2k,j}(\mathbf{r}),\ (j\neq N),\\ \mathcal{M}_{i,N}(\mathbf{R}) &= \phi_{2k,i}^*(\mathbf{R}).\end{aligned} \tag{5.16}$$

Because we are dealing with a finite system, the wave functions $\phi_{2k,i}$ will differ from $\phi_{2k,l,m}$ in Eq. (4.5). However, when N is large, $\phi_{2k,l,m}$ will be a good approximation. We can then calculate the determinant analytically. As shown in App. E, for the $\frac{1}{3}$ fractional QHE state the overlap is given by

$$\begin{aligned}\langle\Psi_{2k,N}^{\rm MF}|\Phi_{N,\mathbf{R}}\rangle &= \frac{1}{[2\pi(N-1)!]^{\frac{1}{2}}\ell_{\rm eff}}\frac{(\zeta^*)^{2N-2}}{\zeta^{N-1}}\exp\left(-\frac{|\zeta|^2}{2}\right)f_N(|\zeta|^2),\\ f_N(x) &= \int_0^x dt\,\left(1-\frac{t}{x}\right)^2\frac{t^{N-2}\exp(-t)}{(N-2)!},\end{aligned} \tag{5.17}$$

where $\zeta = Z/(\ell_{\rm eff}\sqrt{2})$. After substituting into Eq. (5.14) and carrying out the integration we find $|\mathcal{T}(N)|^2 \simeq 0.380N^{-2}$ for $N\gg 1$. We conclude that the mean-field theory reproduces the algebraic decay of the tunneling matrix element for large N, but with a different value of the exponent: $|\mathcal{T}(N)|^2 \propto N^{-2}$ instead of $\propto N^{-1}$ in Refs. [23, 24]. (We have not been able to find a general formula for arbitrary k.) In the present context, the orthogonality catastrophe originates from the correlations created by the gauge transformation (2.6), required to remove the fictitious vector potential from the Hamiltonian (2.2).

6 Summary

The adiabatic mapping of Greiter and Wilczek [10, 11] is an exact prescription for constructing fractional QHE states from integer QHE states. Starting from an incompressible state of the integer QHE, an even number of flux quanta is adiabatically attached to each electron. After a singular gauge transformation, we end up with an incompressible state of the fractional QHE. In general, the adiabatic mapping cannot be carried out exactly and a suitable approximation should be applied. We have investigated the mean-field approximation to the adiabatic mapping, suggested

by the vector-mean-field theory of anyon superconductivity [14]-[16]. In this approximation, the flux tubes are smeared out, resulting in fictitious magnetic and electric fields proportional to the electron density and current density, respectively.

In the case of an unbounded, uniform fractional QHE state, the mean-field equations can be solved exactly, yielding Jain's formula [12] for the hierarchy of fractional QHE filling factors $\nu = p/(2kp+1)$. We calculated the mean-field Coulomb energy per electron and found it to be in reasonable agreement with the exact results. By generalizing the adiabatic mapping to low-lying excited states we were able to recover the fractional charge and statistics of the quasiparticles and quasiholes. The derivation was based on the asymptotic solution of the mean-field equations far away from the excitation. The quasiparticle, quasihole, and excitation gap energies were numerically calculated for $\nu = \frac{1}{3}, \frac{1}{5}$, and $\frac{2}{5}$. The difference with exact results was found to be about $10 - 20\%$.

The hierarchy of filling factors $\nu = p/(2kp+1)$, generated by the adiabatic mapping of the incompressible integer QHE states, is restricted to the values $\nu < \frac{1}{2}$. The mean-field equations, by themselves, allow another hierarchy of filling factors given by $\nu = p/(2kp-1)$. We calculated the Coulomb energy per electron for these "conjugate" states, and determined the charge and statistics of their excitations by an asymptotic analysis similar to the one for the original hierarchy. The initial states which can be mapped onto the conjugate fractional QHE states remain to be identified.

The mean-field theory can be readily applied to confined geometries (quantum dots). We considered a 2D parabolic confinement which is particularly suitable for calculations. For a small number of electrons, we exactly diagonalized the Hamiltonian. The "magic" vlaues of angular momentum, at which the exact ground-state energy shows a cusp, are represented quite well by the adiabatic mapping.

The probability of resonant tunneling through a quantum dot in the fractional QHE regime vanishes algebraically as the number of electrons N in the dot is increased. This orthogonality catastrophe, discovered by Wen and Kinaret *et al.* [23, 24], originates from the non-Fermi-liquid nature of the fractional QHE ground state. For a quantum dot at the filling factor $\nu = \frac{1}{2k+1}$, the tunneling probability vanishes as N^{-k} when $N \to \infty$. The vector-mean-field theory reproduces the orthogonality catastrophe albeit with a wrong exponent. Conventional mean-field theory (Hartree or Hartree-Fock) describes a Fermi-liquid, because the ground state is a Slater determinant. Vector-mean-field theory, in contrast, does not produce a Fermi-liquid because the ground state is no longer a Slater determinant after the singular gauge transformation. The correlations induced by this gauge transformation are the origin of the orthogonality catastrophe in out formulation.

The major shortcoming of the vector-mean-field theory is its inability to give the correct behaviour of the wave function at short separations. In the conventional theory of the fractional QHE the exact pair distribution function in the $\nu = \frac{1}{2k+1}$ state vanishes as $|\mathbf{r}_{12}|^{4k+2}$ as $\mathbf{r}_{12} \to 0$. The mean-field pair distribution function (4.7) for $\nu = \frac{1}{2k+1}$, however, vanishes as $|\mathbf{r}_{12}|^2$ for all values of k. This does not introduce a big error in the ground-state and excitation energies, because of the long-range nature

of the Coulomb interaction. We attribute the failure of the vector-mean-field theory to give the correct expression for the suppression of tunneling to this breakdown at short separations. The same problem is also reflected in the mean-field result for the kinetic energy of the fractional QHE ground state which does not yield the correct value of $\frac{1}{2}\hbar\omega_c$ per electron.

The obtained results might be improved by a projection of the mean-field ground-state onto the lowest Landau level (as in Jain's approach [12]). This would resolve the problem of kinetic energy, but would also make the theory less tractable. One might also think of improving the results by including the (here neglected) exchange terms in the mean-field Hamiltonian, or by going beyond mean-field by taking into account the particle-hole excitations (random phase approximation). Here we have shown that the vector-mean-field theory in its simplest form is able to describe the essential features of the fractional QHE.

A Derivation of the mean-field equations

In this appendix we present a variational derivation of the mean-field Hamiltonian (3.2), and the self-consistency relations (3.3)-(3.5). We shall use the language of second quantization, which is more convenient for keeping track of many different terms appearing in the derivation.

The many-body Hamiltonian (2.2) in second quantized form is

$$\mathcal{H}_\lambda = \mathcal{H}_{\rm kin} + \mathcal{H}_{\rm int} + \mathcal{H}_{\rm ex}, \tag{A.1}$$

$$\mathcal{H}_{\rm kin} = \frac{1}{2m}\int d\mathbf{1}\, \psi^\dagger(\mathbf{1}) \left[\Pi_1 - e\lambda \int d\mathbf{2}\, \mathbf{a}_{12}\psi^\dagger(\mathbf{2})\psi(\mathbf{2})\right]^2 \psi(\mathbf{1}), \tag{A.2}$$

$$\mathcal{H}_{\rm int} = \frac{1}{2}\int d\mathbf{1}d\mathbf{2}\, \psi^\dagger(\mathbf{1})\psi^\dagger(\mathbf{2})u_{12}\psi(\mathbf{2})\psi(\mathbf{1}), \tag{A.3}$$

$$\mathcal{H}_{\rm ex} = \int d\mathbf{1}\, V(\mathbf{1})\psi^\dagger(\mathbf{1})\psi(\mathbf{1}), \tag{A.4}$$

where $\mathbf{i}$ stands for $\mathbf{r}_i$, $\Pi_i \equiv -i\hbar\nabla_i + e\mathbf{A}(\mathbf{r}_i)$, $\mathbf{a}_{ij} \equiv \mathbf{a}(\mathbf{r}_i - \mathbf{r}_j)$, and $u_{ij} \equiv u(\mathbf{r}_i - \mathbf{r}_j)$. In Eq. (A.1) $\mathcal{H}_{\rm kin}$ is the kinetic energy including the vector-potential interaction, $\mathcal{H}_{\rm int}$ is the ordinary electron-electron interaction Hamiltonian, and $\mathcal{H}_{\rm ex}$ represents the interaction with an external potential. The operators $\psi^\dagger$ and ψ satisfy the anticommutation relations

$$\begin{aligned} &\{\psi(\mathbf{1}), \psi(\mathbf{2})\} = \{\psi^\dagger(\mathbf{1}), \psi^\dagger(\mathbf{2})\} = 0, \\ &\{\psi(\mathbf{1}), \psi^\dagger(\mathbf{2})\} = \delta(\mathbf{1} - \mathbf{2}). \end{aligned} \tag{A.5}$$

Using Eq. (A.5), we write $\mathcal{H}_{\rm kin} = \mathcal{H}_1 + \mathcal{H}_2 + \mathcal{H}_3$ with

$$\mathcal{H}_1 = \frac{1}{2m}\int d\mathbf{1}\, \psi^\dagger(\mathbf{1})\Pi_1^2\psi(\mathbf{1}), \tag{A.6}$$

$$\mathcal{H}_2 = -\frac{e\lambda}{m}\int d\mathbf{1}d\mathbf{2}\, \psi^\dagger(\mathbf{1})\psi^\dagger(\mathbf{2})\mathbf{a}_{12}\cdot[\Pi_1 - \frac{e\lambda}{2}\mathbf{a}_{12}]\psi(\mathbf{2})\psi(\mathbf{1}), \tag{A.7}$$

$$\mathcal{H}_3 = \frac{e^2\lambda^2}{2m}\int d\mathbf{1}d\mathbf{2}d\mathbf{3}\, \psi^\dagger(\mathbf{1})\psi^\dagger(\mathbf{2})\psi^\dagger(\mathbf{3})\mathbf{a}_{12}\cdot\mathbf{a}_{13}\psi(\mathbf{3})\psi(\mathbf{2})\psi(\mathbf{1}). \tag{A.8}$$

In the Hartree-Fock approximation, the eigenstates of $\mathcal{H}_\lambda$ are approximated by Slater determinants (3.1) of single-particle wave functions $\phi_i(\mathbf{r})$, $i = 1, \ldots, N$. (To keep the notation simple, the dependence of $\{\phi_i(\mathbf{r})\}$ on λ is not written explicitly.) The corresponding second quantized representation is

$$|\Psi^{\rm MF}\rangle = c_1^\dagger \ldots c_N^\dagger|0\rangle, \tag{A.9}$$

where $c_i^\dagger$ creates a particle in the state ϕ_i by operating on the vaccum state $|0\rangle$. The Hartree-Fock energy is simply

$$E^{\rm HF} = \langle\Psi^{\rm MF}|\mathcal{H}_\lambda|\Psi^{\rm MF}\rangle, \tag{A.10}$$

which can be written in terms of $\{\phi_i\}$ by means of the relation:

$$\langle\psi^\dagger(\mathbf{1})\cdots\psi^\dagger(\mathbf{n})\psi(\mathbf{n}')\cdots\psi(\mathbf{1}')\rangle = \langle\psi^\dagger(\mathbf{1})\psi(\mathbf{1}')\rangle\cdots\langle\psi^\dagger(\mathbf{n})\psi(\mathbf{n}')\rangle + (-1)^\sigma \text{permutations of } \{\mathbf{1}'\ldots\mathbf{n}'\}, \tag{A.11}$$

where

$$\langle\psi^\dagger(\mathbf{r})\psi(\mathbf{r}')\rangle = \sum_i \phi_i(\mathbf{r})\phi_i^*(\mathbf{r}'). \tag{A.12}$$

Here, $\langle\cdots\rangle$ denotes the Hartree-Fock average $\langle\Psi^{\rm MF}|\cdots|\Psi^{\rm MF}\rangle$. Upon substituting Eqs. (A.1)-(A.4) and (A.6)-(A.8) into Eq. (A.10), and using Eqs. (A.11) and (A.12), one finds the following expression for $E^{\rm HF}$:

$$E^{\rm HF} = E_1 + E_2^a + E_2^b + E_2^c + E_2^d + E_3^a + E_3^b + E_3^c + E_3^d + E_{\rm int}^a + E_{\rm int}^b + E_{\rm ex}, \tag{A.13}$$

$$E_1 = \frac{1}{2m}\sum_i \int d\mathbf{1}\, \phi_i^*(\mathbf{1})\Pi_1^2\phi_i(\mathbf{1}), \tag{A.14}$$

$$E_2^a = -\frac{e\lambda}{m}\sum_{ij}\int d\mathbf{1}d\mathbf{2}\, \phi_i^*(\mathbf{1})\phi_j^*(\mathbf{2})\mathbf{a}_{12}\cdot\Pi_1\,\phi_j(\mathbf{2})\phi_i(\mathbf{1}), \tag{A.15}$$

$$E_2^b = \frac{e\lambda}{m}\sum_{ij}\int d\mathbf{1}d\mathbf{2}\, \phi_i^*(\mathbf{1})\phi_j^*(\mathbf{2})\mathbf{a}_{12}\cdot\Pi_1\,\phi_i(\mathbf{2})\phi_j(\mathbf{1}), \tag{A.16}$$

$$E_2^c = \frac{e\lambda}{m}\sum_{ij}\int d\mathbf{1}d\mathbf{2}\, \phi_i^*(\mathbf{1})\phi_j^*(\mathbf{2})|\mathbf{a}_{12}|^2\phi_j(\mathbf{2})\phi_i(\mathbf{1}), \tag{A.17}$$

$$E_2^d = -\frac{e\lambda}{m}\sum_{ij}\int d\mathbf{1}d\mathbf{2}\, \phi_i^*(\mathbf{1})\phi_j^*(\mathbf{2})|\mathbf{a}_{12}|^2\phi_i(\mathbf{2})\phi_j(\mathbf{1}), \tag{A.18}$$

$$E_3^a = \frac{e^2\lambda^2}{2m}\sum_{ijk}\int d\mathbf{1}d\mathbf{2}d\mathbf{3}\, \phi_i^*(\mathbf{1})\phi_j^*(\mathbf{2})\phi_k^*(\mathbf{3})\mathbf{a}_{12}\cdot\mathbf{a}_{13}\phi_k(\mathbf{3})\phi_j(\mathbf{2})\phi_i(\mathbf{1}), \tag{A.19}$$

$$E_3^b = -\frac{e^2\lambda^2}{2m}\sum_{ijk}\int d\mathbf{1}d\mathbf{2}d\mathbf{3}\, \phi_i^*(\mathbf{1})\phi_j^*(\mathbf{2})\phi_k^*(\mathbf{3})\mathbf{a}_{12}\cdot\mathbf{a}_{13}\phi_j(\mathbf{3})\phi_k(\mathbf{2})\phi_i(\mathbf{1}), \tag{A.20}$$

$$E_3^c = \frac{e^2\lambda^2}{m}\sum_{ijk}\int d\mathbf{1}d\mathbf{2}d\mathbf{3}\, \phi_i^*(\mathbf{1})\phi_j^*(\mathbf{2})\phi_k^*(\mathbf{3})\mathbf{a}_{12}\cdot\mathbf{a}_{13}\phi_j(\mathbf{3})\phi_i(\mathbf{2})\phi_k(\mathbf{1}), \tag{A.21}$$

$$E_3^d = -\frac{e^2\lambda^2}{m}\sum_{ijk}\int d\mathbf{1}d\mathbf{2}d\mathbf{3}\, \phi_i^*(\mathbf{1})\phi_j^*(\mathbf{2})\phi_k^*(\mathbf{3})\mathbf{a}_{12}\cdot\mathbf{a}_{13}\phi_k(\mathbf{3})\phi_i(\mathbf{2})\phi_j(\mathbf{1}), \tag{A.22}$$

$$E_{\rm int}^a = \frac{1}{2}\sum_{ij}\int d\mathbf{1}d\mathbf{2}\, \phi_i^*(\mathbf{1})\phi_j^*(\mathbf{2})u_{12}\phi_j(\mathbf{2})\phi_i(\mathbf{1}), \tag{A.23}$$

$$E_{\rm int}^b = -\frac{1}{2}\sum_{ij}\int d\mathbf{1}d\mathbf{2}\, \phi_i^*(\mathbf{1})\phi_j^*(\mathbf{2})u_{12}\phi_i(\mathbf{2})\phi_j(\mathbf{1}), \tag{A.24}$$

$$E_{\rm ex} = \sum_i \int d\mathbf{1}\, V(\mathbf{1})\phi_i^*(\mathbf{1})\phi_i(\mathbf{1}). \tag{A.25}$$

The Hartree-Fock equations are obtained by minimization of $E^{\rm HF}$ with respect to the wave functions $\phi_i(\mathbf{r})$. These equations, however, are rather complicated. Therefore, we have to neglect some of the terms in Eq. (A.13) in order to make the approximation tractable. A natural alternative is the Hartree approximation which satisfies the basic conservation laws, and leads to gauge invariant equations [16]. The Hartree (mean-field) energy functional is given by

$$E^{\rm MF} = E_{\rm kin} + E^a_{\rm int} + E_{\rm ex}, \tag{A.26}$$

where

$$\begin{aligned} E_{\rm kin} &= E_1 + E^a_2 + E^a_3 \\ &= \frac{1}{2m}\sum_i \int d\mathbf{1}\, \phi^*_i(\mathbf{1}) \left[\Pi_1 - e\lambda \int d\mathbf{2}\, \mathbf{a}_{12} \sum_j \phi^*_j(\mathbf{2})\phi_j(\mathbf{2})\right]^2 \phi_i(\mathbf{1}). \end{aligned} \tag{A.27}$$

The Hartree (mean-field) equations can now be found by minimizing $E^{\rm MF}$ with respect to $\phi_i(\mathbf{r})$. The wave functions $\phi_i(\mathbf{r})$ are subject to the normalization condition:

$$\int d\mathbf{r}\, \phi^*_i(\mathbf{r})\phi_i(\mathbf{r}) = 1. \tag{A.28}$$

Hence, one has to solve the equations

$$\frac{\delta E^{\rm MF}}{\delta \phi^*_i(\mathbf{r})} = \epsilon_i \phi_i(\mathbf{r}), \tag{A.29}$$

where ϵ_i $(i = 1, \ldots, N)$ are Lagrange multipliers. Taking the variational derivatives of $E^a_{\rm int}$ and $E_{\rm ex}$ yields

$$\frac{\delta E^a_{\rm int}}{\delta \phi^*_i(\mathbf{r})} = U^{\rm f}(\mathbf{r})\phi_i(\mathbf{r}), \tag{A.30}$$

$$\frac{\delta E_{\rm ex}}{\delta \phi^*_i(\mathbf{r})} = V(\mathbf{r})\phi_i(\mathbf{r}), \tag{A.31}$$

where $U^{\rm f}(\mathbf{r})$ is the usual Hartree potential given by Eq. (3.5). The variational derivative of $E_{\rm kin}$ is more complicated:

$$\frac{\delta E_{\rm kin}}{\delta \phi^*_i(\mathbf{r})} = \frac{1}{2m}\left[-{\rm i}\hbar\nabla + e\mathbf{A}(\mathbf{r}) - e\lambda \mathbf{A}^{\rm f}(\mathbf{r})\right]^2 \phi_i(\mathbf{r}) + e\lambda\Phi^{\rm f}(\mathbf{r}), \tag{A.32}$$

$$\mathbf{A}^{\rm f}(\mathbf{r}) = \int d\mathbf{r}' \mathbf{a}(\mathbf{r}-\mathbf{r}') \sum_j \phi^*_j(\mathbf{r}')\phi_j(\mathbf{r}'), \tag{A.33}$$

$$\Phi^{\rm f}(\mathbf{r}) = \frac{1}{m}\int d\mathbf{r}' \mathbf{a}(\mathbf{r}-\mathbf{r}') \cdot \sum_j \phi^*_j(\mathbf{r}') \left[-{\rm i}\hbar\nabla' + e\mathbf{A}(\mathbf{r}') - e\lambda\mathbf{A}^{\rm f}(\mathbf{r}')\right] \phi_j(\mathbf{r}'). \tag{A.34}$$

Substituting Eqs. (3.6) and (3.7) into Eqs. (A.33) and (A.34) leads to the final expressions (3.3) and (3.4) for the fictitious fields. Collecting the results, one finds the eigenvalue equation $\mathcal{H}^{\rm MF}_\lambda \phi_i = \epsilon_i \phi_i$, where $\mathcal{H}^{\rm MF}_\lambda$ is given by Eq. (3.2).

B Single-particle eigenfunctions in a constant magnetic field with a flux tube at the origin

In this appendix we derive the eigenfunctions of the Hamiltonian

$$H = \frac{1}{2m}\left[-\mathrm{i}\hbar\nabla + e\mathbf{A}^{\mathrm{eff}}(\mathbf{r}) - e\delta\mathbf{a}(\mathbf{r})\right]^2, \tag{B.1}$$

where $\nabla \times \mathbf{A}^{\mathrm{eff}} = B^{\mathrm{eff}}\hat{\mathbf{z}}$ is associated with a constant magnetic field B^{eff} in the z-direction. The vector potential $-\delta\mathbf{a}(\mathbf{r})$, with $\mathbf{a}(\mathbf{r})$ given by Eq. (2.3), is the field of a flux tube at the origin of the strength $-\delta h/e$. Using cilinder coordinates (r,θ), H is written as

$$H = -\frac{\hbar^2}{2m}\frac{1}{r}\frac{\partial}{\partial r}r\frac{\partial}{\partial r} + \frac{1}{2m}\left[\frac{eB^{\mathrm{eff}}r}{2} - \frac{\delta\hbar}{r} - \frac{\mathrm{i}\hbar}{r}\frac{\partial}{\partial\theta}\right]^2. \tag{B.2}$$

Here we have used the symmetric gauge $\mathbf{A}^{\mathrm{eff}} = (eB^{\mathrm{eff}}r/2)\hat{\theta}$, and rewritten Eq. (2.3) as $\mathbf{a}(\mathbf{r}) = (\hbar/er)\hat{\theta}$, where $\hat{\theta}$ is the unit vector in the azimuthal direction. The eigenfunctions $\phi(\mathbf{r})$ of H are next decomposed as

$$\phi(\mathbf{r}) = \frac{1}{\sqrt{2\pi}}\exp(-\mathrm{i}q\theta)\psi(r), \tag{B.3}$$

where q is an integer. After substitution of Eq. (B.3) the eigenvalue equation $H\phi = \epsilon\phi$ becomes

$$-\frac{1}{s}\frac{d}{ds}s\frac{d}{ds}\psi(s) + \left(s - \frac{q+\delta}{s}\right)^2\psi(s) = \frac{4\epsilon}{\hbar\omega_{\mathrm{eff}}}\psi(s), \tag{B.4}$$

where $\ell_{\mathrm{eff}} = (eB^{\mathrm{eff}}/\hbar)^{-1/2}$, $s = r/(\ell_{\mathrm{eff}}\sqrt{2})$, and $\omega_{\mathrm{eff}} = eB^{\mathrm{eff}}/m$. We next substitute

$$\psi(s) = s^{|q+\delta|}\exp\left(-\frac{s^2}{2}\right)f(s^2), \tag{B.5}$$

into Eq. (B.4). The resulting differential equation for $f(x)$ is

$$xf'' + (|q+\delta|+1-x)f' + \left[\frac{\epsilon}{\hbar\omega_{\mathrm{eff}}} + \frac{1}{2}(q+\delta-|q+\delta|-1)\right]f = 0. \tag{B.6}$$

The physically acceptable solutions of Eq. (B.6) are

$$f(x) = L_n^{|q+\delta|}(x), \tag{B.7}$$

$$\epsilon = \hbar\omega_{\mathrm{eff}}\left[n + \frac{1}{2} + \frac{1}{2}(|q+\delta| - q - \delta)\right], \tag{B.8}$$

where n is a nonnegative integer and $L_n^{\alpha}(x)$ is the generalized Laguerre polynomial. The next step is to substitute Eqs. (B.7) and (B.5) back into Eq. (B.3). After normalization we have

$$\phi(\mathbf{r}) = \frac{(n!)^{1/2}s^{|q+\delta|}}{[2\pi\Gamma(|q+\delta|+n+1)]^{1/2}\ell_{\mathrm{eff}}}L_n^{|q+\delta|}(s^2)\exp\left(-\mathrm{i}q\theta\right)\exp\left(-\frac{s^2}{2}\right). \tag{B.9}$$

We introduce the quantum numbers l, m through the relations $l = n + (|q| - q)/2$ and $m = l + q = n + (|q| + q)/2$ (l and m are both nonnegative integers). Since the asymptotic solution in Sec. 4.2 is only valid for electrons far away from the origin, we have to consider the solutions with $m \gg l$. Hence, we have $q = m - l \gg 1$ and $n = l$. Since $|\delta| \leq 2k$, we have $|q + \delta| = m - l + \delta$. Substituting this relation into Eq. (B.9) and using $\xi = s \exp(-\mathrm{i}\theta)$, we recover Eq. (4.20). The area enclosed by the wave function $\phi(\mathbf{r})$ is

$$\langle \phi | \pi r^2 | \phi \rangle = \frac{2\pi l! \ell_{\rm eff}^2}{\Gamma(m+\delta+1)} \int_0^\infty dx\, x^{m-l+\delta+1} \left[L_l^{m-l+\delta}(x) \right]^2 \exp(-x). \tag{B.10}$$

Using the orthogonality property of the Laguerre polynomials

$$\int_0^\infty dx\, x^\alpha \exp(-x) L_n^\alpha(x) L_{n'}^\alpha(x) = \delta_{n,n'}, \tag{B.11}$$

and the recurrent relation

$$(n+1) L_{n+1}^\alpha(x) = (2n + \alpha + 1 - x) L_n^\alpha(x) - (n+\alpha) L_{n-1}^\alpha(x), \tag{B.12}$$

the enclosed area becomes

$$\langle \phi | \pi r^2 | \phi \rangle = 2\pi \ell_{\rm eff}^2 (m + l + \delta + 1). \tag{B.13}$$

C Mean-field equations in a rotationally symmetric geometry

In a rotationally symmetric geometry, all physical quantities including the electron density and current density, will only depend on the distance r from the origin. The three self-consistency relations (3.3)-(3.5) therefore become

$$\mathbf{A}^{\rm f}(\mathbf{r}) = \int_0^\infty r' dr'\, n(r') \int_0^{2\pi} d\theta'\, \mathbf{a}(\mathbf{r} - \mathbf{r}'), \tag{C.1}$$

$$\Phi^{\rm f}(\mathbf{r}) = \int_0^\infty r' dr'\, \mathbf{j}(r') \cdot \int_0^{2\pi} d\theta'\, \mathbf{a}(\mathbf{r} - \mathbf{r}'), \tag{C.2}$$

$$U(\mathbf{r}) = \int_0^\infty r' dr'\, n(r') \int_0^{2\pi} d\theta'\, u(\mathbf{r} - \mathbf{r}'), \tag{C.3}$$

where we have used cilinder coordinates r, θ. The first two equations can be simplified by using the relation

$$\int_0^{2\pi} d\theta'\, \mathbf{a}(\mathbf{r} - \mathbf{r}') = \frac{h}{er}\, \Theta(r - r')\, \hat{\theta}, \tag{C.4}$$

where $\Theta(x) = 1$ for $x > 0$ and $\Theta(x) = 0$ for $x < 0$. $\hat{\theta}$ is the unit vector in the azimuthal direction. Substitution of Eq. (C.4) into Eqs. (C.1) and (C.2) leads to

$$\mathbf{A}^{\rm f}(\mathbf{r}) = A_\theta^{\rm f}(r)\hat{\theta},\ A_\theta^{\rm f}(r) = \frac{h}{er} \int_0^r r' dr'\, n(r'), \tag{C.5}$$

$$\Phi^{\rm f}(\mathbf{r}) = \Phi^{\rm f}(r) = \frac{h}{er} \int_0^r r' dr'\, j_\theta(r'), \tag{C.6}$$

where $A_\theta^{\rm f}$ and j_θ are the azimuthal components of $\mathbf{A}^{\rm f}$ and $\mathbf{j}$, respectively. For the Coulomb potential $u(r) = e^2/r$, we have

$$\int_0^{2\pi} d\theta' \, \frac{e^2}{|\mathbf{r}-\mathbf{r}'|} = w(r,r'),\; w(r,r') = \begin{cases} 4e^2 r^{-1} K(r'/r) & r > r', \\ 4e^2 r'^{-1} K(r/r') & r < r', \end{cases} \tag{C.7}$$

where $K(x)$ is the complete elliptic integral of the first kind. Hence, Eq. (C.3) becomes

$$U(\mathbf{r}) = U(r) = \int_0^\infty r' dr' \, n(r') w(r,r'). \tag{C.8}$$

We now write the mean-field Hamiltonian (3.2) in cilinder coordinates (r,θ) and decompose its eigenfunctions $\phi_{\lambda,i}(\mathbf{r})$ as

$$\phi_{\lambda,i}(\mathbf{r}) = \frac{1}{\sqrt{2\pi}} \exp(-\mathrm{i} q_i \theta) \psi_{\lambda,i}(r). \tag{C.9}$$

Here $q_i = 0, 1, 2, \ldots$ is the angular momentum of i-th electron, and $\psi_{\lambda,i}(r)$ satisfies the ordinary differential equation

$$\mathcal{H}^{\rm MF}_{\lambda,i} \psi_{\lambda,i} = \epsilon_{\lambda,i} \psi_{\lambda,i}, \tag{C.10}$$

$$\mathcal{H}^{\rm MF}_{\lambda,i} = -\frac{\hbar^2}{2m} \frac{1}{r} \frac{d}{dr} r \frac{d}{dr} + \frac{1}{2m} \left[eA_\theta - e\lambda A_\theta^{\rm f} - \frac{\hbar q_i}{r} \right]^2 + e\lambda \Phi^{\rm f} + U + V. \tag{C.11}$$

The electron density $n(r)$ and azimuthal current density $j_\theta(r)$ are expressed in terms of $\psi_{\lambda,i}(r)$ by substituting Eq. (C.9) into Eqs. (3.6) and (3.7):

$$n(r) = \frac{1}{2\pi} \sum_i |\psi_{\lambda,i}(r)|^2, \tag{C.12}$$

$$j_\theta(r) = \frac{1}{2\pi m} \sum_i \left[eA_\theta(r) - e\lambda A_\theta^{\rm f}(r) - \frac{\hbar q_i}{r} \right] |\psi_{\lambda,i}(r)|^2. \tag{C.13}$$

Equation (C.10) together with the self-consistency relations (C.5), (C.6), (C.8), and the definitions (C.12) and (C.13) form the basis of our mean-field calculations.

D Numerical method

The mean-field equations have to be solved for every value of λ, as it is increased adiabatically from 0 to $2k$. Hence, for every value of λ, we have to deal with a set of coupled nonlinear differential equations, which can only be solved by iterative methods. Here, we give a brief account of the method used.

Starting from an appropriate initial guess for the density $n(r)$ and azimuthal current density $j_\theta(r)$, we determine the potentials A_θ, Φ, and U from Eqs. (C.5),(C.6),

and (C.8), respectively, and solve the eigenvalue equation (C.10) to obtain the single-particle eigenfunctions $\psi_i(r)$. Substitution of $\psi_i(r)$ into Eqs. (C.12) and (C.13) yields a new density and current density distribution which is again used to determine the new potentials. This procedure is repeated until the solution converges.

Although simple at first sight, there is no guarantee that the iteration will always converge. A standard technique to controle the convergence is to mix the new density and current density after each iteration with their old values before the iteration:

$$\begin{aligned} n^{(\mathrm{new})} &\to \alpha n^{(\mathrm{new})} + (1-\alpha) n^{(\mathrm{old})}, \\ j_\theta^{(\mathrm{new})} &\to \alpha j_\theta^{(\mathrm{new})} + (1-\alpha) j_\theta^{(\mathrm{old})}. \end{aligned} \tag{D.1}$$

The constant α ($\in [0,1]$) is the mixing parameter, which for simplicity is assumed to be the same for n and j_θ. In general, the range of α for which the iteration converges should be determined by numerical experimentation.

As an illustration suppose that we had to solve the mean-field equations iteratively for a uniform system. If the obtained (constant) density after the i-th iteration step is denoted by $n^{(i)}$, we find the following relation by using Eq. (4.1) and assuming that p Landau levels are filled:

$$n^{(i+1)} = \frac{pe}{h}\left(B - \frac{\lambda h}{e} n^{(i)}\right). \tag{D.2}$$

If $\Delta n^{(i)} \equiv n^{(i)} - n$ denotes the deviation from the final solution n given by Eq. (4.2), then it is easily found that

$$\Delta n^{(i+1)} = (-p\lambda)\Delta n^{(i)}. \tag{D.3}$$

Hence if $p\lambda > 1$, the error will increase at each iteration, and convergence will never occur. Since $p \geq 1$, the iteration diverges if $\lambda > 1$. Let's now modify Eq. (D.2) by including a mixing parameter:

$$n^{(i+1)} = \frac{\alpha pe}{h}\left(B - \frac{\lambda h}{e} n^{(i)}\right) + (1-\alpha) n^{(i)}. \tag{D.4}$$

After some elementary algebra we find

$$\Delta n^{(i+1)} = (1 - \alpha - \alpha p\lambda)\Delta n^{(i)}. \tag{D.5}$$

In order to have convergence we have to choose α such that $|1 - \alpha - \alpha p\lambda| < 1$. This condition is always satisfied if $\alpha < 2(p\lambda + 1)^{-1}$.

In practice, it is not possible to solve the mean-field equations for every λ in the interval $[0, 2k]$. Starting from $\lambda = 0$, we increase λ by small, but finite steps. The obtained solution at each step serves as the initial guess for the iterative solution of the mean-field equations at the next step. Adiabaticity requires that the single-particle eigenfunctions change continuously as λ is increased. This is carried out numerically by requiring the overlap of the wave functions obtained at any two subsequent steps to be near 1.

E Calculation of the tunneling matrix element

In this appendix we calculate the tunneling matrix element

$$\mathcal{T}(N) = \langle \tilde{\Psi}_N^{\rm MF} | c_{\Delta M}^\dagger | \tilde{\Psi}_{N-1}^{\rm MF} \rangle, \tag{E.1}$$

where $\tilde{\Psi}_N^{\rm MF}$ is the N-electron fractional QHE ground state in the mean-field approximation. The operator $c_{\Delta M}^\dagger$ creates an electron in the lowest Landau level with angular momentum $\Delta M = M_N - M_{N-1}$, where M_N is the total angular momentum of the N-electron fractional QHE ground state. M_N is related to the filling factor ν by [2]

$$M_N = \frac{N(N-1)}{2\nu}, \tag{E.2}$$

so that

$$\Delta M = M_N - M_{N-1} = \nu^{-1}(N-1). \tag{E.3}$$

As the first step of the derivation we write the N-electron state $|\tilde{\Phi}_{N,\Delta M}\rangle \equiv c_{\Delta M}^\dagger |\tilde{\Psi}_{N-1}^{\rm MF}\rangle$ as the integral

$$|\tilde{\Phi}_{N,\Delta M}\rangle = \int d\mathbf{R} \phi_{\Delta M}(\mathbf{R}) \psi^\dagger(\mathbf{R}) |\tilde{\Psi}_{N-1}^{\rm MF}\rangle, \tag{E.4}$$

where $\psi^\dagger(\mathbf{R})$ creates an electron at the position $\mathbf{R}$ and $\phi_{\Delta M}(\mathbf{R})$ is the wave function of an electron in the lowest Landau level with the angular momentum ΔM:

$$\phi_{\Delta M}(\mathbf{R}) = \frac{1}{(2\pi \Delta M!)^{1/2}\ell_0} \left(\frac{Z}{\ell_0\sqrt{2}}\right)^{\Delta M} \exp\left(-\frac{|Z|^2}{4\ell_0^2}\right). \tag{E.5}$$

Here $Z = X - {\rm i}Y$ is the complex-plane representation of $\mathbf{R}$. Because of the gauge transformation (2.6), it is more convenient to return to first quantization and work directly with wave functions. The state $|\tilde{\Phi}_{N,\mathbf{R}}\rangle \equiv \psi^\dagger(\mathbf{R})|\tilde{\Psi}_{N-1}^{\rm MF}\rangle$ has the wave function

$$\tilde{\Phi}_{N,\mathbf{R}}(\mathbf{r}_1, \ldots, \mathbf{r}_N) = \frac{1}{\sqrt{N}} \sum_{i=1}^N (-1)^{N-i} \delta(\mathbf{r}_i - \mathbf{R})\, \tilde{\Psi}_{N-1}^{\rm MF}(\mathbf{r}_1, \ldots, \mathbf{r}_{i-1}, \mathbf{r}_{i+1}, \ldots, \mathbf{r}_N). \tag{E.6}$$

The antisymmetry of $\tilde{\Phi}_{N,\mathbf{R}}$ is ensured by the antisymmetry of $\tilde{\Psi}_{N-1}^{\rm MF}$ and the factor $(-1)^{N-i}$. Using Eqs. (3.9) and (2.6), we next write

$$\tilde{\Phi}_{N,\mathbf{R}} = \prod_{i=1}^N \prod_{j=i+1}^N \frac{(z_i - z_j)^{2k}}{|z_i - z_j|^{2k}}\, \Phi_{N,\mathbf{R}}, \tag{E.7}$$

where

$$\begin{aligned} \Phi_{N,\mathbf{R}} = \quad & \frac{1}{\sqrt{N}} \sum_{i=1}^N (-1)^{N-i}\, \delta(\mathbf{r}_i - \mathbf{R}) \times \\ & \prod_{j=1(\neq i)}^N \frac{(Z - z_j)^{-2k}}{|Z - z_j|^{-2k}}\, \Psi_{N-1}^{\rm MF}(\mathbf{r}_1, \ldots, \mathbf{r}_{i-1}, \mathbf{r}_{i+1}, \ldots, \mathbf{r}_N). \end{aligned} \tag{E.8}$$

The wave function $\Psi_{N-1}^{\rm MF}$ is the Slater determinant (3.1) of the single-particle wave functions $\phi_i(\mathbf{r})$, $i = 1, \ldots, N-1$. (We have dropped the subscript $2k$ of $\phi_i(\mathbf{r})$ for the sake of simplicity.) Hence, each term of the form

$$\prod_{j=1(\neq i)}^{N} \frac{(Z-z_j)^{-2k}}{|Z-z_j|^{-2k}} \Psi_{N-1}^{\rm MF}(\mathbf{r}_1, \ldots, \mathbf{r}_{i-1}, \mathbf{r}_{i+1}, \ldots, \mathbf{r}_N),$$

is itself a Slater determinant of the new single-particle wave functions

$$\phi_{i,\mathbf{R}}(\mathbf{r}) = \frac{(Z-z)^{-2k}}{|Z-z|^{-2k}}\, \phi_i(\mathbf{r}). \tag{E.9}$$

Note that $\mathbf{R}$ is just a parameter and not a particle coordinate. ¿From this observation, and using Eq. (E.8) we conclude that $\Phi_{N,\mathbf{R}}$ is a N-particle Slater determinant of the form

$$\Phi_{N,\mathbf{R}} = \frac{1}{\sqrt{N!}} \sum_{\sigma} \mathrm{sgn}(\sigma)\, \phi_{\sigma(1),\mathbf{R}}(\mathbf{r}_1) \cdots \phi_{\sigma(N),\mathbf{R}}(\mathbf{r}_{N-1}) \delta(\mathbf{r}_N - \mathbf{R}). \tag{E.10}$$

Let's now return to the tunneling matrix element (E.1) which we rewrite as

$$\mathcal{T}(N) = \langle \tilde{\Psi}_N^{\rm MF} | \tilde{\Phi}_N \rangle = \int d\mathbf{R}\, \langle \tilde{\Psi}_N^{\rm MF} | \tilde{\Phi}_{N,\mathbf{R}} \rangle\, \phi_{\Delta M}(\mathbf{R}), \tag{E.11}$$

by using Eq. (E.8). It now becomes clear why we applied the transformation (E.7) in the first place. Because of unitarity, the N-particle gauge transformations in $\tilde{\Psi}_N^{\rm MF}$ and $\tilde{\Phi}_{N,\mathbf{R}}$ cancel against each other, and we find

$$\mathcal{T}(N) = \int d\mathbf{R}\, \langle \Psi_N^{\rm MF} | \Phi_{N,\mathbf{R}} \rangle\, \phi_{\Delta M}(\mathbf{R}), \tag{E.12}$$

where both $\Psi_N^{\rm MF}$ and $\Phi_{N,\mathbf{R}}$ are Slater determinants.

The overlap of two Slater determinants can be evaluated easily. Consider two N-particle wave functions $F(\mathbf{r}_1, \ldots, \mathbf{r}_N)$ and $G(\mathbf{r}_1, \ldots, \mathbf{r}_N)$ which are Slater determinants of the single-particle wave functions $f_i(\mathbf{r})$ and $g_i(\mathbf{r})$, respectively ($i = 1, \ldots, N$). Then their overlap is given by

$$\langle F | G \rangle = \det \langle f_i | g_j \rangle. \tag{E.13}$$

Using this relation, together with Eqs. (3.1) and (E.10), we find

$$\langle \Psi_N^{\rm MF} | \Phi_{N,\mathbf{R}} \rangle = \mathrm{Det}\, \mathcal{M}_{i,j}(\mathbf{R}), \tag{E.14}$$

where $\mathcal{M}_{i,j}(\mathbf{R})$ is a $N \times N$ matrix with the elements

$$\begin{aligned} \mathcal{M}_{i,j}(\mathbf{R}) &= \langle \phi_i | \phi_{j,\mathbf{R}} \rangle = \int d\mathbf{r}\, \frac{(z-Z)^{-2k}}{|z-Z|^{-2k}}\, \phi_i^*(\mathbf{r}) \phi_j(\mathbf{r}),\ (j \neq N), \\ \mathcal{M}_{i,N}(\mathbf{R}) &= \phi_i^*(\mathbf{R}). \end{aligned} \tag{E.15}$$

In principle, one now has to determine $\phi_i(\mathbf{r})$ numerically for a finite number of electrons N, and calculate the matrix elements (E.15) and the determinant (E.14). Instead, however, we approximate $\phi_i(\mathbf{r})$ by the solution in an infinite uniform system given by Eq. (4.5). This will allow us to find analytical expressions for the determinant (E.14), as we shall see below.

For simplicity we only calculate the tunneling probability for the fundamental filling factors $\nu = \frac{1}{2k+1}$, corresponding to $p = 1$ in the hierarchy formula (4.4). The single-particle wave functions are obtained from Eq. (4.5) by equating $l_i = 0$:

$$\phi_{2k,0,m}(\mathbf{r}) = \frac{1}{(2\pi m!)^{1/2}\ell_{\text{eff}}} \left(\frac{z}{\ell_{\text{eff}}\sqrt{2}}\right)^m \exp\left(-\frac{|z|^2}{4\ell_{\text{eff}}^2}\right), \tag{E.16}$$

where $m = 0, \ldots, N-1$. After substituting Eq. (E.16) into Eq. (E.15), the elements of the matrix $\mathcal{M}$ become

$$\mathcal{M}_{m,n} = \int_0^\infty r dr\, \psi_m(r)\psi_n(r)\, f_{2k,n-m}(r;\mathbf{R}),\ n \neq N-1, \tag{E.17}$$

$$\psi_m(r) = \frac{1}{(m!)^{1/2}\ell_{\text{eff}}} \left(\frac{r}{\ell_{\text{eff}}\sqrt{2}}\right)^m \exp\left(-\frac{r^2}{4\ell_{\text{eff}}^2}\right), \tag{E.18}$$

$$f_{2k,q}(r;\mathbf{R}) = \int_0^{2\pi} \frac{d\theta}{2\pi}\, \frac{(z-Z)^{-2k}}{|z-Z|^{-2k}}\, \exp(-\mathrm{i}q\theta), \tag{E.19}$$

$$\mathcal{M}_{m,N-1} = \frac{1}{(2\pi m!)^{1/2}\ell_{\text{eff}}} \left(\frac{Z^*}{\ell_{\text{eff}}\sqrt{2}}\right)^m \exp\left(-\frac{|Z|^2}{4\ell_{\text{eff}}^2}\right). \tag{E.20}$$

In deriving Eq. (E.17) we have put $z = r\exp(-\mathrm{i}\theta)$ where r, θ are cilinder coordinates.

The function $f_{2k,q}(r;\mathbf{R})$ can be evaluated by rewriting the integral in Eq. (E.19) as a contour integral in the complex z-plane, by means of the substitutions

$$\frac{d\theta}{2\pi}\, \exp(-\mathrm{i}q\theta) = -\frac{1}{r^q}\, \frac{dz}{2\pi\mathrm{i}} z^{q-1}, \tag{E.21}$$

$$\frac{(z-Z)^{-2k}}{|z-Z|^{-2k}} = \left(\frac{z^*-Z^*}{z-Z}\right)^k = (-Z^*)^k\, \frac{1}{z^k}\, \left(\frac{z-Y}{z-Z}\right)^k, \tag{E.22}$$

with $Y = z^*z/Z^* = r^2/Z^*$. The result is

$$f_{2k,q}(r;\mathbf{R}) = \frac{(-Z^*)^k}{r^q} \oint_{\mathrm{C}} \frac{dz}{2\pi\mathrm{i}}\, z^{q-k-1}\, \left(\frac{z-Y}{z-Z}\right)^k. \tag{E.23}$$

The integral is taken along a circle C of radius r in the positive (counter-clockwise) direction. The contour integral in Eq. (E.23) can be evaluated directly by applying Cauchy's theorem. However, the calculation is complicated and it is better to first simplify the determinant (E.14) further.

It is known from the theory of determinants that the determinant of a matrix does not change if to a row or column one adds a linear combination of other rows

or columns of that matrix. ¿From Eqs. (E.17), (E.18), and (E.23) it follows that the elements of the first $N-1$ columns of the matrix $\mathcal{M}_{m,n}$ are given by

$$\mathcal{M}_{m,n} = C_{m,n}(-Z^*)^k \int_0^\infty dr\, r^{2m+1} \exp\left(-\frac{r^2}{2\ell_{\rm eff}^2}\right) \oint_{\rm C} \frac{dz}{2\pi {\rm i}}\, z^{n-m-k-1} \left(\frac{z-Y}{z-Z}\right)^k, \quad \text{(E.24)}$$

where

$$C_{m,n} = \frac{1}{(m!n!2^{m+n})^{1/2}\ell_{\rm eff}^{m+n+2}},\ n \neq N-1. \quad \text{(E.25)}$$

To each column n of $\mathcal{M}_{m,n}$ with $0 \leq n \leq N-k-2$, we now add a linear combination of the next k columns by the substitution

$$\mathcal{M}_{m,n} \to \mathcal{M}'_{m,n} = \mathcal{M}_{m,n} + \sum_{i=1}^{k} \left(\frac{C_{m,n}}{C_{m,n+i}}\right) \left(\begin{array}{c} k \\ i \end{array}\right) (-Z)^{-i} \mathcal{M}_{m,n+i}. \quad \text{(E.26)}$$

Eqs. (E.24) and (E.26) yield

$$\mathcal{M}'_{m,n} = \left(\frac{Z^*}{Z}\right)^k C_{m,n} \int_0^\infty dr\, r^{2m+1} \exp\left(-\frac{r^2}{2\ell_{\rm eff}^2}\right) \oint_{\rm C} \frac{dz}{2\pi {\rm i}}\, z^{n-m-k-1} (z-Y)^k. \quad \text{(E.27)}$$

The contour integral in Eq. (E.27) is much easier to calculate than the one in Eq. (E.19). Application of Cauchy's theorem leads to

$$\begin{aligned} \oint_{\rm C} \frac{dz}{2\pi {\rm i}}\, z^{n-m-k-1} (z-Y)^k &= \left(\begin{array}{c} k \\ n-m \end{array}\right) (-Y)^{n-m} \ \ m \leq n \leq m+k, \\ &= 0 \ \text{otherwise.} \end{aligned} \quad \text{(E.28)}$$

Hence, the elements $\mathcal{M}'_{m,n}$ with $m > n$ are zero. The determinant (E.14) therefore reduces to

$$\langle \Psi_N^{\rm MF} | \Phi_{N,\mathbf{R}} \rangle = \prod_{m=0}^{N-k-2} \mathcal{M}'_{m,m} \times \det \left| \begin{array}{ccc} \mathcal{M}_{N-k-1,N-k-1} & \cdots & \mathcal{M}_{N-k-1,N-1} \\ \cdot & \cdots & \cdot \\ \cdot & \cdots & \cdot \\ \mathcal{M}_{N-1,N-k-1} & \cdots & \mathcal{M}_{N-1,N-1} \end{array} \right|. \quad \text{(E.29)}$$

Using Eqs. (E.25), (E.27), and (E.28), we find

$$\prod_{m=0}^{N-k-2} \mathcal{M}'_{m,m} = \left(\frac{Z^*}{Z}\right)^{k(N-k-1)}. \quad \text{(E.30)}$$

The elements of the first k columns of the $(k+1) \times (k+1)$ determinant in Eq. (E.29), given by $\mathcal{M}_{m,n}$, $m = N-k-1, \ldots, N-1$, $n = N-k-1, \ldots, N-2$, are calculated by using Eq. (E.24). We expand the factor $(z-Y)^k$ as a binomial sum in the contour integral in Eq. (E.24):

$$\oint_{\rm C} \frac{dz}{2\pi {\rm i}}\, z^{q-k-1} \left(\frac{z-Y}{z-Z}\right)^k = \sum_{i=0}^{k} \left(\begin{array}{c} k \\ i \end{array}\right) (-Y)^i \oint_{\rm C} \frac{dz}{2\pi {\rm i}}\, \frac{z^{q-i-1}}{(z-Z)^k}, \quad \text{(E.31)}$$

where $q = n - m$. Each contour integral in Eq. (E.31) is now evaluated by applying Cauchy's theorem:

$$\oint_{\rm C} \frac{dz}{2\pi {\rm i}} \frac{z^{q-i-1}}{(z-Z)^k} = \frac{1}{(i-q)!} \left[\left(\frac{d}{dz} \right)^{i-q} (z-Z)^{-k} \right]_{z=0} \Theta_{i-q} + \frac{1}{(k-1)!} \left[\left(\frac{d}{dz} \right)^{k-1} z^{q-i-1} \right]_{z=Z} \Theta(r-R), \tag{E.32}$$

where $\Theta(x) = 1$ when $x \geq 0$ and $\Theta(x) = 0$ when $x < 0$. Similarly, $\Theta_n = 1$ when $n \geq 0$ and $\Theta_n = 0$ when $n < 0$. Taking the derivatives in Eq. (E.32), one finds

$$\oint_{\rm C} \frac{dz}{2\pi {\rm i}} \frac{z^{q-i-1}}{(z-Z)^k} = \frac{(-k)(-k-1)\cdots(-k-i+q+1)}{(i-q)!} (-Z)^{-k-i+q} \Theta_{i-q} + \frac{(q-i-1)(q-i-2)\cdots(q-i-k+1)}{(k-1)!} Z^{-k-i+q} \Theta(r-R). \tag{E.33}$$

The first term on the r.h.s. of Eq. (E.33) vanishes when $q-i > 0$ because of the factor Θ_{i-q}. The second term also vanishes for $q-i > 0$ which can be seen as follows. Since $q = n - m$ with $m = N-k-1, \ldots, N-1$, $n = N-k-1, \ldots, N-2$, we have $q < k$, so that $q - i < k$. Hence one of the factors $(q-i-1)\cdots(q-i-k+1)$ will inevitably vanish if $q - i > 0$. Using this result together with the relation $\Theta(-x) = 1 - \Theta(x)$, we find after some algebra

$$\oint_{\rm C} \frac{dz}{2\pi {\rm i}} \frac{z^{q-i-1}}{(z-Z)^k} = (-1)^k \left(\begin{array}{c} i-q+k-1 \\ k-1 \end{array} \right) Z^{-k-i+q} \Theta(R-r) \Theta_{i-q}. \tag{E.34}$$

Substituting Eq. (E.34) back into Eqs. (E.31), and (E.24), and equating $Y = r^2/Z^*$, $q = n - m$ leads to

$$\mathcal{M}_{m,n} = C_{m,n} \left(\frac{Z^*}{Z} \right)^k Z^{n-m} \sum_{i=0}^{k} \Theta_{i-n+m} \left(\begin{array}{c} k \\ i \end{array} \right) \times \left(\begin{array}{c} i-n+m+k-1 \\ k-1 \end{array} \right) (-R^2)^{-i} \int_0^R dr r^{2m+2i+1} \exp\left(-\frac{r^2}{2\ell_{\rm eff}^2} \right). \tag{E.35}$$

After calculating the integral on the r.h.s. of Eq. (E.35) and substituting Eq. (E.25) into Eq. (E.35) we find

$$\mathcal{M}_{m,n} = \left(\frac{Z^*}{Z} \right)^k \left(\frac{Z}{\ell_{\rm eff}\sqrt{2}} \right)^{n-m} \sum_{i=0}^{k} \Theta_{i-n+m} \left(\begin{array}{c} k \\ i \end{array} \right) \times \left(\begin{array}{c} i-n+m+k-1 \\ k-1 \end{array} \right) \frac{(m+i)!}{(m!n!)^{1/2}} \left(-\frac{|Z|^2}{2\ell_{\rm eff}^2} \right)^{-i} Q_{m+i} \left(-\frac{|Z|^2}{2\ell_{\rm eff}^2} \right), \tag{E.36}$$

where

$$Q_m(x) = \frac{1}{m!} \int_0^x dt\, t^m \exp(-t) = 1 - \exp(-x) \sum_{j=0}^{m} \frac{x^j}{j!}. \tag{E.37}$$

Let's now consider the specific case of $k = 1$ ($\nu = \frac{1}{3}$). Using Eqs. (E.29), (E.36), and (E.20), we find

$$\langle \Psi_N^{\rm MF} | \Phi_{N,\mathbf{R}} \rangle = \frac{\exp(-|\zeta|^2/2)}{[2\pi(N-1)!]^{1/2}\,\ell_{\rm eff}} \frac{(\zeta^*)^{2N-2}}{\zeta^{N-1}} f_N(|\zeta|^2), \tag{E.38}$$

where $\zeta = Z/(\ell_{\rm eff}\sqrt{2})$ and

$$\begin{aligned} f_N(x) = &\quad Q_{N-2}(x) - \frac{2(N-1)}{x} Q_{N-1}(x) + \frac{N(N-1)}{x^2} Q_N(x) \\ = &\quad \int_0^x dt\, \left(1 - \frac{t}{x}\right)^2 \frac{t^{N-2}\exp(-t)}{(N-2)!}. \end{aligned} \tag{E.39}$$

Substituting this result together with Eq. (E.5) into Eq. (E.12) yields

$$\mathcal{T}(N) = \frac{(\ell_{\rm eff}/\ell_0)^{3N-2}}{[(N-1)!(3N-3)!]^{1/2}} \int_0^\infty dx\, x^{2N-2} f_N(x) \exp(-ax), \tag{E.40}$$

where $a = \frac{1}{2}(1 + \ell_{\rm eff}^2/\ell_0^2)$. Equating $\ell_{\rm eff}/\ell_0 = \nu^{-1/2}$, we find $a = 2$ for $\nu = \frac{1}{3}$. The integral in Eq. (E.40) is calculated by using the following results:

$$\begin{aligned} \int_0^\infty dx\, \exp(-2x) x^{2N-2} Q_{N-2}(x) &= \frac{(2N-2)!}{2^{2N-1}} - \sum_{i=0}^{N-2} \frac{(2N-2+i)!}{3^{2N-1+i}\, i!}, \\ \int_0^\infty dx\, \exp(-2x) x^{2N-3} Q_{N-1}(x) &= \frac{(2N-3)!}{2^{2N-2}} - \sum_{i=0}^{N-1} \frac{(2N-3+i)!}{3^{2N-2+i}\, i!}, \\ \int_0^\infty dx\, \exp(-2x) x^{2N-3} Q_N(x) &= \frac{(2N-4)!}{2^{2N-3}} - \sum_{i=0}^{N} \frac{(2N-4+i)!}{3^{2N-3+i}\, i!}. \end{aligned} \tag{E.41}$$

The summations in Eq. (E.41) cannot be carried out analytically and have to be evaluated numerically. ¿From Eqs. (E.40) and (E.41), we find $|\mathcal{T}(N)|^2 \simeq 0.380/N^2$ for large N.

References

[1] R.B. Laughlin, Phys. Rev. Lett. **50**, 1395 (1983).

[2] S.A. Trugman and S. Kivelson, Phys. Rev. B **31**, 5280 (1985).

[3] S. Kivelson and V. L. Pokrovsky, Phys. Rev. B **40**, 1373 (1989).

[4] F.D.M. Haldane, Phys. Rev. Lett. **51**, 605 (1983).

[5] B.I. Halperin, Phys. Rev. Lett. **52**, 1583 (1984).

[6] H. Fukuyama, P.M. Platzman, and P.W. Anderson, Phys. Rev. B **19**, 5211 (1979).

[7] D. Yoshioka, Phys. Rev. B **27**, 3637 (1983).

[8] D. Yoshioka and P.A. Lee, Phys. Rev. B **27**, 4986 (1983).

[9] K. Maki and X. Zotos, Phys. Rev. B **28**, 4349 (1983).

[10] M. Greiter and F. Wilczek, Mod. Phys. Lett. B **4**, 1063 (1990).

[11] M. Greiter and F. Wilczek, Nucl. Phys. B **370**, 577 (1992).

[12] J.K. Jain, Phys. Rev. Lett. **63**, 199 (1989); Adv. in Phys. **41**, 105 (1992).

[13] B. Rejaei and C.W.J. Beenakker, Phys. Rev. B **46**, 15566 (1992).

[14] C. Gros, S.M. Girvin, G.S. Canright, and M.D. Johnson, Phys. Rev. B **43**, 5883 (1991).

[15] R.B. Laughlin, Phys. Rev. Lett. **60**, 2677 (1988).

[16] A.L. Fetter and C.B. Hanna, Phys. Rev. B **45**, 2335 (1992).

[17] B. Rejaei and C.W.J. Beenakker, Phys. Rev. B **43**, 11392 (1991).

[18] S.C. Zhang, T.H. Hansson, and S. Kivelson, Phys. Rev. Lett. **62**, 82 (1989).

[19] N. Read, Phys. Rev. Lett. **62**, 86 (1989).

[20] A. Lopez and E. Fradkin, Phys. Rev. B **44**, 5246 (1991).

[21] S.G. Ovchinnikov, Pis'ma Zh. Eksp. Teor. Fiz. **54**, 579 (1991) [JETP Lett. **54**, 583 (1991)].

[22] A. Perez Martinez and A. Cabo, Mod. Phys. Lett. B **5**, 1703 (1991).

[23] X.G. Wen, Int. J. Mod. Phys. B **6**, 1711 (1992).

[24] J.M. Kinaret, Y. Meir, N.S. Wingreen, P.A. Lee, and X.G. Wen, Phys. Rev. B **45**, 9489 (1992).

[25] G. Fano and F. Ortolani, Phys. Rev. B **37**, 8179 (1988).

[26] C. Gros and A.H. MacDonald, Phys. Rev. B **42**, 9514 (1990).

[27] *The Quantum Hall Effect*, eds. R.E. Prange and S.M. Girvin (Springer, New York, 1987).

[28] *The Fractional Quantum Hall Effect*, by T. Chakraborty and P. Pietiläinen (Springer, Berlin, 1988).

[29] D. Arovas, J.R. Schrieffer, and F. Wilczek, Phys. Rev. Lett. **53**, 722 (1984).

[30] S. Kivelson, Phys. Rev. Lett. **65**, 3369 (1990).

[31] A.H. MacDonald and S.M. Girvin, Phys. Rev. B **34**, 5639 (1986).

[32] R. Morf and B.I. Halperin, Phys. Rev. B **33**, 2221 (1986).

[33] N. d'Ambrumenil and R. Morf, Phys. Rev. B **40**, 6108 (1989).

[34] S.M. Girvin, Phys. Rev. B **29**, 6012 (1984).

[35] V. Fock, Z. Phys. **47**, 446 (1928); C.G. Darwin, Proc. Camb. Phil. Soc. **27**, 86 (1930).

[36] F.C. Zhang, V.Z. Vulovic, Y. Guo, and S. Das Sarma, Phys. Rev. B **32**, 6920 (1985).

[37] C.W.J. Beenakker, H. van Houten, and A.A.M. Staring, in *Granular Nanoelectronics*, eds. D.K. Ferry, J.R. Berten, and C. Jacobson, NATO ASI series B **251** (Plenum, New York, 1991).

[38] C.W.J. Beenakker and B. Rejaei, Physica B **189**, 147 (1993).

[39] Y. Meir and N.S. Wingreen, Phys. Rev. Lett. **68**, 2512 (1992).

Chapter 5

Exact solution for the distribution of transmission eigenvalues in a disordered wire and comparison with random-matrix theory

1 Introduction

A fundamental problem of mesoscopic physics is to find the statistical distribution of the scattering matrix in an ensemble of disordered conductors. Once this is known, one can compute all moments of the conductance, and of any other transport property, at temperatures which are sufficiently low that the conductor is fully phase-coherent. Random-matrix theory (RMT) addresses this problem on the basis of the assumption that all correlations between the transmission eigenvalues are due to the jacobian from matrix to eigenvalue space.[1, 2, 3] The transmission eigenvalues $T_1, T_2, \ldots T_N$ are the eigenvalues of the matrix product $tt^\dagger$, where t is the $N \times N$ transmission matrix of the conductor. The jacobian is

$$J(\{\lambda_n\}) = \prod_{i<j} |\lambda_j - \lambda_i|^\beta, \tag{1.1}$$

where $\lambda_i \equiv (1 - T_i)/T_i$ is the ratio of reflection to transmission probabilities ($\lambda \geq 0$, since $0 \leq T \leq 1$), and $\beta \in \{1, 2, 4\}$ is the symmetry index of the ensemble of scattering matrices. [In the absence of time-reversal symmetry, one has $\beta = 2$; In the presence of time-reversal symmetry, one has $\beta = 1\,(4)$ in the presence (absence) of spin-rotation symmetry.]

If all correlations are due to the jacobian, then the probability density $P(\{\lambda_n\})$ of the λ's should have the form $P \propto J \prod_i f(\lambda_i)$, or equivalently,

$$P(\{\lambda_n\}) = C \exp\Big[-\beta\Big(\sum_{i<j} u(\lambda_i, \lambda_j) + \sum_i V(\lambda_i)\Big)\Big], \tag{1.2}$$

$$u(\lambda_i, \lambda_j) = -\ln|\lambda_j - \lambda_i|, \tag{1.3}$$

with $V = -\beta^{-1} \ln f$ and C a normalization constant. Eq. (1.2) has the form of a Gibbs distribution at temperature β^{-1} for a fictitious system of classical particles

moving in one dimension in an external potential V, with a logarithmically repulsive interaction u. All microscopic parameters (sample length L, width W, mean free path l, Fermi wave length $\lambda_{\rm F}$) are contained in the single function $V(\lambda)$. The logarithmic repulsion is independent of microscopic parameters, because of its geometric origin.

The RMT probability distribution (1.2), due to Muttalib, Pichard, and Stone, was justified by a maximum-entropy principle for quasi-one-dimensional (quasi-1D) conductors.[2, 3] Quasi-1D means $L \gg W$. In this limit one can assume that the distribution of scattering matrices is only a function of the transmission eigenvalues (isotropy assumption). The distribution (1.2) then maximizes the information entropy subject to the constraint of a given density of eigenvalues. The function $V(\lambda)$ is determined by this constraint and is not specified by RMT.

It was initially believed that Eq. (1.2) would provide an exact description in the quasi-1D limit, if only $V(\lambda)$ were suitably chosen.[3, 4] However, it was shown recently by one of us[5] that RMT is not exact, even in the quasi-1D limit. If one computes from Eq. (1.2) in the metallic regime the variance $\mathrm{Var}\, G$ of the conductance $G = G_0 \sum_n T_n$ (with $G_0 = 2e^2/h$), one finds[5]

$$\mathrm{Var}\, G/G_0 = \frac{1}{8}\beta^{-1}, \tag{1.4}$$

independent of the form of $V(\lambda)$. The diagrammatic perturbation theory[6, 7] of universal conductance fluctuations (UCF) gives instead

$$\mathrm{Var}\, G/G_0 = \frac{2}{15}\beta^{-1} \tag{1.5}$$

for a quasi-1D conductor. The difference between the coefficients $\frac{1}{8}$ and $\frac{2}{15}$ is tiny, but it has the fundamental implication that the interaction between the λ-variables is not precisely logarithmic, or in other words, that there exist correlations between the transmission eigenvalues over and above those induced by the jacobian.

What then is the status of the random-matrix theory of quantum transport? It is obviously highly accurate, so that the true eigenvalue interaction should be close to logarithmic. Is there perhaps a cutoff for large separation of the λ's? Or is the true interaction a many-body interaction, which can not be reduced to the sum of pairwise interactions? That is the problem addressed in this paper. A brief account of our results was reported in a recent Letter.[8]

The transport problem considered here has a counterpart in equilibrium. The Wigner-Dyson RMT of the statistics of the eigenvalues $\{E_n\}$ of a random hamiltonian yields a probability distribution of the form (1.2), with a logarithmic repulsion between the energy levels.[9] It was shown by Efetov[10] and by Al'tshuler and Shklovskiĭ[11] that the logarithmic level repulsion in a small disordered particle (diameter L, diffusion constant D) holds for energy separations small compared to the Thouless energy $E_{\rm c} \equiv \hbar D/L^2$. For larger separations the interaction potential decays algebraically.[12] As we will see, the way in which the RMT of quantum transport breaks down is quite different: The interaction $u(\lambda_i, \lambda_j) = -\ln|\lambda_j - \lambda_i|$ is exact for

$\lambda_i, \lambda_j \ll 1$, i.e. for strongly transmitting scattering channels (recall that $\lambda \ll 1$ implies $T \equiv (1+\lambda)^{-1}$ close to unity). For weakly transmitting channels the repulsion is still logarithmic, but reduced by a factor of two from what one would expect from the jacobian. This modified interaction explains the $\frac{1}{8}$ — $\frac{2}{15}$ discrepancy in the UCF in the metallic regime,[5] and it also explains a missing factor of two in the width of the log-normal distribution of the conductance in the insulating regime.[13]

Our analysis is based on the Dorokhov-Mello-Pereyra-Kumar (DMPK) equation

$$l\frac{\partial P}{\partial L} = \frac{2}{\beta N + 2 - \beta}\sum_{i=1}^{N}\frac{\partial}{\partial \lambda_i}\lambda_i(1+\lambda_i)J\frac{\partial}{\partial \lambda_i}J^{-1}P, \tag{1.6}$$

with ballistic initial condition $\lim_{L\to 0} P = \prod_i \delta(\lambda_i - 0^+)$, which describes the evolution of the eigenvalue distribution function in an ensemble of disordered wires of increasing length. Eq. (1.6) was derived by Dorokhov,[14] (for $\beta = 2$) and by Mello, Pereyra, and Kumar,[15] (for $\beta = 1$, with generalizations to $\beta = 2, 4$ in Refs. [16, 17]) by computing the incremental change of the transmission eigenvalues upon attachment of a thin slice to the wire. It is assumed that the conductor is weakly disordered, $l \gg \lambda_{\rm F}$, so that the scattering in the thin slice can be treated by perturbation theory. A key simplification is the isotropy assumption that the flux incident in one scattering channel is, on average, equally distributed among all outgoing channels. This assumption restricts the applicability of the DMPK equation to the quasi-1D regime $L \gg W$, since it ignores the finite time scale for transverse diffusion.

Eq. (1.6) has the form of a diffusion equation in a complicated N-dimensional space (identified as a certain Riemannian manifold in Ref. [18]). For a coordinate-free "supersymmetry formulation" of this diffusion process, see Refs. [19, 20]. The similarity to diffusion in real space has been given further substance by the demonstration [21] that Eq. (1.6) holds on length scales $\gg l$ regardless of the microscopic scattering properties of the conductor.

The diffusion equation (1.6) has been studied extensively for more than ten years. Exact solutions have been obtained by Mel'nikov[22] and Mello[23] for the case $N = 1$ of a single degree of freedom (when $J \equiv 1$). For $N > 1$ the strong coupling of the scattering channels by the jacobian (1.1) prevented an exact solution by standard methods. The problem simplifies drastically deep in the localized regime ($L \gg Nl$), when the scattering channels become effectively decoupled. Pichard[13] has computed from Eq. (1.6) the log-normal distribution of the conductance in this regime, and has found an excellent agreement with numerical simulations of a quasi-1D Anderson insulator. In the metallic regime ($L \ll Nl$), Mello and Stone[16, 24] were able to compute the first two moments of the conductance, in precise agreement with the diagrammatic perturbation theory of weak localization and UCF [Eq. (1.5)] in the quasi-1D limit. (Their method of moments has also been applied to the shot noise,[25] where there is no diagrammatic theory to compare with.) More general calculations of the weak localization effect[26] and of universal fluctuations[27] [for arbitrary transport properties of the form $A = \sum_n a(T_n)$] were recently developed, based on linearization of Eq. (1.6) in the fluctuations of the λ's around their mean

positions (valid in the large-N metallic regime, when the fluctuations are small). The work of Chalker and Macêdo[27] was motivated by the same $\frac{1}{8}$ — $\frac{2}{15}$ discrepancy[5] as the present paper and Ref. [8], with which it has some overlap.

None of these calculations suffices to determine the form of the eigenvalue interaction, which requires knowledge of the complete distribution function. Here we wish to present (in considerable more detail than in our Letter[8]) the exact solution of Eq. (1.6) for $\beta = 2$.

The outline of this paper is as follows. In Sec. II we solve Eq. (1.6) exactly, for all N and L, for the case $\beta = 2$. The method of solution is a mapping onto a model of non-interacting fermions, inspired by Sutherland's mapping of a different diffusion equation.[28] The case $\beta = 2$ is special, because for other values of β the mapping introduces interactions between the fermions. The free-fermion problem, which is obtained for $\beta = 2$, has the character of a one-dimensional scattering problem in imaginary time. The absence of a ground state is a significant complication, compared with Sutherland's problem.[29, 30, 31] The exact solution which we obtain has the form of a determinant of an $N \times N$ matrix. The determinant can be evaluated in closed form in the metallic regime $L \ll Nl$ and in the insulating regime $L \gg Nl$. These two opposite regimes are discussed separately in Secs. III and IV. We conclude in Sec. V with a comparison of the solution of Eq. (1.6) with the probability distribution (1.2) of random-matrix theory.

2 Exact solution

The solution of the Dorokhov-Mello-Pereyra-Kumar (DMPK) equation (1.6) proceeds in a series of steps, which we describe in separate subsections.

2.1 Transformation of variables

The DMPK equation (1.6) can be written in the form of an N-dimensional Fokker-Planck equation,

$$\frac{\partial}{\partial s} P(\{\lambda_n\}, s) = \sum_{i=1}^{N} \frac{\partial}{\partial \lambda_i} D(\lambda_i) \left(\frac{\partial P}{\partial \lambda_i} + \beta P \frac{\partial}{\partial \lambda_i} \Omega(\{\lambda_n\}) \right), \tag{2.1}$$

$$D(\lambda) = \frac{2}{\gamma} \lambda(1+\lambda), \tag{2.2}$$

$$\Omega(\{\lambda_n\}) = -\sum_{i<j} \ln|\lambda_j - \lambda_i|, \tag{2.3}$$

where we have abbreviated $s = L/l$, $\gamma = \beta N + 2 - \beta$. Eq. (2.1) is the diffusion equation in "time" s of a one-dimensional gas of N classical particles with a logarithmically repulsive interaction potential Ω. The diffusion takes place at temperature β^{-1} in a fictitious non-uniform viscous fluid with diffusion coefficient $D(\lambda)$.

The position dependence of the diffusion coefficient is problematic. We seek to eliminate it by a transformation of variables. Let $\{x_n\}$ be a new set of N independent variables, related to the λ's by $\lambda_n = f(x_n)$. The new probability distribution $P(\{x_n\}, s) = P(\{\lambda_n\}, s) \prod_i |f'(x_i)|$ still satisfies a Fokker-Planck equation, but with a new potential $\Omega(\{x_n\})$ and a new diffusion coefficient $D(x)$. The potential transforms as $\Omega \to \Omega - \beta^{-1} \sum_i \ln |f'(x_i)|$, while the diffusion coefficient transforms as $D \to D/f'(x)^2$. In order to obtain an x-independent diffusion coefficient, we thus need to choose $f(x)$ such that $f(x)[1 + f(x)]/f'(x)^2 =$ constant. The choice $f(x) = \sinh^2 x$ does it.

We therefore transform to a new set of variables $\{x_n\}$, defined by

$$\lambda_n = \sinh^2 x_n, \quad T_n = 1/\cosh^2 x_n. \tag{2.4}$$

Since $T_n \in [0, 1]$, $x_n \geq 0$. The probability distribution of the x-variables satisfies a Fokker-Planck equation with *constant* diffusion coefficient,

$$\frac{\partial}{\partial s} P(\{x_n\}, s) = \frac{1}{2\gamma} \sum_{i=1}^{N} \frac{\partial}{\partial x_i} \left(\frac{\partial P}{\partial x_i} + \beta P \frac{\partial}{\partial x_i} \Omega(\{x_n\}) \right), \tag{2.5}$$

$$\Omega(\{x_n\}) = -\sum_{i<j} \ln |\sinh^2 x_j - \sinh^2 x_i| - \frac{1}{\beta} \sum_i \ln |\sinh 2x_i|. \tag{2.6}$$

It turns out that the x-variables have a special physical significance: The ratio L/x_n equals the channel-dependent localization length of the conductor.[3]

2.2 From Fokker-Planck to Schrödinger equation

Sutherland[28] has shown that a Fokker-Planck equation with constant diffusion coefficient and with a logarithmic interaction potential can be mapped onto a Schrödinger equation with an inverse-square interaction which *vanishes* for $\beta = 2$. The Fokker-Planck equation (2.5) does have a constant diffusion coefficient, but the interaction is not logarithmic. It is not obvious that Sutherland's mapping onto a free-fermion problem should work for the non-translationally invariant interaction (2.6), but surprisingly enough it does.

To map the Fokker-Planck equation (2.5) onto a Schrödinger equation we substitute

$$P(\{x_n\}, s) = \exp\left[-\frac{1}{2} \beta \Omega(\{x_n\}) \right] \Psi(\{x_n\}, s). \tag{2.7}$$

This is a variation on Sutherland's transformation,[28] which we used in Ref. [31] in a different context. Substitution of Eq. (2.7) into Eq. (2.5) yields for Ψ the equation

$$-\frac{\partial \Psi}{\partial s} = -\frac{1}{2\gamma} \sum_{i=1}^{N} \frac{\partial^2 \Psi}{\partial x_i^2} + \frac{\beta}{4\gamma} \Psi \sum_{i=1}^{N} \left[\frac{\beta}{2} \left(\frac{\partial \Omega}{\partial x_i} \right)^2 - \frac{\partial^2 \Omega}{\partial x_i^2} \right]. \tag{2.8}$$

The expression between square brackets is evaluated as follows (we abbreviate $\xi_i = \cosh 2x_i$):

$$\begin{aligned}\sum_{i=1}^{N} \frac{\partial^2 \Omega}{\partial x_i^2} &= 4 \sum_i \sum_{j(\neq i)} \left(\frac{\xi_i^2 - 1}{(\xi_j - \xi_i)^2} + \frac{\xi_i}{\xi_j - \xi_i} \right) + \frac{4}{\beta} \sum_i \frac{1}{\xi_i^2 - 1} \\ &= 4 \sum_i \sum_{j(\neq i)} \frac{\xi_i^2 - 1}{(\xi_j - \xi_i)^2} + \frac{4}{\beta} \sum_i \frac{1}{\xi_i^2 - 1} - 4 \binom{N}{2}, \end{aligned} \tag{2.9}$$

$$\begin{aligned}\sum_{i=1}^{N} \left(\frac{\partial \Omega}{\partial x_i} \right)^2 &= 4 \sum_i \sum_{j(\neq i)} \sum_{k(\neq i)} \frac{\xi_i^2 - 1}{(\xi_j - \xi_i)(\xi_k - \xi_i)} - \frac{8}{\beta} \sum_i \sum_{j(\neq i)} \frac{\xi_i}{\xi_j - \xi_i} + \frac{4}{\beta^2} \sum_i \frac{\xi_i^2}{\xi_i^2 - 1} \\ &= 4 \sum_i \sum_{j(\neq i)} \frac{\xi_i^2 - 1}{(\xi_j - \xi_i)^2} + \frac{4}{\beta^2} \sum_i \frac{1}{\xi_i^2 - 1} + \frac{4}{\beta^2} N + \frac{8}{\beta} \binom{N}{2} + 8 \binom{N}{3}. \end{aligned} \tag{2.10}$$

In the final equality we have used that for any three distinct indices i, j, k

$$\frac{\xi_i^2 - 1}{(\xi_j - \xi_i)(\xi_k - \xi_i)} + \frac{\xi_j^2 - 1}{(\xi_i - \xi_j)(\xi_k - \xi_j)} + \frac{\xi_k^2 - 1}{(\xi_i - \xi_k)(\xi_j - \xi_k)} \equiv 1, \tag{2.11}$$

so that the triple sum over $k \neq i \neq j$ collapses to a double sum over $i \neq j$. Collecting results, we find that Ψ satisfies a Schrödinger equation in imaginary time,

$$-\frac{\partial \Psi}{\partial s} = (\mathcal{H} - U)\Psi, \tag{2.12}$$

$$\mathcal{H} = -\frac{1}{2\gamma} \sum_i \left(\frac{\partial^2}{\partial x_i^2} + \frac{1}{\sinh^2 2x_i} \right) + \frac{\beta(\beta - 2)}{2\gamma} \sum_{i<j} \frac{\sinh^2 2x_j + \sinh^2 2x_i}{(\cosh 2x_j - \cosh 2x_i)^2}, \tag{2.13}$$

$$U = -\frac{N}{2\gamma} - N(N-1)\frac{\beta}{\gamma} - N(N-1)(N-2)\frac{\beta^2}{6\gamma}. \tag{2.14}$$

The interaction potential in the hamiltonian (2.13) is attractive for $\beta = 1$ and repulsive for $\beta = 4$. For $\beta = 2$ the interaction vanishes identically, reducing $\mathcal{H}$ to a sum of single-particle hamiltonians $\mathcal{H}_0$,

$$\mathcal{H}_0 = -\frac{1}{4N} \frac{\partial^2}{\partial x^2} - \frac{1}{4N \sinh^2 2x}. \tag{2.15}$$

(Note that $\gamma = 2N$ for $\beta = 2$.) It might be possible to solve also the interacting Schrödinger equation (2.12) for $\beta = 1$ or 4, by some modification of techniques developed for the Sutherland hamiltonian,[28, 29, 30] but in this paper we focus on the simplest case $\beta = 2$ of broken time-reversal symmetry.

To complete the mapping onto a single-particle problem, we need to consider the boundary condition at the edge $x = 0$. (Recall that $x \geq 0$.) Conservation of probability implies for P the boundary condition (one for each $i = 1, 2, \ldots N$)

$$\lim_{x_i \to 0} \left(\frac{\partial P}{\partial x_i} + \beta P \frac{\partial \Omega}{\partial x_i} \right) = 0. \tag{2.16}$$

According to Eq. (2.7), the corresponding boundary condition on Ψ is

$$\lim_{x_i \to 0} \left(\frac{\partial \Psi}{\partial x_i} + \frac{1}{2} \beta \Psi \frac{\partial \Omega}{\partial x_i} \right) = 0, \tag{2.17}$$

which in view of Eq. (2.6) simplifies to

$$\lim_{x_i \to 0} \left(\frac{\partial \Psi}{\partial x_i} - \frac{\Psi}{\sinh 2x_i} \right) = 0, \tag{2.18}$$

independent of β. Fortunately, the boundary condition does not couple different degrees of freedom, so that we have indeed obtained a single-particle problem for $\beta = 2$.

2.3 From probability distribution to fermion Green's function

We seek a solution $P(\{x_n\}, s \,|\, \{y_n\})$ of the Fokker-Planck equation (2.5) with symmetrized delta-function initial condition

$$P(\{x_n\}, 0 \,|\, \{y_n\}) = \frac{1}{N!} \sum_{\pi} \prod_{i=1}^{N} \delta(x_i - y_{\pi_i}). \tag{2.19}$$

The sum in Eq. (2.19) is over all $N!$ permutations of $1, 2, \ldots N$. Eventually, we will take the limit $\{y_n\} \to 0$ of a ballistic initial condition, but it is convenient to first consider the more general initial condition (2.19). In this subsection we use the mapping onto a Schrödinger equation of the previous subsection to relate the probability distribution $P(\{x_n\}, s \,|\, \{y_n\})$ to the N-fermion Green's function $G(\{x_n\}, s \,|\, \{y_n\})$.

We first note that, since $\exp(-\beta\Omega)$ is an s-independent solution of the Fokker-Planck equation (2.5), $\exp(-\frac{1}{2}\beta\Omega)$ is an s-independent solution of the Schrödinger equation (2.12) [in view of the mapping (2.7)]. For a particular ordering of the x_n's, the function $\Psi_0 \propto \exp(-\frac{1}{2}\beta\Omega)$ is therefore an eigenfunction of the N-fermion hamiltonian $\mathcal{H}$ with eigenvalue U. Anti-symmetrization yields the fermion eigenstate

$$\Psi_0(\{x_n\}) = C \exp\left[-\frac{1}{2} \beta \Omega(\{x_n\}) \right] \prod_{i<j} \frac{x_j - x_i}{|x_j - x_i|}, \tag{2.20}$$

with C a normalization constant.

We obtain the N-fermion Green's function G from the probability distribution P by the similarity transformation

$$G(\{x_n\}, s \,|\, \{y_n\}) = \Psi_0^{-1}(\{x_n\}) P(\{x_n\}, s \,|\, \{y_n\}) \Psi_0(\{y_n\}). \tag{2.21}$$

To verify this, we first observe that G is by construction anti-symmetric under a permutation of two x or two y variables. For a given order of the x_n's, the function G satisfies the Schrödinger equation

$$-\frac{\partial G}{\partial s} = (\mathcal{H} - U) G, \tag{2.22}$$

in view of Eqs. (2.7), (2.12), and (2.20). Finally, Eq. (2.19) implies the initial condition

$$G(\{x_n\}, 0 \,|\, \{y_n\}) = \frac{1}{N!} \sum_{\pi} \sigma_\pi \prod_{i=1}^{N} \delta(x_i - y_{\pi_i}), \tag{2.23}$$

with σ_π the sign of the permutation. Hence G is indeed the N-fermion Green's function.

The relation (2.21) holds for any β. In the remainder of this paper we consider the non-interacting case $\beta = 2$. The eigenstate (2.20) then takes the form

$$\Psi_0(\{x_n\}) = C \prod_{i<j} (\sinh^2 x_j - \sinh^2 x_i) \prod_i (\sinh 2x_i)^{1/2}. \tag{2.24}$$

The N-fermion Green's function G becomes a Slater determinant of the single-particle Green's function G_0,

$$G(\{x_n\}, s \,|\, \{y_n\}) = \frac{\mathrm{e}^{Us}}{N!} \operatorname{Det} G_0(x_n, s \,|\, y_m), \tag{2.25}$$

where $\operatorname{Det} a_{nm}$ denotes the determinant of the $N \times N$ matrix with elements a_{nm}. The function $G_0(x, s \,|\, y)$ is a solution of the single-particle Schrödinger equation $-\partial G_0/\partial s = \mathcal{H}_0 G_0$ in the variable x, with initial condition $G(x, 0 \,|\, y) = \delta(x - y)$. In the following subsection we will compute the single-particle Green's function G_0. The probability distribution P, for $\beta = 2$, then follows from Eqs. (2.21), (2.24), and (2.25):

$$P(\{x_n\}, s \,|\, \{y_n\}) = \frac{\prod_{i<j} (\sinh^2 x_j - \sinh^2 x_i) \prod_i (\sinh 2x_i)^{1/2}}{\prod_{i<j} (\sinh^2 y_j - \sinh^2 y_i) \prod_i (\sinh 2y_i)^{1/2}} \frac{\mathrm{e}^{Us}}{N!} \operatorname{Det} G_0(x_n, s \,|\, y_m). \tag{2.26}$$

2.4 Computation of Green's function

To compute the Green's function G_0 of the single-particle hamiltonian (2.15) we need to solve the eigenvalue equation

$$-\frac{1}{4N} \frac{d^2}{dx^2} \psi(x) - \frac{1}{4N} \frac{\psi(x)}{\sinh^2 2x} = \varepsilon \psi(x), \tag{2.27}$$

with the boundary condition dictated by Eq. (2.18),

$$\lim_{x \to 0} \left(\frac{d\psi}{dx} - \frac{\psi}{\sinh 2x} \right) = 0. \tag{2.28}$$

We have found that the substitution

$$\psi(x) = (\sinh 2x)^{1/2} f(\cosh 2x) \tag{2.29}$$

transforms Eq. (2.27) into Legendre's differential equation in the variable $z = \cosh 2x$,

$$\frac{d}{dz}\left[(1-z^2)\frac{d}{dz}f(z)\right] = (N\varepsilon + \frac{1}{4})f(z). \tag{2.30}$$

The boundary condition (2.28) restricts the solutions of Eq. (2.30) to the Legendre functions of the first kind $\mathrm{P}_\nu(z)$. The index ν is given by $\nu = -\frac{1}{2} + \frac{1}{2}\mathrm{i}k$ with k a real number. (These Legendre functions are also known as "toroidal functions", because they appear as solutions to the Laplace equation in toroidal coordinates.) The numbers ν, k, and ε are related by $-\nu(\nu+1) = N\varepsilon + \frac{1}{4}$ and $\varepsilon = \frac{1}{4}k^2/N$. We can restrict ourselves to $k \geq 0$, since the functions $\mathrm{P}_{-\frac{1}{2}+\frac{1}{2}\mathrm{i}k}$ and $\mathrm{P}_{-\frac{1}{2}-\frac{1}{2}\mathrm{i}k}$ are identical.

We conclude that the spectrum of $\mathcal{H}_0$ is continuous, with positive eigenvalues $\varepsilon = \frac{1}{4}k^2/N$. The eigenfunctions $\psi_k(x)$ are real functions given by

$$\psi_k(x) = [\pi k \tanh(\frac{1}{2}\pi k)\sinh(2x)]^{1/2}\,\mathrm{P}_{\frac{1}{2}(\mathrm{i}k-1)}(\cosh 2x). \tag{2.31}$$

They form a complete and orthonormal set,

$$\int_0^\infty dk\,\psi_k(x)\psi_k(x') = 2\pi\delta(x-x'), \tag{2.32}$$

$$\int_0^\infty dx\,\psi_k(x)\psi_{k'}(x) = 2\pi\delta(k-k'), \tag{2.33}$$

in accordance with the inversion formula in Ref. [32]. The single-particle Green's function G_0 has the corresponding spectral representation

$$\begin{aligned} G_0(x,s\,|\,y) &= (2\pi)^{-1}\int_0^\infty dk\,\exp(-\frac{1}{4}k^2 s/N)\,\psi_k(x)\psi_k(y) \\ &= \frac{1}{2}(\sinh 2x \sinh 2y)^{1/2}\int_0^\infty dk\,\exp(-\frac{1}{4}k^2 s/N)k\tanh(\frac{1}{2}\pi k) \\ &\qquad \times \mathrm{P}_{\frac{1}{2}(\mathrm{i}k-1)}(\cosh 2x)\mathrm{P}_{\frac{1}{2}(\mathrm{i}k-1)}(\cosh 2y). \end{aligned} \tag{2.34}$$

2.5 Ballistic initial condition

Equations (2.26) and (2.34) together determine the probability distribution $P(\{x_n\}, s\,|\,\{y_n\})$ with initial condition (2.19),

$$\begin{aligned} P &= C(s)\frac{\prod_{i<j}(\sinh^2 x_j - \sinh^2 x_i)\prod_i(\sinh 2x_i)}{\prod_{i<j}(\sinh^2 y_j - \sinh^2 y_i)} \\ &\quad \times \mathrm{Det}\left[\int_0^\infty dk\,\exp(-\frac{1}{4}k^2 s/N)k\tanh(\frac{1}{2}\pi k)\mathrm{P}_{\frac{1}{2}(\mathrm{i}k-1)}(\cosh 2x_n)\mathrm{P}_{\frac{1}{2}(\mathrm{i}k-1)}(\cosh 2y_m)\right] \\ &= C(s)\prod_{i<j}(\sinh^2 x_j - \sinh^2 x_i)\prod_i(\sinh 2x_i)\int_0^\infty dk_1\int_0^\infty dk_2\cdots\int_0^\infty dk_N \\ &\quad \times \prod_i\left[\exp(-\frac{1}{4}k_i^2 s/N)k_i\tanh(\frac{1}{2}\pi k_i)\mathrm{P}_{\frac{1}{2}(\mathrm{i}k_i-1)}(\cosh 2x_i)\right]\frac{\mathrm{Det}\,\mathrm{P}_{\frac{1}{2}(\mathrm{i}k_n-1)}(\cosh 2y_m)}{\prod_{i<j}(\sinh^2 y_j - \sinh^2 y_i)}. \end{aligned} \tag{2.35}$$

We have absorbed all x and y independent factors into the function $C(s)$, which is fixed by the requirement that P is normalized to unity,

$$\int_0^\infty dx_1 \int_0^\infty dx_2 \cdots \int_0^\infty dx_N \, P = 1. \tag{2.36}$$

In the second equality in Eq. (2.35) we have applied the identity $\mathrm{Det}\,(b_n a_{nm}) = (\prod_i b_i)\mathrm{Det}\, a_{nm}$ to isolate the factors containing the y-variables.

Now it remains to take the limit $\{y_n\} \to 0$ of a ballistic initial condition. The limit is tricky because it involves a cancellation of zeroes of the determinant in the numerator with zeroes of the alternating function in the denominator. It is convenient to first write the alternating function as a Vandermonde determinant,

$$\prod_{i<j} (\sinh^2 y_j - \sinh^2 y_i) = \mathrm{Det}\,(\sinh^2 y_m)^{n-1}. \tag{2.37}$$

Next, we expand the Legendre function in powers of $\sinh^2 y$,

$$\mathrm{P}_{\frac{1}{2}(\mathrm{i}k-1)}(\cosh 2y) = \sum_{p=1}^{\infty} c_p(k)(\sinh^2 y)^{p-1}. \tag{2.38}$$

The factors $c_p(k)$ are polynomials in k^2, with $c_1(k) \equiv 1$ and

$$c_p(k) = (-1)^{p-1}[2^{p-1}(p-1)!]^{-2}\,(k^2+1^2)(k^2+3^2)\cdots(k^2+(2p-3)^2) \tag{2.39}$$

for $p \geq 2$. In the limit $y \to 0$, we can truncate the expansion (2.38) after the first N terms, that is to say,

$$\lim_{\{y_n\}\to 0} \frac{\mathrm{Det}\,\mathrm{P}_{\frac{1}{2}(\mathrm{i}k_n-1)}(\cosh 2y_m)}{\prod_{i<j}(\sinh^2 y_j - \sinh^2 y_i)} = \lim_{\{y_n\}\to 0} \frac{\mathrm{Det}\left[\sum_{p=1}^{N} c_p(k_n)(\sinh^2 y_m)^{p-1}\right]}{\mathrm{Det}\,(\sinh^2 y_m)^{n-1}}. \tag{2.40}$$

The numerator on the r.h.s. of Eq. (2.40) factors as the product of two determinants, one of which is just the Vandermonde determinant in the denominator, so that the whole quotient reduces to the single determinant $\mathrm{Det}\, c_m(k_n)$. This determinant can be simplified by means of the identity

$$\mathrm{Det}\, c_m(k_n) = c_0\, \mathrm{Det}\,(k_n^2)^{m-1}, \tag{2.41}$$

with c_0 a numerical coefficient. Eq. (2.41) holds because the determinant of a matrix is unchanged if any one column of the matrix is added to any other column, so that we can reduce the polynomial $c_m(k)$ in k^2 of degree $m-1$ to just its highest order term $k^{2(m-1)}$ times a numerical coefficient.

Collecting results, we find

$$\lim_{\{y_n\}\to 0} \frac{\mathrm{Det}\,\mathrm{P}_{\frac{1}{2}(\mathrm{i}k_n-1)}(\cosh 2y_m)}{\prod_{i<j}(\sinh^2 y_j - \sinh^2 y_i)} = c_0\, \mathrm{Det}\,(k_n^2)^{m-1}. \tag{2.42}$$

Substituting into Eq. (2.35), and absorbing the coefficient c_0 in the function $C(s)$, we obtain the probability distribution $P(\{x_n\}, s)$ for a ballistic initial condition,

$$P(\{x_n\},s) = C(s)\prod_{i<j}(\sinh^2 x_j - \sinh^2 x_i)\prod_i(\sinh 2x_i) \times \mathrm{Det}\left[\int_0^\infty dk\, \exp(-\frac{1}{4}k^2 s/N)\tanh(\frac{1}{2}\pi k)k^{2m-1}\, \mathrm{P}_{\frac{1}{2}(ik-1)}(\cosh 2x_n)\right]. \tag{2.43}$$

This is the exact solution of the DMPK equation for the case $\beta = 2$.

3 Metallic regime

3.1 Probability distribution

The solution (2.43) holds for any s and N. It can be simplified in the regime $1 \ll s \ll N$ of a conductor which is long compared to the mean free path l but short compared to the localization length Nl. This is the metallic regime. The dominant contribution to the integral over k in Eq. (2.43) then comes from the range $k > (N/s)^{1/2} \gg 1$. In this range $\tanh(\frac{1}{2}\pi k) \to 1$ and the Legendre function simplifies to a Bessel function, [1]

$$\mathrm{P}_{\frac{1}{2}(ik-1)}(\cosh 2x) = J_0(kx)\left(\frac{2x}{\sinh 2x}\right)^{\frac{1}{2}} \quad \text{for } k \gg 1,\ x \gg 1/k. \tag{3.1}$$

The second condition $x \gg 1/k$ on Eq. (3.1) implies the restriction $x \gg (s/N)^{1/2}$, which is irrelevant since $s/N \ll 1$. The k-integration can now be carried out analytically,

$$\int_0^\infty dk\, \exp(-k^2 s/4N)k^{2m-1}\, J_0(kx_n) = \frac{1}{2}(m-1)!\,(4N/s)^m \exp(-x_n^2 N/s)L_{m-1}(x_n^2 N/s), \tag{3.2}$$

with L_{m-1} a Laguerre polynomial. We then apply the determinantal identity

$$\mathrm{Det}\, L_{m-1}(x_n^2 N/s) = c\,\mathrm{Det}\,(x_n^2)^{m-1} = c\prod_{i<j}(x_j^2 - x_i^2), \tag{3.3}$$

with c an x-independent number [which can be absorbed in $C(s)$]. Eq. (3.3) is derived in the same way as Eq. (2.41), by combining columns of the matrix of polynomials in x^2. Collecting results, we find that the general solution (2.43) simplifies in the metallic regime to

$$P(\{x_n\},s) = C(s)\prod_{i<j}\left[(\sinh^2 x_j - \sinh^2 x_i)(x_j^2 - x_i^2)\right]\prod_i\left[\exp(-x_i^2 N/s)(x_i \sinh 2x_i)^{1/2}\right]. \tag{3.4}$$

[1] The useful asymptotic relation (3.1) between a Legendre function and a Bessel function does not appear in the handbooks on special functions which we consulted. We obtained it by combining the two asymptotic expansions (8.10.7) and (9.2.1) in the *Handbook of Mathematical Functions*, ed. by M. Abramowitz and I. A. Stegun, (Dover, New York, 1972).

In the remainder of this section we use the probability distribution (3.4) to compute various statistical quantities of interest. For that purpose it is convenient to write P as a Gibbs distribution,

$$P(\{x_n\},s) = C(s)\exp\Big[-\beta\Big(\sum_{i<j}u(x_i,x_j)+\sum_i V(x_i,s)\Big)\Big], \tag{3.5}$$

$$u(x_i,x_j) = -\frac{1}{2}\ln|\sinh^2 x_j-\sinh^2 x_i| - \frac{1}{2}\ln|x_j^2-x_i^2|, \tag{3.6}$$

$$V(x,s) = \frac{1}{2}Ns^{-1}x^2 - \frac{1}{4}\ln(x\sinh 2x), \tag{3.7}$$

with $\beta=2$ understood.

3.2 Eigenvalue density

The mean density $\langle\rho(x)\rangle_s$ of the x-variables is defined as the ensemble average with distribution $P(\{x_n\},s)$ of the microscopic density $\rho(x)$:

$$\rho(x) = \sum_{n=1}^{N}\delta(x-x_n), \tag{3.8}$$

$$\langle\rho(x)\rangle_s = \int_0^\infty dx_1\int_0^\infty dx_2\cdots\int_0^\infty dx_N\, P(\{x_n\},s)\rho(x). \tag{3.9}$$

The mean density is determined to leading order in N by the integral equation

$$-\int_0^\infty dx'\,\langle\rho(x')\rangle_s\, u(x,x') = V(x,s)+\text{const.} \tag{3.10}$$

The additive constant (which may depend on s but is independent of x) is fixed by the normalization condition

$$\int_0^\infty dx\,\langle\rho(x)\rangle_s = N. \tag{3.11}$$

Eq. (3.10) can be understood intuitively as the condition for mechanical equilibrium of a fictitious one-dimensional gas with two-body interaction u in a confining potential V. Dyson[33] has shown that corrections to Eq. (3.10) are an order $N^{-1}\ln N$ smaller than the terms retained, and are β-dependent. [2] These corrections are responsible for the weak-localization effect in the conductance.[26] Here we consider only the leading order contribution to the density, which is of order N and which is independent of β.

Substituting the functions $u(x,x')$ and $V(x,s)$ from Eq. (3.5) into Eq. (3.10), and taking the derivative with respect to x to eliminate the additive constant, we obtain the equation

$$\frac{s}{2N}\int_0^\infty dx'\,\langle\rho(x')\rangle_s\left(\frac{\sinh 2x}{\sinh^2 x-\sinh^2 x'}+\frac{2x}{x^2-x'^2}\right) = x+\mathcal{O}(1/N). \tag{3.12}$$

[2] Dyson's derivation of Eq. (3.10) is for a logarithmic interaction potential, but it is readily generalized to other repulsive interactions $u(x,x')$.

We note that

$$\begin{aligned}\int_0^s dx' \left(\frac{\sinh 2x}{\sinh^2 x - \sinh^2 x'} + \frac{2x}{x^2 - x'^2} \right) &= \ln \left| \frac{\sinh(s+x)}{\sinh(s-x)} \right| + \ln \left| \frac{s+x}{s-x} \right| \\ &= 2x + \mathcal{O}(x/s), \quad \text{for } s \gg 1,\ s \gg x. \end{aligned} \tag{3.13}$$

It follows that the uniform density

$$\langle \rho(x) \rangle_s = \frac{N}{s} \theta(s-x) \tag{3.14}$$

is the solution of Eq. (3.12) in the regime $s \gg 1$, $s \gg x$. (The function $\theta(\xi)$ equals 1 for $\xi > 0$ and 0 for $\xi < 0$.) The result (3.14) was first obtained by Mello and Pichard, by direct integration of the DMPK equation.[4] To order N, the x-variables have a uniform density of Nl/L, with a cutoff at L/l such that the normalization (3.11) is satisfied. In the cutoff region $x \sim L/l$ the density deviates from uniformity, but this region is irrelevant since the transmission eigenvalues are exponentially small for $x \gg 1$.

3.3 Correlation function

The two-point correlation function $K(x, x', s)$ is defined by

$$K(x, x', s) = \langle \rho(x) \rangle_s \langle \rho(x') \rangle_s - \langle \rho(x) \rho(x') \rangle_s. \tag{3.15}$$

We compute the two-point correlation function by the general method of Ref. [5], which is based on an exact relationship between K and the functional derivative of the mean eigenvalue density $\langle \rho \rangle$ with respect to the eigenvalue potential V:

$$K(x, x', s) = \frac{1}{\beta} \frac{\delta \langle \rho(x) \rangle_s}{\delta V(x', s)}. \tag{3.16}$$

Eq. (3.16) holds for any probability distribution of the form (3.5), regardless of whether the interaction is logarithmic or not. In the large-N limit the functional derivative can be evaluated from the integral equation (3.10). The functional derivative $\delta \langle \rho \rangle / \delta V$ equals the solving kernel of

$$-\int_0^\infty dx'\, \psi(x') u(x, x') = \phi(x) + \text{const}, \tag{3.17}$$

where the additive constant has to be chosen such that ψ has zero mean,

$$\int_0^\infty dx\, \psi(x) = 0, \tag{3.18}$$

since the variations in $\langle \rho \rangle$ have to occur at constant N. Because of Eq. (3.16), the integral solution

$$\psi(x) = \int_0^\infty dx'\, \beta K(x, x') \phi(x') \tag{3.19}$$

of Eq. (3.17) directly determines the two-point correlation function. It turns out that $K(x,x') \equiv K(x,x',s)$ is independent of s in the metallic regime.

The integral equation (3.17) can be solved analytically by the following method. We extend the functions ψ and ϕ symmetrically to negative x, by defining $\psi(-x) \equiv \psi(x)$, $\phi(-x) \equiv \phi(x)$. We then note that the decomposition

$$\begin{aligned} u(x,x') &= -\frac{1}{2}\mathcal{U}(x-x') - \frac{1}{2}\mathcal{U}(x+x') + \ln 2, && (3.20)\\ \mathcal{U}(x) &= \ln|2x\sinh x|, && (3.21)\end{aligned}$$

transforms the integral equation (3.17) into a convolution,

$$\int_{-\infty}^{\infty} dx'\,\psi(x')\,\mathcal{U}(x-x') = 2\phi(x) + \text{const}, \tag{3.22}$$

which is readily solved by Fourier transformation. The Fourier transformed kernel is

$$\mathcal{U}(k) \equiv \int_{-\infty}^{\infty} dx\,\mathrm{e}^{\mathrm{i}kx}\,\mathcal{U}(x) = -\frac{\pi}{|k|}[1 + \operatorname{cotanh}(\tfrac{1}{2}\pi|k|)]. \tag{3.23}$$

The k-space solution to Eq. (3.22) is $\psi(k) = 2\phi(k)/\mathcal{U}(k)$, which automatically satisfies the normalization (3.18). In x-space the solution becomes

$$\begin{aligned} \psi(x) &= 2\int_{-\infty}^{\infty} dx'\,\mathcal{K}(x-x')\phi(x') \\ &= 2\int_{0}^{\infty} dx'\,[\mathcal{K}(x-x') + \mathcal{K}(x+x')]\,\phi(x'), && (3.24)\\ \mathcal{K}(x) &= \frac{1}{2\pi}\int_{-\infty}^{\infty} dk\,\mathrm{e}^{-\mathrm{i}kx}\,\frac{1}{\mathcal{U}(k)} = \frac{1}{\pi}\int_{0}^{\infty} dk\,\frac{\cos kx}{\mathcal{U}(k)}. && (3.25)\end{aligned}$$

Combining Eqs. (3.19), (3.23), and (3.24), we find that the two-point correlation function is given by

$$\begin{aligned} K(x,x') &= \mathcal{K}(x-x') + \mathcal{K}(x+x'), && (3.26)\\ \mathcal{K}(x) &= -\frac{2}{\beta\pi^2}\int_{0}^{\infty} dk\,\frac{k\cos kx}{1+\operatorname{cotanh}(\frac{1}{2}\pi k)}, && (3.27)\end{aligned}$$

with $\beta = 2$. The inverse Fourier transform (3.27) evaluates to

$$\begin{aligned} \mathcal{K}(x) &= \frac{1}{2\beta\pi^2}\,\frac{d^2}{dx^2}\ln[1+(\pi/x)^2] \\ &= \frac{1}{\beta\pi^2}\,\mathrm{Re}\left[(x+\mathrm{i}0^+)^{-2} - (x+\mathrm{i}\pi)^{-2}\right], && (3.28)\end{aligned}$$

where 0^+ is a positive infinitesimal.

We derived[8] these expressions for the two-point correlation function for the case $\beta = 2$. A direct integration of the DMPK equation by Chalker and Macêdo[27] shows that the function $K(x,x')$ has in fact the $1/\beta$ dependence indicated in Eq. (3.28), as expected from general considerations.[5]

3.4 Universal conductance fluctuations

Now that we have the two-point correlation function, we can compute the variance $\operatorname{Var} A = \langle A^2 \rangle - \langle A \rangle^2$ of any linear statistic $A = \sum_{n=1}^{N} a(x_n)$ on the transmission eigenvalues (recall that $T_n \equiv \cosh^{-2} x_n$). By definition

$$\operatorname{Var} A = -\int_0^\infty dx \int_0^\infty dx'\, a(x)a(x')K(x,x'). \tag{3.29}$$

Substituting Eq. (3.28) we find

$$\operatorname{Var} A = \frac{1}{\beta\pi^2} \int_0^\infty dk\, \frac{k|a(k)|^2}{1 + \operatorname{cotanh}(\frac{1}{2}\pi k)}, \tag{3.30}$$

$$a(k) = 2\int_0^\infty dx\, a(x) \cos kx, \tag{3.31}$$

or equivalently,

$$\operatorname{Var} A = -\frac{1}{2\beta\pi^2} \int_0^\infty dx \int_0^\infty dx' \left(\frac{da(x)}{dx}\right)\left(\frac{da(x')}{dx'}\right) \ln\left(\frac{1+\pi^2(x+x')^{-2}}{1+\pi^2(x-x')^{-2}}\right). \tag{3.32}$$

To obtain the variance of the conductance $G/G_0 = \sum_n T_n$ (with $G_0 = 2e^2/h$), we substitute $a(x) = \cosh^{-2} x$, hence $a(k) = \pi k/\sinh(\frac{1}{2}\pi k)$, hence

$$\operatorname{Var} G/G_0 = \frac{2}{15}\,\beta^{-1}, \tag{3.33}$$

in agreement with Eq. (1.5). In the same way one can compute the variance of other transport properties. For example, for the shot-noise power[34] $P/P_0 = \sum_n T_n(1-T_n)$ (with $P_0 = 2e|V|G_0$ and V the applied voltage) we substitute $a(x) = \cosh^{-2} x - \cosh^{-4} x$, hence $a(k) = \frac{1}{6}\pi k(2-k^2)(\sinh\frac{1}{2}\pi k)^{-1}$, hence

$$\operatorname{Var} P/P_0 = \frac{46}{2835}\,\beta^{-1}, \tag{3.34}$$

in agreement with the result obtained by a moment expansion of the DMPK equation [25]. Another example is the conductance $G_{\rm NS}$ of a normal-superconductor junction, which for $\beta = 1$ is a linear statistic,[35] $G_{\rm NS}/G_0 = \sum_n 2T_n^2(2-T_n)^{-2}$. We substitute $a(x) = 2\cosh^{-4} x\,(2-\cosh^{-2} x)^2 = 2\cosh^{-2}(2x)$, hence $a(k) = \frac{1}{2}\pi k/\sinh(\frac{1}{4}\pi k)$, hence

$$\operatorname{Var} G_{\rm NS}/G_0 = \frac{16}{15} - \frac{48}{\pi^4}. \tag{3.35}$$

Finally, for the variance of the critical current $I_{\rm c}$ of a point-contact Josephson junction (which is also a linear statistic for $\beta = 1$)[36, 37] we compute

$$\operatorname{Var} I_{\rm c}/I_0 = 0.0890, \tag{3.36}$$

with $I_0 = e\Delta/\hbar$ and Δ the superconducting energy gap.

As in the previous subsection, we note that our results are derived for $\beta = 2$, and that the $1/\beta$ dependence of the variance in Eq. (3.32) needs the justification provided by the calculation of Chalker and Macêdo.[27]

4 Insulating regime

The solution (2.43) can also be simplified in the regime $1 \ll N \ll s$ of a conductor which is long compared to the localization length Nl. This is the insulating regime. It is sufficient to consider the range $x_n \gg 1$, since the probability that $x < 1$ is of order N/s which is $\ll 1$. The appropriate asympotic expansion of the Legendre function is

$$\mathrm{P}_{\frac{1}{2}(\mathrm{i}k-1)}(\cosh 2x) = (2\pi \sinh 2x)^{-1/2}\,\mathrm{Re}\,\frac{2\Gamma(\frac{1}{2}\mathrm{i}k)\mathrm{e}^{\mathrm{i}kx}}{\Gamma(\frac{1}{2}+\frac{1}{2}\mathrm{i}k)} \quad \text{for } x \gg 1. \tag{4.1}$$

For $s/N \gg 1$, the dominant contribution to the integral over k in Eq. (2.43) comes from the range $k \ll 1$. In this range $\tanh(\frac{1}{2}\pi k) \to \frac{1}{2}\pi k$ and the ratio of Gamma functions in Eq. (4.1) simplifies to

$$\frac{\Gamma(\frac{1}{2}\mathrm{i}k)}{\Gamma(\frac{1}{2}+\frac{1}{2}\mathrm{i}k)} = (\frac{1}{2}\mathrm{i}k\sqrt{\pi})^{-1} \quad \text{for } k \ll 1. \tag{4.2}$$

The k-integration can now be carried out analytically,

$$\begin{aligned}\int_0^\infty dk\, \exp(-k^2 s/4N)\, k^{2m-1}\, \sin(kx_n) = \\ (-1)^{m-1}\pi^{1/2}(N/s)^m \exp(-x_n^2 N/s) H_{2m-1}(x_n\sqrt{N/s}),\end{aligned} \tag{4.3}$$

with H_{2m-1} a Hermite polynomial. We then apply the determinantal identity [cf. Eq. (3.3)]

$$\mathrm{Det}\, H_{2m-1}(x_n\sqrt{N/s}) = c\,\mathrm{Det}\, x_n^{2m-1} = c\prod_i x_i \prod_{i<j}(x_j^2 - x_i^2), \tag{4.4}$$

with c an x-independent number. Collecting results, we find that the general solution (2.43) reduces in the insulating regime to

$$P(\{x_n\},s) = C(s)\prod_{i<j}\left[(\sinh^2 x_j - \sinh^2 x_i)(x_j^2 - x_i^2)\right]\prod_i\left[\exp(-x_i^2 N/s)x_i(\sinh 2x_i)^{1/2}\right]. \tag{4.5}$$

(This formula was cited incorrectly in our Letter.[8])

The result (4.5) can be simplified further by ordering the x_n's from small to large and using that $1 \ll x_1 \ll x_2 \ll \cdots \ll x_N$ in the insulating regime ($s \gg N$). The distribution function then factorizes,

$$\begin{aligned} P(\{x_n\},s) &= C(s)\prod_{i=1}^N \exp\left[(2i-1)x_i - x_i^2 N/s\right] \\ &= (\pi s/N)^{-N/2}\prod_{i=1}^N \exp\left[-(N/s)(x_i - \bar{x}_i)^2\right]. \end{aligned} \tag{4.6}$$

The x_n's have a gaussian distribution with mean $\bar{x}_n = \frac{1}{2}(s/N)(2n-1)$ and variance $\frac{1}{2}s/N$. The width of the gaussian is smaller than the mean spacing by a factor $(N/s)^{1/2}$, which is $\ll 1$, so that indeed $1 \ll x_1 \ll x_2 \ll \cdots \ll x_N$, as anticipated.

The conductance $G/G_0 = \sum_n \cosh^{-2} x_n$ is dominated by x_1, i.e. by the smallest of the x_n's. Since $x_1 \gg 1$ we may approximate $G/G_0 = 4\exp(-2x_1)$. It follows that the conductance has a log-normal distribution, with mean $\langle \ln G/G_0 \rangle = -s/N + \mathcal{O}(1)$ and variance $\mathrm{Var}\, \ln G/G_0 = 2s/N$. Hence we conclude that

$$\mathrm{Var}\, \ln G/G_0 = -2\langle \ln G/G_0 \rangle, \tag{4.7}$$

in agreement with the result obtained by Pichard,[13] by directly solving the DMPK equation in the localized regime.

The results obtained here are for the case $\beta = 2$. Pichard has shown that the relationship (4.7) between mean and variance of $\ln G/G_0$ remains valid for other values of β, since both the mean and the variance have a $1/\beta$ dependence on the symmetry index.

5 Comparison with random-matrix theory

The random-matrix theory of quantum transport[2, 3] is based on the postulate that all correlations between the transmission eigenvalues are due to the jacobian (1.1). The resulting distribution function (1.2) has the form of a Gibbs distribution with a logarithmic repulsive interaction in the variables $\lambda_n \equiv (1 - T_n)/T_n$. There exists a maximum-entropy argument for this distribution,[2, 3] but it has no microscopic justification. In this paper we have shown, for the case of a quasi-1D geometry without time-reversal symmetry, that the prediction of RMT is highly accurate but not exact.

In the *metallic regime* ($L \ll Nl$), the distribution is given by Eq. (3.5). In terms of the λ-variables ($\lambda \equiv \sinh^2 x$), the distribution takes the form (1.2) of RMT, but with a different interaction

$$u(\lambda_i, \lambda_j) = -\frac{1}{2}\ln|\lambda_j - \lambda_i| - \frac{1}{2}\ln|\mathrm{arcsinh}^2\lambda_j^{1/2} - \mathrm{arcsinh}^2\lambda_i^{1/2}|. \tag{5.1}$$

For $\lambda \ll 1$ (i.e. for T close to unity) $u(\lambda_i, \lambda_j) \to -\ln|\lambda_j - \lambda_i|$, so we derive the logarithmic eigenvalue repulsion (1.3) for the strongly transmitting scattering channels. However, for $\lambda \approx 1$ the interaction (5.1) is *non-logarithmic*. For fixed $\lambda_i \ll 1$, $u(\lambda_i, \lambda_j)$ as a function of λ_j crosses over from $-\ln|\lambda_j - \lambda_i|$ to $-\frac{1}{2}\ln|\lambda_j - \lambda_i|$ as $\lambda_j \to \infty$ (see Fig. 1). It is remarkable that, for weakly transmitting channels, the interaction is twice as small as predicted by considerations based solely on the jacobian. We have no intuitive argument for this result. The reduced level repulsion for weakly transmitting channels enhances the variance of the conductance fluctuations above the prediction (1.4) of RMT. Indeed, as shown in Sec. III.D, a calculation along the lines of Ref. [5], but for the non-logarithmic interaction (5.1), resolves the $\frac{1}{8}$ — $\frac{2}{15}$ discrepancy between RMT and diagrammatic perturbation theory, discussed in the Introduction. The discrepancy is so small because only the weakly transmitting channels (which contribute little to the conductance) are affected by the non-logarithmic interaction.

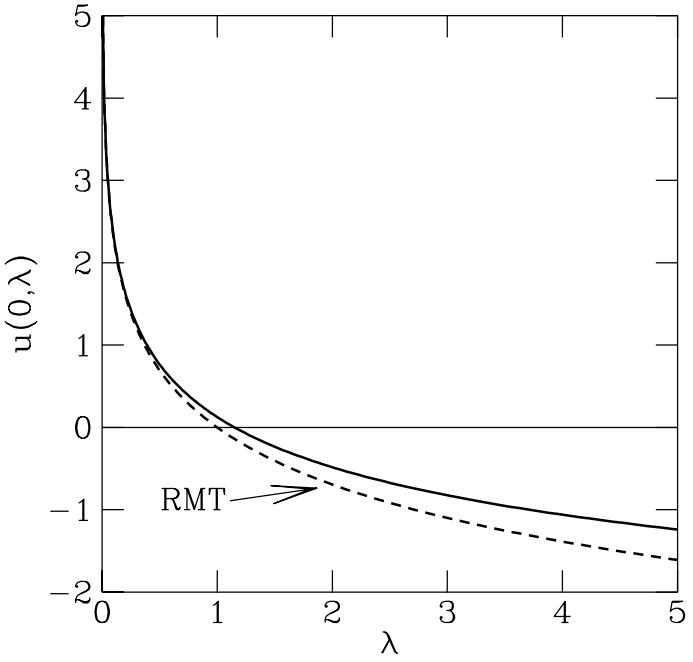

Fig. 5.1. Interaction potential $u(\lambda_i, \lambda_j)$ for $\lambda_i = 0$ as a function of $\lambda_j \equiv \lambda$. The solid curve is the result (5.1) from the DMPK equation. The dashed curve is the logarithmic repulsion (1.3) predicted by random-matrix theory. For $\lambda \ll 1$ the two curves coincide. For $\lambda \to \infty$ their ratio approaches a factor of two.

In the *insulating regime* ($L \gg Nl$), the distribution is given by Eq. (4.5). In terms of the λ's the distribution takes the form (1.2) of RMT, but again with the non-logarithmic interaction (5.1). Since $\ln \lambda \gg 1$ in the insulating regime, the interaction (5.1) may be effectively simplified to $u(\lambda_i, \lambda_j) = -\frac{1}{2} \ln |\lambda_j - \lambda_i|$, which is a factor of two smaller than the interaction (1.3) predicted by RMT. This explains the factor-of-two discrepancy between the results of RMT and of numerical simulations for the width of the log-normal distribution of the conductance:[13] RMT predicts $\mathrm{Var} \ln G/G_0 = -\langle \ln G/G_0 \rangle$, which is twice as small as the correct result (4.7).

We conclude by mentioning some directions for future research. We have only solved the case $\beta = 2$ of broken time-reversal symmetry. In that case the DMPK equation (1.6) can be mapped onto a free-fermion problem. For $\beta = 1, 4$ the Sutherland-type mapping which we have considered is onto an interacting Schrödinger equation. It might be possible to solve this equation exactly too, using techniques developed recently for the Sutherland hamiltonian.[29, 30] From the work of Chalker and Macêdo[27] we know that the two-point correlation function in the large-N limit has a simple $1/\beta$ dependence on the symmetry index. This poses strong restrictions on a possible β-dependence of the eigenvalue interaction.

Another technical challenge is to compute the exact two-point correlation function $K(x, x', s)$ from the distribution function $P(\{x_n\}, s)$. Our result (3.5) for P is exact, but the large-N asymptotic result (3.28) for K ignores fine structure on the scale of the eigenvalue spacing. (This large-N result for K corresponds to the regime of validity of the diagrammatic perturbation theory of UCF,[6, 7] while the exact result for P goes beyond perturbation theory.) In RMT there exists a technique known as the method of orthogonal polynomials,[9] which permits an exact computation of K.[38] A logarithmic interaction seems essential for this method to work, and we see no obvious way to generalize it to the non-logarithmic interaction (5.1).

It might be possible to come up with another maximum-entropy principle, different from that of Muttalib, Pichard, and Stone,[2] which yields the correct eigenvalue interaction (5.1) instead of the logarithmic interaction (1.3). Slevin and Nagao[39] have recently proposed an alternative maximum-entropy principle, but their distribution function does not improve the agreement with Eq. (1.5). [3]

To go beyond quasi-one-dimensional geometries (long and narrow wires) remains an outstanding problem. A numerical study of Slevin, Pichard, and Muttalib[40] has indicated a significant break-down of the logarithmic repulsion for two- and three-dimensional geometries (squares and cubes). A generalization of the DMPK equation (1.6) to higher dimensions has been the subject of some recent investigations.[41, 42] It remains to be seen whether the method developed here for Eq. (1.6) is of use for that problem.

[3] The distribution function of Ref. [39] yields $\mathrm{Var}\, G/G_0 = 0.148\, \beta^{-1}$, which is more than 10% above Eq. (1.5) [K. Slevin, private communication].

References

[1] Y. Imry, Europhys. Lett. **1**, 249 (1986).

[2] K.A. Muttalib, J.-L. Pichard, and A.D. Stone, Phys. Rev. Lett. **59**, 2475 (1987).

[3] A.D. Stone, P.A. Mello, K.A. Muttalib, and J.-L. Pichard, in *Mesoscopic Phenomena in Solids*, ed. by B.L. Al'tshuler, P.A. Lee, and R.A. Webb (North-Holland, Amsterdam, 1991).

[4] P.A. Mello and J.-L. Pichard, Phys. Rev. B **40**, 5276 (1989).

[5] C.W.J. Beenakker, Phys. Rev. Lett. **70**, 1155 (1993); Phys. Rev. B **47**, 15763 (1993).

[6] B.L. Al'tshuler, Pis'ma Zh. Eksp. Teor. Fiz. **41**, 530 (1985) [JETP Lett. **41**, 648 (1985)].

[7] P.A. Lee and A.D. Stone, Phys. Rev. Lett. **55**, 1622 (1985); P.A. Lee, A.D. Stone, and H. Fukuyama, Phys. Rev. B **35**, 1039 (1987).

[8] C.W.J. Beenakker and B. Rejaei, Phys. Rev. Lett. (to be published).

[9] M.L. Mehta, *Random Matrices*, 2nd ed. (Academic, New York, 1991).

[10] K.B. Efetov, Adv. Phys. **32**, 53 (1983).

[11] B.L. Al'tshuler and B.I. Shklovskiĭ, Zh. Eksp. Teor. Fiz. **91**, 220 (1986) [Sov. Phys. JETP **64**, 127 (1986)].

[12] R.A. Jalabert, J.-L. Pichard, and C.W.J. Beenakker, Europhys. Lett. **24**, 1 (1993).

[13] J.-L. Pichard, in *Quantum Coherence in Mesoscopic Systems*, edited by B. Kramer, NATO ASI Series B254 (Plenum, New York, 1991).

[14] O.N. Dorokhov, Pis'ma Zh. Eksp. Teor. Fiz. **36**, 259 (1982) [JETP Lett. **36**, 318 (1982)].

[15] P.A. Mello, P. Pereyra, and N. Kumar, Ann. Phys. **181**, 290 (1988).

[16] P.A. Mello and A.D. Stone, Phys. Rev. B **44**, 3559 (1991).

[17] A.M.S. Macêdo and J.T. Chalker, Phys. Rev. B **46**, 14985 (1992).

[18] A. Hüffmann, J. Phys. A **23**, 5733 (1990).

[19] S. Iida, H.A. Weidenmüller, and J.A. Zuk, Phys. Rev. Lett. **64**, 583 (1990).

[20] M.R. Zirnbauer, Phys. Rev. Lett. **69**, 1584 (1992).

[21] P.A. Mello and B. Shapiro, Phys. Rev. B **37**, 5860 (1988).

[22] V.I. Mel'nikov, Fiz. Tverd. Tela **23**, 782 (1981) [Sov. Phys. Solid State **23**, 444 (1981)].

[23] P.A. Mello, J. Math. Phys. **27**, 2876 (1986).

[24] P.A. Mello, Phys. Rev. Lett. **60**, 1089 (1988).

[25] M.J.M. de Jong and C.W.J. Beenakker, Phys. Rev. B **46**, 13400 (1992).

[26] C.W.J. Beenakker, Phys. Rev. B (to be published).

[27] J.T. Chalker and A.M.S. Macêdo, Phys. Rev. Lett. (to be published).

[28] B. Sutherland, Phys. Rev. A **5**, 1372 (1972).

[29] B.D. Simons, P.A. Lee, and B.L. Altshuler, Phys. Rev. Lett. **70**, 4122 (1993).

[30] E.R. Mucciolo, B.S. Shastry, B.D. Simons, and B.L. Altshuler (preprint).

[31] C.W.J. Beenakker and B. Rejaei, submitted to Physica A.

[32] A. Erdélyi, editor, *Higher Transcendental Functions* (McGraw-Hill, New York, 1953): Vol. 1, p. 175.

[33] F.J. Dyson, J. Math. Phys. **13**, 90 (1972).

[34] M. Büttiker, Phys. Rev. Lett. **65**, 2901 (1990).

[35] C.W.J. Beenakker, Phys. Rev. B **46**, 12841 (1992).

[36] C.W.J. Beenakker, Phys. Rev. Lett. **67**, 3836 (1991); **68**, 1442(E) (1992).

[37] C.W.J. Beenakker, in *Transport Phenomena in Mesoscopic Systems*, ed. by H. Fukuyama and T. Ando (Springer, Berlin, 1992).

[38] K.A. Muttalib, Y. Chen, M.E.H. Ismail, and V.N. Nicopoulos, Phys. Rev. Lett. **71**, 471 (1993).

[39] K. Slevin and T. Nagao, Phys. Rev. Lett. **70**, 635 (1993).

[40] K. Slevin, J.-L. Pichard, and K.A. Muttalib, J. Physique I (France) **3**, 1387 (1993).

[41] P.A. Mello and S. Tomsovic, Phys. Rev. Lett. **67**, 342 (1991).

[42] J.T. Chalker and M. Bernhardt, Phys. Rev. Lett. **70**, 982 (1993).

Summary

On the conductivity of strongly correlated low-dimensional systems

Traditionally, low-dimensional models, *i.e.*, models with spatial dimensions lower than three, have served as pedagogical tools for studying real, three-dimensional systems. Very often, systems whose theoretical description in three dimensions is quite complicated, allow simple and sometimes even exact treatments in lower dimensions. Many theoretical concepts have their roots in low-dimensional, artificial models. There is, however, another reason for studying low-dimensional systems. Recent progress in the manufacturing technology and the availability of very pure semiconducting materials, have made it possible to realize and investigate a number of low-dimensional condensed matter systems in the laboratory. This has led to the discovery of a number of interesting phenomena which can only occur in dimensions lower than three.

This thesis deals with three topics from the physics of low-dimensional systems: anyon superconductivity, the fractional quantum Hall effect, and the electrical conductivity of a disordered wire. A common feature of all these systems is that strong correlations play a crucial role. Consequently, the perturbative techniques, which have proved to be quite successful in other branches of condensed matter physics, turn out to be of little use in these systems.

Chapter 2 deals with the mean-field theory of anyon superconductivity. The notion of anyons is inherently related to the definition of quantum statistics in two dimensions. It is now well-known that the usual definition of quantum statistics, which follows from the change of the sign of the wave function under particle exchange, can be replaced by a more general definition where the phase acquired by the wave function depends on the exchange path. Whereas in three dimensions this definition yields the usual bosons and fermions, in two dimensions it opens the possibility for a whole new range of particles interpolating between bosons and fermions. These new particles are referred to as anyons or particles obeying fractional statistics. In an alternative, but equivalent picture, an anyon is a composite particle consisting of a charged boson or fermion pierced by an infinitely thin tube containing fictitious magnetic flux perpendicular to the two-dimensional plane. The attached flux tubes

induce a long-range vector-potential interaction between the particles. Although there is still no experimental evidence, it has been suggested by R.B. Laughlin that the charged excitations in the high-temperature superconductors are anyons. To see how fractional statistics implies superconductivity, in chapter 2 we apply the mean-field approximation to the vector-potential interaction.

One of the most remarkable phenomena discovered recently is the quantum Hall effect (QHE) which occurs in the two-dimensional electron gas (2DEG), a thin layer of highly mobile electrons whose motion perpendicular to the layer is quantized so that the motion of the electrons is confined to a plane. It is found that at very high perpendicular magnetic fields and very low temperatures, the Hall conductance of the 2DEG is quantized in the units of e^2/h where e is the electron charge and h is the Planck constant. There are two types of QHE: the integer QHE where the Hall conductance is an integer multiple of e^2/h, and the fractional QHE where the Hall conductance is a rational fraction of e^2/h. In both cases, the origin of the quantization of the Hall conductance is the incompressibility of the 2DEG at special values of the electron density. However, while the incompressibility in the integer QHE is a property of the noninteracting electrons, the incompressibility in the fractional QHE is a genuine many-body effect caused by strong correlations between the electrons.

In chapter 3 we investigate the similarities between the ground-state energy spectra in the integer and the fractional QHE's. The analysis is based on numerical results, and an adiabatic principle due to M. Greiter and F. Wilczek which continuously relates the incompressible states of the integer QHE to the incompressible states of the fractional QHE. The adiabatic principle of Greiter and Wilczek is based on the introduction of a fictitious long-range vector-potential interaction between the electrons. The same kind of interaction is studied in connection with anyons. It is assumed that the incompressible states of the integer QHE evolve continuously into the incompressible states of the fractional QHE by adiabatically switching on the vector-potential interaction, *i.e.* by adiabatically attaching flux to the electrons.

The adiabatic principle is an exact prescription for constructing the fractional QHE states from the integer QHE states, but it cannot be carried out in practice unless suitable approximations are made. One possibility is the vector-mean-field theory discussed in chapter 4. The vector-mean-field theory is quite similar to the mean-field theory of anyon superconductivity (considered in chapter 2) where the fictitious vector-potential interaction is treated in mean-field. Unlike the ordinary Hartree-Fock calculations in which the mean-field approximation is applied to the Coulomb interaction, the vector-mean-field theory successfully recovers the properties of the uniform, unbounded fractional QHE states. In addition, the theory can be easily applied to confined or non-uniform systems.

Finally, chapter 5 deals with the electrical conductivity of a (quasi) one-dimensional system, a disordered wire. The motion of the electrons across the wire is quantized, leading to a set of discrete modes similar to the discrete modes of the electromagnetic field in a waveguide. The conductivity of the wire is determined by the transmission eigenvalues of the individual modes, *i.e.*, the probability for each mode to propagate

through the wire. Usually, we are interested not in a particular sample, but in an ensemble of disordered wires, each with a different realization of the disorder. The average conductivity of the ensemble can then be calculated if one knows the probability density of the transmission eigenvalues. The latter can be determined by solving the scaling equation which governs the evolution of the probability density of the transmission eigenvalues as the length of the sample increases. The scaling equation is a diffusion (or Fokker-Planck) equation in the space of transmission eigenvalues. The strong correlations in this problem result from the effective repulsion of these eigenvalues. In chapter 5 we present an exact solution based on a mapping onto a free-fermion problem. The obtained results are then used to test the predictions of an alternative approach, the random matrix theory of the transmission eigenvalues.

Samenvatting

Over het geleidingsvermogen van sterk gecorreleerde laagdimensionale systemen

Laagdimensionale modellen, dat wil zeggen modellen waarin de dimensie van de ruimte kleiner is dan drie, dienen vaak als leermodellen voor het bestuderen van reële driedimensionale systemen. Het komt vaker voor dat een driedimensionaal model met een gecompliceerde theoretische beschrijving, een veel eenvoudigere, soms zelfs exacte analyse toelaat in lagere dimensies. Veel van de begrippen uit de fysica van de gecondenseerde materie hebben hun oorsprong in de hypothetische laagdimensionale modellen. Er bestaat bovendien een andere reden voor het bestuderen van laagdimensionale systemen. De recente ontwikkelingen in de fabricagetechnologie en de beschikbaarheid van zeer zuivere halfgeleidermaterialen hebben het mogelijk gemaakt om een aantal laagdimensionale systemen in het laboratorium te vervaardigen en te onderzoeken. Dit heeft geleid tot de ontdekking van een aantal nieuwe verschijnselen die slechts in één of twee dimensies kunnen voorkomen.

Dit proefschrift behandelt drie onderwerpen uit de fysica van de laagdimensionale systemen: anyon supergeleiding, het fractionele quantum Hall effect, en de elektrische geleiding van een wanordelijke draad. Een gemeenschappelijk kenmerk van al deze systemen is, dat er een cruciale rol wordt gespeeld door sterke correlaties. Daarom komen de technieken gebaseerd op storingsrekening, die hun nut bewezen hebben in vele andere takken van de fysica van de gecondenseerde materie, hier niet van pas.

In hoofdstuk 2 behandelen we de gemiddelde-veld theorie van anyon supergeleiding. Het begrip anyon is gerelateerd aan de definitie van de quantumstatistiek in twee dimensies. Het is nu wel bekend dat de gangbare definitie van de quantumstatistiek, die volgt uit de tekenverandering van de veeldeeltjesgolffunctie onder verwisseling van identieke deeltjes, kan worden vervangen door een veel algemenere definitie waarin de fase verkregen door de golffunctie afhangt van de baan van de deeltjes. Terwijl deze nieuwe definitie in drie dimensies de gewone bosonen en fermionen oplevert, leidt het in twee dimensies tot een breed scala van nieuwe deeltjes die interpoleren tussen bosonen en fermionen. Deze deeltjes worden anyonen, of deeltjes met fractionele statistiek genoemd. In een andere aanpak wordt een anyon voorgesteld als een samengesteld deeltje dat bestaat uit een geladen boson of fermion gebonden aan een oneindig dunne

buis. Het buisje bevat fictieve magnetische flux die loodrecht staat op het tweedimensionale vlak. De fluxbuisjes induceren een vector-potentiaal wisselwerking tussen de deeltjes. Hoewel men nog niet beschikt over een empirisch bewijs, heeft R.B. Laughlin een theorie voorgesteld waarin de geladen excitaties van de hogetemperatuur supergeleiders anyonen zijn. Om te zien hoe de fractionele statistiek kan leiden tot supergeleiding, passen we in hoofdstuk 2 de gemiddelde-veld benadering toe op de vector-potentiaal wisselwerking.

Een van de meest opmerkelijke ontdekkingen van de laatste twintig jaar is de ontdekking van het quantum Hall effect (QHE) dat wordt waargenomen in een tweedimensionaal elektronengas (2DEG), een dunne laag van zeer beweeglijke elektronen waarin de transversale beweging is gekwantiseerd zodat de elektronen zich alleen maar kunnen bewegen in een vlak. Men heeft ontdekt dat bij zeer sterke transversale magnetische velden en zeer lage temperaturen de Hall geleiding van het 2DEG gekwantiseerd is in de eenheden van e^2/h, waarin e de lading is van een elektron en h is de constante van Planck. Men onderscheidt twee soorten QHE: het integer QHE waarbij de Hall geleiding een gehele veelvoud is van e^2/h, en het fractionele QHE waarbij de Hall geleiding een rationele fractie is van e^2/h. In beide gevallen moet de oorsprong van de geleidingskwantisatie worden gezocht in de incompressibiliteit van het 2DEG bij speciale elektronendichtheden. Echter, terwijl de incompressibiliteit in het integer QHE een eigenschap is van niet-wisselwerkende elektronen, wordt de incompressibiliteit in het fractionele QHE veroorzaakt door de sterke correlatie tussen de elektronen.

In hoofdstuk 3 bestuderen we de overeenkomst tussen de grondtoestand spectra in het integer en het fractionele QHE. De analyse is gebaseerd op numerieke resultaten en het adiabatisch principe van M. Greiter en F. Wilczek dat een integer QHE grondtoestand continu relateert aan een fractionele QHE grondtoestand. Het adiabatische principe van Greiter en Wilczek maakt gebruik van een fictieve vector-potentiaal wisselwerking tussen de elektronen. Een soortgelijke wisselwerking wordt bestudeerd in verband met anyonen. Met neemt aan dat een integer QHE grondtoestand continu evolueert in een fractionele QHE grondtoestand door het adiabatisch inschakelen van de vector-potentiaal wisselwerking, dat wil zeggen door het adiabatisch toevoegen van flux aan elektronen.

Het adiabatische principe is een exact voorschrift voor het construeren van de fractionele QHE toestanden uit de integer QHE toestanden. Het kan echter niet in de praktijk worden uitgevoerd tenzij er geschikte benaderingen worden gemaakt. Een mogelijkheid is de vectoriële-gemiddelde-veld theorie die wordt behandeld in hoofdstuk 4. De vectoriële-gemiddelde-veld theorie lijkt op de gemiddelde-veld theorie van anyon-supergeleiding waar men de gemiddelde-veld benadering toepast op de vector-potentiaal wisselwerking. In tegenstelling tot een gewone Hartree-Fock berekening waar de Coulomb wisselwerking behandeld wordt in de gemiddelde-veld benadering, is de vectoriële-gemiddelde-veld theorie in staat de eigenschappen van de homogene fractionele QHE toestanden te verklaren. Bovendien kan men de vectoriële-gemiddelde-veld theorie eenvoudig generalizeren om ook de inhomogene fractionele

QHE toestanden te kunnen beschrijven.

Tenslotte behandelen we in hoofdstuk 5 het elektrische geleidingsvermogen van een (quasi) ééndimensionale wanordelijke geleider (wanordelijke draad). Door de kwantisatie van de transversale beweging van de elektronen in de draad, ontstaan er discrete modes vergelijkbaar met de discrete modes van het elektromagnetische veld in een golfgeleider. Het geleidingsvermogen van de draad wordt bepaald door de transmissie-eigenwaarden: de transmissie-eigenwaarde van elke mode is per definitie de waarschijnlijkheid dat hij zich langs de draad kan voortplanten. Men is in het algemeen geïntresseerd in een ensemble van wanordelijke geleiders, elk met een eigen realisatie van de wanorde. Het gemiddelde geleidingsvermogen kan dan worden berekend als men beschikt over de gezamenlijke kansdichtheid van de transmissie-eigenwaarden. Deze kan worden gevonden door het oplossen van de schaalvergelijking die aangeeft hoe de gezamenlijke kansdichtheid verandert met de toenemende lengte van de draad. De schaalvergelijking is een gecompliceerde diffusie (of Fokker-Planck) vergelijking in de ruimte van transmissie-eigenwaarde. De sterke correlaties in dit probleem zijn afkomstig van de effectieve repulsie van de transmissie-eigenwaarden. In hoofdstuk 5 lossen we deze vergelijking exact op door hem af te beelden op een systeem van vrije fermionen. De resultaten worden vervolgens vergeleken met die van een alternatieve aanpak, de random-matrix theorie van de transmissie-eigenwaarden.

List of publications

1. *Exchange interaction in type II quantum wells,*
   B. Rejaei and G.E.W. Bauer,
   Physical Review B **39**, 1970–1972 (1989).

2. *Superconductivity in the mean-field anyon gas,*
   B. Rejaei and C.W.J. Beenakker,
   Physical Review B **43**, 11392–11395 (1991).

3. *Vector-mean-field theory of the fractional quantum Hall effect,*
   B. Rejaei and C.W.J. Beenakker,
   Physical Review B **46**, 15566–15569 (1992).

4. *Single-electron tunneling in the fractional quantum Hall effect regime,*
   C.W.J. Beenakker and B. Rejaei,
   Physica B **189**, 147–156 (1993).

5. *Quasi-Landau-level structure in the fractional quantum Hall effect,*
   B. Rejaei,
   Physical Review B **48**, 18016–18023 (1993).

6. *Non-logarithmic repulsion of transmission eigenvalues in a disordered wire,*
   C.W.J. Beenakker and B. Rejaei,
   Physical Review Letters **71**, 3689–3692 (1993).

7. *Random-matrix theory of parametric correlations in the spectra of disordered metals and chaotic billiards,*
   C.W.J. Beenakker and B. Rejaei,
   Physica A **203**, 61–90 (1994).

8. *Exact solution for the distribution of transmission eigenvalues in a disordered wire and comparison with random-matrix theory,*
   C.W.J. Beenakker and B. Rejaei,
   Physical Review B, 15 March 1994.

9. *Scaling theory of conduction through a normal-superconductor microbridge,*
   C.W.J. Beenakker, B. Rejaei, and J.A. Melsen,
   submitted for publication.

Curriculum Vitae

van Behzad Rejaei-Salmassi

Ik ben geboren op 15 mei 1965 te Teheran, Iran. Bepaalde omstandigheden, waaronder een geringe mogelijkheid tot studie, hebben mij ertoe gedwongen om na het behalen van mijn middelbare schooldiploma in 1983 mijn vaderland te verlaten. Enigszins door toeval belandde ik in 1984 in Nederland, waar ik na het leren van de Nederlandse taal en het afleggen van de benodigde examens, in september 1985 aan de studie elektrotechniek begon aan de Technische Universiteit Delft. Het propaedeutisch examen legde ik (met lof) af in juni 1986. In de zomer van 1988 heb ik een stage gedaan bij het Philips Natuurkundig Laboratorium in Eindhoven. Daar heb ik, onder begeleiging van prof.dr.ir. G.E.W. Bauer, berekeningen gedaan aan de sterkte van de exchange wisselwerking in een quantumput. Het afstudeeronderzoek vond plaats binnen de vakgroep Elektromagnetisme bij prof.dr.ir. H. Blok. Het onderzoek betrof het ontwikkelen van een nieuwe oplossingsmethode voor inverse verstrooingsproblemen in elektromagnetische media. Het doctoraalexamen haalde ik (met lof) in maart 1990.

In februari 1990 ben ik in dienst getreden van het Philips Natuurkundig Laboratorium in Eindhoven, bij de groep Theoretische Natuurkunde die toen onder leiding stond van prof.dr.ir. M.F.H. Schuurmans. Daar begon ik aan een promotie onderzoek onder begeleiding van prof.dr.ir. C.W.J. Beenakker. Na het vertrek van prof. Beenakker naar Leiden in 1992, heb ik mijn promotie-onderzoek voortgezet als assistent in opleiding in dienst van de Rijksuniversiteit Leiden. In augustus 1992 bezocht ik de zomerschool "Low-Dimensional Field Theories in Condensed Matter" in Trieste, Italië, en in maart 1993 de March-Meeting van de American Physical Society in Seattle, VS. Als onderwijstaak heb ik gedurende twee semesters het werkcollege Elektromagnetisme II aan tweedejaars studenten gegeven.

Stellingen

1. De gelijkenis in de energiespectra van niet-wisselwerkende elektronen in het heeltallige gekwantiseerde Hall-effect en wisselwerkende elektronen in het fractionele gekwantiseerde Hall-effect kan worden gezien als het resultaat van de inductie van quasi-Landau-niveaus door de repulsie tussen de elektronen in het laagste Landau-niveau.

2. In tegenstelling tot bosonen lijden fermionen met hun grote kinetische energie aan een statistische frustratie. Deze kan voor een deel worden gecompenseerd door een magneetveld.

   G.S. Canright en M.D. Johnson, Comments Cond. Mat. Phys. **15**, 77 (1990).

3. De volledige statistische verdeling van het geleidingsvermogen van een wanordelijke draad met twee tunnelbarrières is onafhankelijk van de plaats van de barrières langs de draad, mits de afstand veel groter is dan de Fermi-golflengte.

4. Dyson's Brownse-beweging-model voor parametrische spectrale correlaties is equivalent met de supersymmetrie-theorie van Simons, Lee en Altshuler.

   B.D. Simons, P.A. Lee en B.L. Altshuler, Phys. Rev. Lett. **70**, 4122 (1993).

5. De weerstand van een wanordelijke draad verbonden aan een supergeleider voldoet niet aan de wet van Ohm.

6. De hagelruis van een junctie tussen een normale metaal en een supergeleider is twee keer zo groot als in de normale toestand.

7. De afbeelding op de omslag van het boek *Theory of Simple Liquids* door J.-P. Hansen en I.R. McDonald is niet die van een vloeistof.

B. Rejaei-Salmassi, Leiden, februari 1994.